Synapses of the inner plexiform layer of kitten retina during postnatal development: a quantitative study.

A thesis submitted for the degree of

Doctor of Philosophy

by

Jill Crooks

February, 1990

Institute of Physiology

University of Glasgow

CONTENTS

LIST OF FIGURES

LIST OF TABLES

ACKNOWLEDGEMENTS

I would like to thank Dr Jim Morrison for his advice and encouragement, which was greatly appreciated.

I would also like to thank the following:

-Professor Jennett for the use of the facilities in the Institute of Physiology.

-The Royal National Institute for the Blind for funding me during this project.

-The Vision Research Trust for additional funding.

-Dr Hugh Elder, Mr Bill Biddlecombe and Dr Ian Montgomery of the EM unit, with particular thanks to Mr John Pediani, for useful advice and assistance.

-Dr Jim Reilly and Dr Christine Kay for their friendship during our shared years of study in the Vision Unit.

Finally I would like to give a special thanks to my family and friends for their continuous support and encouragement.

SUMMARY

The development of the synapses of the inner plexiform layer (IPL) was studied in a reproducible area of cat retina which was chosen to be the area centralis. The number of bipolar cell ribbons and conventional synapses during development has been counted from large montages of electron micrographs in 17 kittens of ages ranging from newborn to 200 days and also in three adult cats. Measurements of synaptic profile size and their orientation and distribution within the IPL were also taken, in case there was a systematic change with age which would affect the frequency of occurrence of the profiles.

A very considerable degree of bipolar cell synaptogenesis was shown to occur in the postnatal period, indicated by the increase in frequency of bipolar cell synaptic ribbons and floating ribbons. This synaptogenesis followed an exponential growth pattern, levelling off at about 100 days of age. This change was not dependent upon any age related shift in ribbon size or orientation; therefore it was inferred that retinal ganglion cells must receive a considerable increase in excitatory input during the postnatal period.

In addition, the profiles of the bipolar cell ribbon synapses were then also subdivided into monads and dyads. While there was a considerable increase of dyad frequency, monad frequency was

found to remain constant. This was interpreted to add support to the sequence of dyad formation requiring the initial formation of a floating ribbon then intermediate formation of a monad.

Bipolar cell ribbons were uniformly distributed throughout the 5 strata of the IPL in the neonatal retina whilst a peak was present in strata 3 and 4 in the mature retina. Possible reasons for this finding are discussed.

In marked contrast to the ribbon synapses of bipolar cells, conventional synapses remained invariant in number during postnatal development. In addition, the length of the synapse and the number of vesicles per synapse remained constant. Furthermore, the range of orientations and distribution through the depth of the IPL was mature at birth, as was the number of serial conventional synapses.

The considerable increase in bipolar cell ribbon frequency and the constancy of conventional synapse frequency during postnatal development are discussed with relation to the conflicting electrophysiological evidence during development.

INTRODUCTION

1.1 Retinal structure

1.1.1 Introduction

The vertebrate retina, which is an outgrowth of the diencephalon, is part of the central nervous system. It consists of discrete layers of neurones and neuropil (Fig. 1). The outermost layer consists of photoreceptors which, under the electron microscope, can be seen to be closely enmeshed by processes of the pigment epithelium.

The photoreceptor layer consists of two types of receptors - rods and cones - which occur in varying proportions according to the species lifestyle i.e. whether nocturnal or diurnal. The former have an all rod retina e.g. the rat, while diurnal animals may have a mixed rod/cone retina e.g. primates, or an entirely cone retina e.g. hen. The receptors constitute three layers. The bacillary layer consists of those parts that lie beyond the outer limiting membrane *viz* the outer and inner segments. The nuclei of the receptors form the outer nuclear layer (ONL) while the synaptic terminals lie within the outer plexiform layer (OPL). The latter also contains the dendrites of neurones located in the inner nuclear layer (INL): these are the dendrites of bipolar cells, the dendrites and axons terminals of horizontal cells and the axon terminals of interplexiform cells. The bipolar cells which are generally regarded as second order neurones, though by an alternative

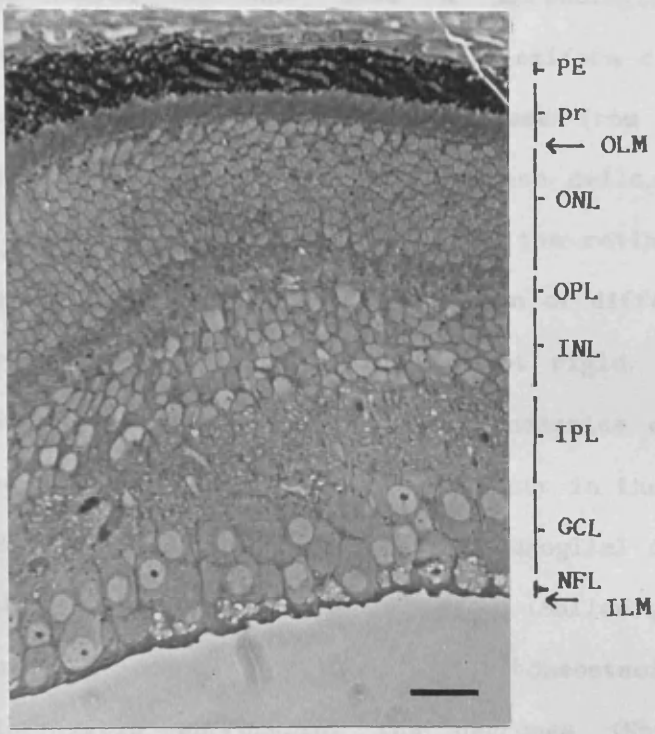

Figure 1

Light micrograph of area centralis of adult cat retina, showing pigment epithelium (PE), photoreceptors (pr), outer limiting membrane (OLM), outer nuclear layer (ONL), outer plexiform layer (OPL), inner nuclear layer (INL), inner plexiform layer (IPL), ganglion cell layer (GCL), nerve fibre layer (NFL) and inner limiting membrane (ILM). Scale bar is 20μm.

classification may be counted as first order neurones, project to the inner plexiform layer (IPL) along with the processes of amacrine cells (which do not have a morphologically identifiable axon) and the dendrites of interplexiform cells. The third order neurones which receive synapses from both bipolar cells and amacrine cells are the ganglion cells, the axons of which pass over the inner surface of the retina to leave the eye in the optic nerve. The demarcation of different classes of neurones into specific layers is not rigid. Many neurones in the ganglion cell layer (GCL) are amacrine cells and, in addition, ganglion cells are known to occur in the INL and IPL (displaced cells of Dogiel). Numerous neuroglial cells are also present in the retina. The astrocytes (Müller glial cells) play a supportive role in maintaining the homeostasis of the extracellular fluid surrounding the neurones (Newman, 1984). Their cell bodies lie in the INL and their fibres radiate through the depth of the retina. Their boundaries extend from the outer limiting membrane to the inner limiting membranes. The ganglion cell layer also contains microglial cells which are generally associated with the blood vessels.

1.1.2 Area centralis

In most diurnal vertebrates, there is a specialised central area in the retina (Walls, 1942), which in the cat is called the ***area centralis.*** The area centralis, which is analagous to the human fovea, lies on the visual axis and is the part of the retina that fixates upon the visual scene. In the adult cat,

the area centralis is approximately elliptical in shape, with the long axis in the horizontal plane, and is located 3.1 mm temporal and 1.4mm dorsal to the optic disc (Bishop, Kozack & Vakkur, 1962). There is a single layer of ganglion cells across most of the retina but at the area centralis it generally forms a double layer of tightly packed cells. The area centralis, as measured by the presence of a double layer of ganglion cells is approximately 1.2mm in horizontal extent and 0.5mm maximum dorso-ventral extent at the centre (Tucker, 1978).

In cat, the area centralis has the highest density of cones, with a ratio of 10 rods to 1 cone compared with a ratio of 100:1 outside the area centralis (Steinberg, Reid & Lacey, 1973). Also, the number of INL cells is highest at the area centralis, with about 5 layers of cells compared to a thickness of about 2 cells in peripheral retina (Donovan, 1966). The area centralis is also characterised by the absence of major blood vessels, an absence of large glial end processes and an absence of an identifiable nerve fibre layer, all of which are very evident in non-central retina.

1.2 Inner plexiform layer

1.2.1 Structural and functional division of the inner plexiform layer

Bipolar cells and interplexiform cells project their axon and dendrites, respectively, into the IPL. Ganglion cells, the axons of which form the optic nerve, and amacrine cells which do not have axons, only project dendrites into the IPL.

Processes from glial Müller cells also traverse the IPL.

Cajal (1892), using the Golgi staining technique, classified numerous subpopulations of bipolar cells, amacrine cells and ganglion cells which branched at different levels within the IPL and he accordingly subdivided the IPL into 5 strata of equal depth. Although most cells ramified in a particular stratum only, some ganglion cells and amacrine cells could be seen to branch in more than one stratum. In addition, some 'diffuse' amacrine cells were observed to ramify throughout the depth of the IPL. However, the processes of the interplexiform cell are not usually confined to a single stratum of the IPL and may branch diffusely (Boycott, Dowling, Fisher, Kolb & Laties, 1975).

Famiglietti & Kolb (1976) divided the IPL into two sublaminae, according to the levels of axonal arborisation of cone bipolar cells and dendritic branching of ganglion cells. The outer third, adjacent to the INL, was termed sublamina *a* and the inner two thirds, adjacent to the GCL, was termed sublamina *b*. Flat cone bipolar cells have terminal arborisations only in sublamina *a* while invaginating cone bipolar cells ramify in sublamina *b*. Rod bipolar cells also ramify in sublamina *b*, their axon terminals lying very close to the GCL, as had been observed much earlier by Cajal (1892). Almost all ganglion cells restrict their dendrites to one or other of the sublaminae. Ganglion cells surmised to receive synapses from flat cone bipolar cells in sublamina *a* respond to darkening of a stimulus and are termed OFF-centre ganglion

cells, while those surmised to receive synapses from invaginating cone bipolar cells in sublamina *b* respond to brightening of the stimulus and are termed ON-centre ganglion cells (Nelson, Famiglietti & Kolb, 1978). In addition, Kolb, Nelson & Mariani (1981) found that many of the sub-types of amacrine cell identified branched in either sublamina *a* or sublamina *b*.

1.2.2 Inner plexiform layer synapses

Kidd (1962) classified IPL synapses into conventional, spine, serial and ribbon synapses. Conventional and spine synapses have both been identified in the retina on the basis of membrane and cleft specialisation, the presence or absence of pre- and postsynaptic thickenings and the synaptic vesicles clustered near the presynaptic membrane. The profiles of spine synapses were identified as lying in an invagination into a postsynaptic process. In primates, Dowling & Boycott (1966) did not distinguish between conventional synapses and spine synapses, both of which they found to be made only by amacrine cells. They found that the postsynaptic process at a conventional synapse can belong to either another amacrine cell dendrite, a bipolar cell terminal or a ganglion cell dendrite. It was later shown, in cat retina, that conventional synapses are also formed by interplexiform cells onto amacrine cells and onto both rod and cone bipolar cells in the IPL (Kolb & West, 1977; Nakamura, McGuire & Sterling, 1980).

Ribbon synapses, in profile, are characterised by having a

lamellar ribbon structure in proximity to the presynaptic membrane. The ribbon is usually surrounded by a halo of synaptic vesicles. Dowling & Boycott (1966) have shown that the element containing the ribbon is always a bipolar cell axon terminal.

The appearance of a ribbon in cross-section is due to the presence of a plate-like membrane structure surrounded by vesicles in the bipolar cell terminals. Usually two postsynaptic processes are associated with each synaptic ribbon site; therefore, Dowling & Boycott termed this type of synaptic contact a 'dyad'. In cat retina, the cone bipolar cell dyad consists mainly of either two ganglion cell dendrites or a ganglion cell dendrite plus an amacrine cell neurite. By contrast, the rod bipolar cell dyad always consists of two amacrine cell neurites (Kolb, 1979).

1.2.3 Inner plexiform layer synaptic pathways

The "ON"-cone pathways are proposed to be mediated via invaginating cone bipolar cells which synapse onto the dendrites of ON-centre ganglion cells in sublamina *b*, while the "OFF"-cone pathway is proposed to be mediated via flat cone bipolar cells which synapse onto the dendrites of OFF-centre ganglion cells in sublamina *a* (Nelson et al, 1978). Gap junctions also occur between neighbouring flat cone bipolar cells (Kolb, 1979).

Since rod bipolar cells form synapses onto a pair of amacrine cell neurites (from AI and AII amacrine cells) but not

onto ganglion cell dendrites (Kolb, 1979), the rod pathway must include amacrine cell interneurones to pass rod signals to ganglion cells. There are rod pathways to both ON- and OFF-centre ganglion cells as indicated by the dark adaptation study of Barlow, Fitzhugh & Kuffler (1957). Therefore, there must be rod pathways to supply signals to ganglion cells stratifying in both sublaminae. OFF-centre ganglion cells appear to receive an input from amacrine cells which are postsynaptic to rod bipolar cells. Rod information may pass to ON-centre ganglion cells in sublamina *b* via the gap junctions between AII amacrine cells and invaginating cone bipolar cells (Kolb, 1979).

Rod bipolar cells are also presynaptic to the AI amacrine cells. AI amacrine cells form conventional synapses onto the rod bipolar cell terminals at the site of the ribbon synapses in a configuration that is termed a reciprocal synapse. AI amacrine cells interconnect neighbouring rod bipolar cells (Kolb, 1979).

Conventional synapses are also formed by interplexiform cells. It is probable that, in the cat retina, interplexiform cells are postsynaptic at amacrine cell conventional synapses and presynaptic to bipolar cells and amacrine cells (Kolb & West, 1977; Nakamura et al, 1980).

Thus, rod bipolar ribbon synapses are presynaptic onto a pair of amacrine cell neurites, while cone bipolar cells may be presynaptic to either two ganglion cell dendrites or to a ganglion cell dendrite and an amacrine cell neurite. Amacrine cell conventional synapses may be presynaptic to

bipolar cells, ganglion cells, to other amacrine cells and to interplexiform cells.

1.3 Conventional synapses

Gray (1959) has described two morphological types of synapse in the cerebral cortex. Although both types were characterised by a cluster of synaptic vesicles associated with a membrane density, or thickening, there were several morphological differences between the types. In type 1 conventional synapses, the gap between the pre- and postsynaptic membrane widens at the synaptic cleft which contains a band of material. There is an accumulation of electron-dense material at the postsynaptic membrane which is greater than at the presynaptic membrane, resulting in an asymmetrical appearance. Both the pre- and postsynaptic membranes display membrane thickening over almost the full extent.

Type 2 conventional synapses do not show an obvious increase in distance between membranes at the synaptic cleft and there is no clearly defined band of material within it. There is a modest but symmetrical membrane thickening on both pre- and postsynaptic processes which extends for about 40% of the total length of the apposed membranes.

In the cerebellum, synapses known to be excitatory contain spherical vesicles while synapses known to be inhibitory contain ellipsoidal vesicles (Uchizono, 1965), though this was not remarked upon by Gray in his study of cerebral cortex. Uchizono concluded that excitatory (E-type) synapses were

equivalent to Gray's type 1 synapses and the inhibitory synapses (I-type) were equivalent to Gray's type 2 synapses.

Conventional synapses in the IPL appear to be predominantly type 1 (Kidd, 1962), as demonstrated by the presence of a widened cleft containing a dense matrix of material, which would suggest that they are excitatory synapses. However, the thickening of the synaptic membranes has been described as symmetrical (Dowling & Boycott, 1966; Raviola & Raviola, 1967; 1982; Kolb & West, 1977).

The freeze fracture study by Raviola & Raviola (1982) has indicated that the majority of conventional synapses, including all amacrine to bipolar cell synapses, are in fact inhibitory. These conventional synapses have an unspecialised postsynaptic membrane, thus resembling the inhibitory synapses of the olfactory bulb, the cerebellum and the organ of Corti. A second type of conventional synapse has a cluster of intramembrane particles preferentially associated with the *inner* leaflet of the postsynaptic membrane. The functional properties of this type of synapse are unknown. A third possible type is characterised by an aggregate of particles in the *outer* leaflet within the postsynaptic membrane, which resembles excitatory synapses in the olfactory bulb, cerebellum and cochlear nucleus. Raviola & Raviola (1982) indicate that the particle aggregate corresponds to the membrane density.

The evidence of Raviola & Raviola (1982) that most amacrine cells are inhibitory is consistent with autoradiographic studies which show an accumulation of exogenous glycine and the

presence of endogenous glycine in some 45-50% of amacrine cells in the cat retina (Wässle, Schäfer-Trenkler & Voigt, 1986; Pourcho & Goebel, 1987a; 1987b). Glycine has been reported to be inhibitory either to all ganglion cells (Bolz, Thier, Voigt & Wässle, 1985) or only to OFF-centre ganglion cells (Ikeda & Sheardown, 1983). Amacrine cells have also been observed to accumulate gamma-aminobutyric acid (GABA) (Freed, Nakamura & Sterling, 1983; Bolz, Frumkes, Voigt & Wässle, 1985) which has been described as having an inhibitory effect on ON-centre ganglion cells only (Ikeda & Sheardown, 1983) or onto all ganglion cells (Bolz, Frumkes, Voigt & Wässle, 1985).

However, other amacrine cells appear to be excitatory, with acetylcholine as the transmitter substance. Amacrine cells have been observed to accumulate acetylcholine and to contain acetylcholine synthesizing enzymes (Masland, Mills & Cassidy, 1984; Masland, Mills & Hayden, 1984; Pourcho & Osman, 1986; Schmidt, Humphrey & Wässle, 1987). There have been several studies implicating acetylcholine as excitatory to ganglion cells. Ikeda & Sheardown (1982a), studying the effects of ionophoretically applied acetylcholine and its antagonists on ganglion cells, proposed that cholinergic nicotinic receptors mediated the excitatory input to the Y-ganglion cells which exhibited a periphery effect. Another ionophoretic study by Schmidt et al (1987) indicates that acetylcholine is excitatory to all brisk-responding ganglion cells, i.e. both X and Y types. In a combined electrophysiological and auto-radiographical study in the rabbit retina, Masland, Mills &

Cassidy (1984) demonstrated the release of acetylcholine at the onset and cessation of light. Hochstein & Shapley (1976) concluded that the Y-ganglion cell pathway contained an additional rectifying component which would be consistent with a spike-generating cell like an amacrine cell.

Vaney & Young (1988) have described cholinergic amacrine cells in the rabbit which also exhibit GABA-like immunoreactivity. This raises the possibility of dual release of both excitatory and inhibitory transmitters. This may, in fact, prove to be rather widespread, since a considerable number of amacrine cells in the retinae of several species appear to contain a wide range of substances other than GABA, glycine and acetylcholine, including dopamine and serotonin, which are well-established as neurotransmitters, and also eight neuropeptides *viz.* substance P, enkephalin, neurotensin, somatostatin, neuropeptide Y, vasoactive intestinal peptide, cholecystokinin and glucagon (reviewed by Dowling, 1987).

1.4 Bipolar cell ribbon synapses

Ribbon synapses have been characterised in profile by having a lamellar ribbon structure associated with the presynaptic membrane at the synaptic site (e.g. Kidd, 1962; Dowling & Boycott, 1966; Raviola & Raviola, 1967). The ribbon is usually surrounded by a halo of synaptic vesicles and usually two postsynaptic processes are associated with each synaptic ribbon site. The cleft between the presynaptic bipolar process and the two postsynaptic processes is enlarged and may contain a matrix

of dense material. The synaptic ribbon is generally orthogonal to the synaptic cleft and there is usually a presynaptic specialisation in the form of a rudimentary arciform density, which is a dense matrix of material, at the site of ribbon apposition to the membrane. There is thickening of the postsynaptic membranes. In these respects, the membrane and cleft specialisation are similar to the type 1 excitatory conventional synapse. The freeze fracture study of Raviola & Raviola (1982) showed that there is a particle aggregate on the *outer* leaflet of the postsynaptic membrane at ribbon synapses, implying that the synapses are excitatory.

The function of bipolar cell ribbons is not totally clear but Gray & Pease (1971) have suggested that synaptic ribbons in receptor terminals act to guide the synaptic vesicles towards the site of release. This is supported by the presence of vesicle attachment sites in the presynaptic membrane on either side of the ribbon (Raviola & Raviola, 1982). These authors have suggested that such a configuration allows the two postsynaptic processes to be activated simultaneously.

Dowling & Boycott (1966) established that only bipolar cells form ribbon synapses. The morphological evidence that the ribbon synapses formed by most bipolar cells are excitatory is supported by electrophysiological evidence that glutamate and aspartate are excitatory to ganglion cells and may be released by bipolar cells (Bloomfield & Dowling, 1985; Massey & Miller, 1988). An ionophoretic study in the cat indicates that aspartate but not glutamate may be an excitatory

neurotransmitter onto ganglion cells (Ikeda & Sheardown, 1982b). Intracellular recording followed by horseradish peroxidase (HRP) injection of rod bipolar cells in the rabbit, to allow identification of the neurone and freeze-fracture electron microscopy, led Raviola & Dacheux (1987) to conclude that rod bipolar cells release an excitatory transmitter. In addition, evidence obtained from transretinal stimulation (Toyodo & Fujimoto, 1984) indicates that bipolar cells are excitatory to amacrine cells.

The possible presence of bipolar cells which release the inhibitory transmitter glycine has been suggested by autoradiographical and immunocytochemical techniques (Cohen & Sterling, 1986; Wässle et al, 1986; Pourcho & Goebel, 1987a; 1987b). However, the actual degree of labelling in the autoradiographic studies is low compared to the amount of [^{3}H] glycine accumulated by amacrine cells (Pourcho & Goebel, 1987a). Even the two most highly labelled cone bipolar cell types demonstrated only about 40% of glycine accumulation as did the most heavily labelled amacrine cell. In addition, some cone bipolar cells did not label much more strongly for glycine than amacrine cells that are thought to be GABAergic (Pourcho & Goebel, 1987a). Therefore, the question of the release of an inhibitory transmitter by bipolar cells still requires clarification.

1.5 Serial synapses and reciprocal synapses

Kidd (1962) described a serial conventional synapse as one in which a process was both presynaptic and postsynaptic. He observed two types of these synapse: those involving a ribbon synapse and those involving conventional synapses only.

Dowling & Boycott (1966) renamed Kidd's definition of a serial synapse involving a ribbon, noting that in the configuration which they called a 'reciprocal synapse', an amacrine cell process involved in a dyad made a synapse back onto the presynaptic bipolar axon terminal near the ribbon synapse. Kolb (1979) named a specific type of amacrine cell involved in reciprocal synapses as 'AI' type amacrine cells. Dowling (1968) confined the term 'serial synapse' to the situation in which an amacrine cell process was presynaptic to a second amacrine cell process, which itself was presynaptic to a third element. The third element could be a bipolar cell terminal, a ganglion cell dendrite or another amacrine cell process.

1.6 Development of the retina

1.6.1 Differentiation of retinal cells

All the retinal cell types appear to derive from a single proliferative cell type, the ventricular cell in the embryonic optic cup (Mann, 1928). Autoradiographic studies in the mouse retina show that ganglion cells and amacrine cells are the first cells to start developing, followed by horizontal cells

and photoreceptor cells, then bipolar cells and neuroglial cells (Sidman, 1961).

Following mitosis, cells either remain attached to the basement membrane of the ventricular layer or become detached from it (Hinds & Hinds, 1979). Then, a vitreal process either grows into the inner part of the ventricular layer or remains in the outer part of the ventricular layer. Cells detached from the basement membrane with short vitreal processes differentiate into horizontal cells, while those remaining attached become photoreceptors. Detached cells with long vitreal processes differentiate into ganglion cells if the vitreal process becomes a viable axon. If the process is not viable, the cell becomes an amacrine cell and, provided that the IPL has not yet formed, migrates outwards to the inner ventricular layer. Subsequent to the formation of the IPL, another population of amacrine cells is formed, which appears to develop directly from the ventricular layer (Hinds & Hinds, 1983). Bipolar cells form later but little is known about the process.

1.6.2 Ganglion cell development

In the embryonic cat, ganglion cells are 'born' mainly between the 21st and 31st embryonic days (E21-E31) (Walsh, Polley, Hickey & Guillery, 1983), They form first in central retina around the optic nerve head and nasal to the area centralis, then arising from locations which describe approximately a spiral pattern first superior and nasal to the

area centralis, then forming progressively in the inferior nasal retina and inferior temporal retina (Walsh & Polley, 1985). Medium sized ganglion cells are generated before large ganglion cells, indicating that beta-ganglion cells are formed prior to alpha-ganglion cells (Walsh et al, 1983). Small ganglion cells, which are first generated at E21, continue to form until at least E36, by which time the generation of medium and large ganglion cells is complete. The ganglion cell layer begins to separate from the ventricular layer in the late E20s (Maslim & Stone, 1986) and the distribution of cells in the GCL indicates that there is a rudimentary area centralis present even as early as E35 (Lia, Williams & Chalupa, 1987).

Retinal ganglion cell axons arrive at the lateral geniculate nucleus from the contralateral nasal retina first at E32, followed by those from the ipsilateral temporal retina at E35 (Shatz, 1983). They are intermingled and do not fully segregate into the appropriate eye layers until birth (Shatz, 1983).

The number of axons in the optic nerve increases from E30 to E45-E55, when it is 450,000-483,000. The number then falls rapidly during the week after birth, reaching a mature level of 185,000 by the 15th postnatal day (P15) (Ng & Stone, 1982). Ganglion cell soma size increases with development, becoming mature at the area centralis by P20, although it is not until P80 that all ganglion cells reach a mature size (Rapaport & Stone, 1983).

1.6.3 Postnatal retinal development

The gestation period of the cat is 61-69 days and by the time of birth all cell division in the central retina has ceased, indicating that all cell types are present by this stage (Johns, Rusoff & Dubin, 1979). However, in non-central retina, although all ganglion cells are present at birth, mitosis of cells in the INL and ONL continues up to 3 weeks after birth. These cells differentiate into photoreceptors and other neurons or into Müller cells. At the time of birth, the ganglion cells form a discrete single cell layer, except at the area centralis, where the ganglion cell layer is 2-3 cells thick. The cells of the INL mature in the central region at approximately 2 weeks and peripherally at approximately 4 weeks postnatally. At the time of birth, Donovan (1966) found the OPL to be present only in central retina. The nuclei of the receptor cells are slowest to mature, appearing mature in all areas of the retina by about 5 weeks of age. Immature rod and cone outer segments were present in the area centralis after birth, attaining a high degree of development at the end of the second week and reaching maturity by the end of the fifth week (Morrison, 1982) although outer segments did not reach a mature length in peripheral retina until about 9 weeks of age (Donovan, 1966).

1.6.4. Inner plexiform layer development

The GCL begins to separate from the ventricular layer in the late E20s and at E45 the IPL contains many compact processes (Maslim & Stone, 1986). Conventional synapses were unambiguously identified at E45 in both central and peripheral retina (Maslim & Stone, 1986). It is thought that membrane densities appear first at the developing synaptic site at E36 in the embryonic cat and synaptic vesicles subsequently become associated with the presynaptic membrane. Studies on postnatal kitten retina show that there are numerous conventional synapses present at birth which are mature in morphology (Vogel, 1978; Morrison, 1982; Maslim & Stone, 1986).

In the cat, the first bipolar cell ribbons appeared at birth at the area centralis but not until the 5th day in peripheral retina (Maslim & Stone, 1986). Although Morrison (1982) did not study prenatal retina, he observed a few bipolar cell ribbons in a monad configuration with a ganglion cell dendrite at the area centralis at birth. Cone bipolar cells appear to form synapses earlier than rod bipolar cells and by 18-23 days a high degree of maturity was present in both cell types (Morrison, 1982).

Serial sectioning of immature retinae have demonstrated the presence of 'true' floating ribbons and monads prior to the occurrence of dyads (McArdle, Dowling & Masland, 1977; Morrison, 1982). Therefore, the sequence has been proposed that, initially, floating ribbons are generated and these become associated with one postsynaptic process to form a monad

prior to the alignment of a second postsynaptic process to form a dyad (McArdle et al, 1977; Morrison, 1982).

1.7 Present study

The retina of the cat is, therefore, an accessible part of the central nervous system for which there is a considerable body of evidence relating to the physiology and neural circuitry of the mature retina (e.g. Nelson et al, 1978; Kolb, 1979). In the developing retina, a high degree of maturity was observed by qualitative electron microscopy of the IPL at 18-23 days postnatal (Morrison, 1982). The functional development of the retina, in terms of the b-wave of the electroretinogram, indicates a more extended time course of development, becoming fully mature only at 10-14 weeks postnatal (Hamasaki & McGuire, 1985; Jacobson, Ikeda & Ruddock, 1987).

The present study is concerned with the morphological changes correlating to the development of ganglion cell responses, which also show an extended time course of development (Hamasaki & Flynn, 1977; Rusoff & Dubin, 1977; Hamasaki & Sutija, 1979). Ganglion cell responses are determined by the interaction of inhibitory and excitatory inputs from IPL synapses. Thus, it was appropriate to undertake a quantitative study of the time course of development of synapses in the IPL by electron microscopy. Accordingly, the number of bipolar cell ribbons and conventional synapses has

been counted at different postnatal ages to provide a measure of the development of excitatory and inhibitory synapses in the IPL.

However, there are several associated problems. First, it is essential that exactly the same region of retina be examined at each age, since the peripheral retina develops more slowly than the centre (Donovan, 1966; Johns et al, 1979; Maslim & Stone, 1986) and contains fewer ganglion cells (Stone, 1965; 1978) which possess larger dendritic fields (Boycott & Wässle, 1974). The most readily identifiable part of the retina, apart from the optic disc, is the area centralis which is characterised by a multiple layer of ganglion cells (Donovan, 1966). It also lies on the visual axis and is, hence, of considerable functional significance. Second, a systematic change in the size or orientation of the the conventional synapse or ribbon during development would affect the frequency with which the synapses were observed in ultrathin sections; hence measurements of both the length and orientation of profiles were made. Third, the counts must be made across the entire depth of the IPL, since sampling from small areas results in atypical results (Dubin, 1970). Of particular relevance is the fact that the flat cone bipolar cell axons arborise in sublamina *a* of the IPL while invaginating cone bipolar cell axons and rod bipolar cell axons terminate in sublamina *b* (Kolb, 1979) Therefore, the positions of conventional synapses and ribbons within the IPL were also measured at different

ages. The results of this study have been presented as a preliminary communication (Crooks & Morrison, 1986) and in a fuller account (Crooks & Morrison, 1989).

MATERIALS AND METHODS

2.1 Materials

Seventeen healthy kittens and three adult cats were used in this study. They were obtained from the University of Edinburgh Breeding Station and from the Animal House, Institute of Physiology, Glasgow University. The age of the kittens was known to the nearest half day and ranged from newborn to 200 days old. The ages of the kittens, with the numbers in parentheses, were: newborn (2), 2 days (3), 5 days (1), 6 days (1), 10 days (1), 18 days (2), 23 days (1), 41 days (1), 43 days (1), 73 days (1), 100 days (1), 200 days (2), adult (3). Ten of these retinae have been used in earlier studies (Morrison, 1982; 1983). The retinae were fixed by immersion as described below.

2.2 Procedure for immersion fixation of retinae

The animal was deeply anaesthetised with an intra-peritoneal dose of Sagatal (50-170 mg/kg body weight). The outer canthus was compressed to blanche the tissue. A deep incision was made into the outer canthus and the conjunctiva was incised and the nictitating membrane removed. A suture was made at the dorsal pole of the eye to aid subsequent alignment of the retina. The eyelids were held open with Mosquito clips and the eye was gently freed by dissection of the extraocular muscles and fascia. The optic nerve and ophthalmic artery were then cut. When both eyes were removed for electron microscopy, the optic nerve (containing the ophthalmic artery) of the first eye was clamped before enucleation to prevent haemorrhage with its

consequent reduction in blood flow to the second eye.

The eye was removed to a petri dish containing cold Krebs' solution bubbled with 100% oxygen and was sectioned just posterior to the limbus. Holding the eye by the optic nerve, the vitreous body was gently parted from the retina by drawing it across filter paper to which it adhered.

The posterior segment of the eye was then fixed by immersion for one hour in 1% glutaraldehyde and 0.5% paraformaldehyde in 0.05M phosphate buffer, pH7.4 and final osmolality *ca* 300mosmoles/kg (See Appendix 1). It was then rinsed several times in 0.15M phosphate buffer over a minimum period of one hour. If the retina had been removed late in the day, so that osmication and embedding were not possible until the following day, it was stored in buffer in the refrigerator overnight. Prior to osmication, the retina was pinned out on dental wax and photographed. Relief cuts were made in the periphery to facilitate pinning out, as shown in Fig. 2. The retina was then post-fixed in 1% OsO_4 in 0.1M phosphate buffer for one hour in the cold and the entire retina embedded in Epon/Araldite. Previous trials had indicated that this mixture gave superior results to either Epon or Araldite alone. It was preferable to embed the entire retina in order to prevent the choroid and sclera separating from the retina and to reduce deformation of the tissue which sometimes occurs with smaller pieces. It also made the entire retina available for analysis.

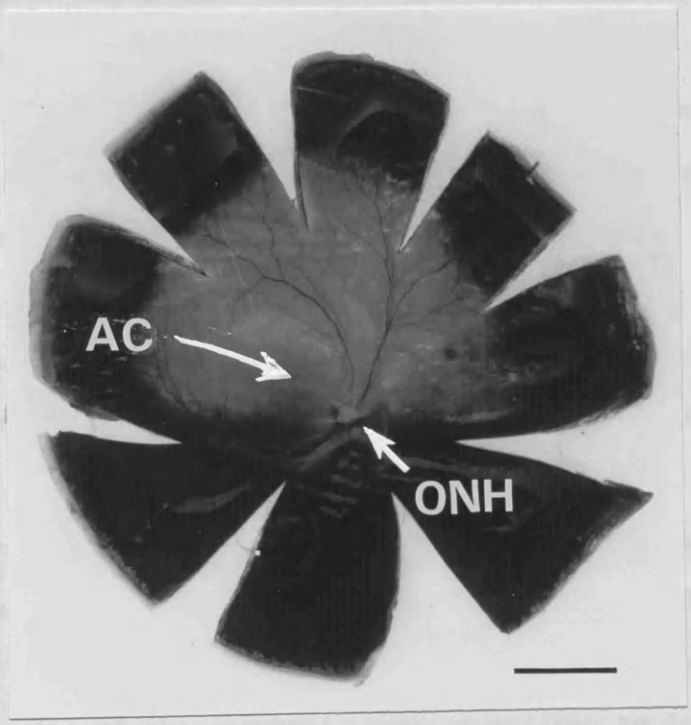

Figure 2

Photograph taken of the left retina of an adult cat, prior to embedding, to show the position of the optic nerve head (ONH) and the area centralis (AC). Scale bar is 5mm.

2.3 Localisation of the area centralis

This was done from the photograph which gives the position of the optic nerve head and the approximate location of the area centralis as judged from the region free of major blood vessels (Fig. 2). A wedge from the temporal retina with the optic nerve head at the apex and containing the area centralis was then removed, using a piercing saw with a fine blade.

2.4 Sectioning procedure

The wedge of temporal retina was trimmed from the apex with a razor blade until the optic nerve became visible. It was then sectioned on a dry glass knife on a LKB III ultramicrotome until the temporal edge of the optic nerve head was reached. Then, the block was divided 2mm from this point with a sharp blade and sectioning of the temporal piece undertaken to locate the area centralis. This was done by taking a series of 3-5μm sections covering a total thickness of 100μm followed by inspection of the sections, mounted on glass in immersion oil, under phase-contrast microscopy. The criteria for confirmation of the area centralis was the presence of a multiple layer of ganglion cells free of prominent glial end processes and blood vessels. The 2mm wedge was retained in the event that it contained the area centralis, as occasionally occurred.

At the area centralis, 1μ sections were then taken and stained with toluidine blue for bright field microscopy or phenylene diamine for phase contrast microscopy (see Appendix 1 for staining procedures).

2.5 Ultrathin sections

Ultrathin sections coloured grey/silver, judged by their interference colours to be 50-60nm thick, were then cut at the area centralis, using a glass knife, and mounted on 3mm formvar coated copper multi slot grids. The sections were stained conventionally with uranyl acetate solution for 5 minutes followed by lead citrate solution for 5 minutes (See Appendix 1). These were viewed with the Zeiss EM109 electron microscope at 7.1K machine magnification. This machine has a low pin cushion distortion, making it particularly suitable for the construction of montages.

2.6 Montages

Large montages were constructed across the depth of the IPL from electron micrographs printed at 2.5X enlargement, thus giving a total magnification of 17.8K. Areas containing blemishes were avoided. At each age, usually 2 or 3 montages from different regions of the area centralis were constructed. The total area covered by the montages for each retina was 737-2775μm^2. Measurements of the area of the montages excluded any capillaries and large glial tracts.

2.7 Measurement of frequency of occurrence of synaptic profiles

Ribbon synapses, floating ribbons, conventional synapses, serial conventional synapses and reciprocal synapses were counted, according to criteria set out in the Results. Incomplete profiles falling on the edge of a montage were

counted at the left but not the right margin of the montage, with the INL uppermost. Each montage was scanned carefully on three separate occasions to identify and classify synapses. Dr J.D.Morrison then independently examined the montages. When there were different opinions about synapse classification, this was decided on a synapse by synapse basis.

2.8 Measurement of dimensions, orientation and position

These measurements were particularly important in case there was a systematic change with age, which would affect the frequency of occurrence of the profiles.

The profile size of each conventional synapse and bipolar cell ribbon was measured with a micrometer to the nearest 0.5mm, which was approximately equivalent to 0.03μm. When measuring conventional synapses or bipolar ribbons, any curvature in the profiles was ignored thus causing a slight underestimate in some measurements. When there was no measurable synaptic density at conventional synapses, the extent of the vesicle cluster was measured.

Measurement of orientation was carried out using a protractor. Zero degrees was parallel to the GCL/IPL border and a T-square was used to position the protractor. A tangent was drawn on the conventional synapse or ribbon and the angle was measured to the nearest 1°, ranging from 0°-179°.

The position of the profile was based on the division of the IPL into 5 strata of equal width, numbered 1-5 from the INL to the GCL and the number of synapses falling into each stratum was counted.

The line of the INL/IPL and IPL/GCL borders was judged by eye, as the cells did not always project evenly into the IPL. When a synapse fell on the boundary of two strata, it was allocated to the stratum nearer to the GCL. Therefore, a synapse falling on the boundary between strata 3 and 4 was allocated to stratum 4.

2.9 Statistical tests

Statistical tests were carried out on the quantitative data using the Minitab statistical package (Ryan, Joiner & Ryan, 1985) on the Glasgow University mainframe computer.

Linear regression analysis was applied to the results for synaptic profile frequencies and synaptic profile sizes with age (days), $\sqrt{}$age and $\log_{10}$age, and the correlation coefficient was calculated. To enable the logarithmic and square root transformation of the data, newborn was counted as 1 day and adult as 300 days.

The data conforming to a Gaussian distribution were compared using the t-test; otherwise the Mann-Whitney test was employed. The χ^2-squared test was applied to determine whether the distributions of the histograms for orientation and position of the synapses in the IPL were random.

Results are tabulated giving the linear regression equation of y on x, the standard deviation of y (S.D. of y), the correlation coefficient (r) and the probability of the null hypothesis (P) for linear, logarithmic and square root (abbreviated Sqrt) functions of age. For practical purposes the age scale was plotted as $\log_{10}$age in the figures.

RESULTS

3.1 Microscopy

3.1.1 Light microscopy of the area centralis

In the adult cat, the area centralis is characterised by a multiple layer of closely packed ganglion cells in a layer of up to 2 cells deep (Fig. 1). There is an absence of a prominent nerve fibre layer, of large glial cell end processes and of large blood vessels and the INL is 5 neurons deep. This also holds true for the neonatal retina though the ganglion cells, which are not so closely packed, may be arranged in a layer up to 3 cells deep (Fig. 3). Both neonatal and mature retinae have an INL approximately 5 cells deep and an IPL of similar depth. The photoreceptor outer segments are much smaller in the neonatal retina, in which the ONL neurones still show characteristically clumped chromatin in the nuclei, whereas in the adult these have fully differentiated. The OPL of the neonatal retina is also much thinner than that of the mature retina. Under the light microscope, the developing cat retina attains a mature appearance by 41 days in the area centralis, though in peripheral non-tapetal retina there is an additional 2 weeks before maturity is attained.

3.1.2 Electron microscopy of the inner plexiform layer

Under the electron microscope, bipolar cell terminals are distinguished by the presence of one or more synaptic ribbons, each of which is adjacent to a pair of postsynaptic processes

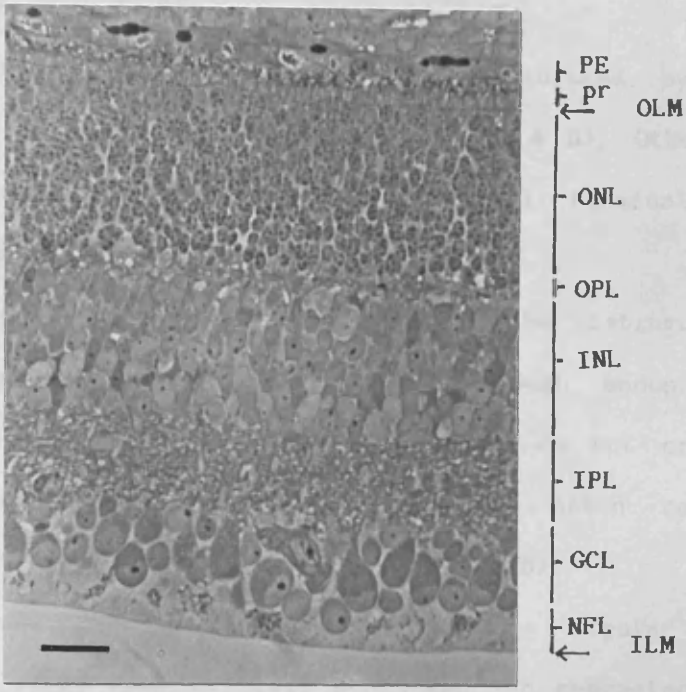

Figure 3

Light micrograph of area centralis of 6 day kitten retina, showing pigment epithelium (PE), photoreceptors (pr), outer limiting membrane (OLM), outer nuclear layer (ONL), outer plexiform layer (OPL), inner nuclear layer (INL), inner plexiform layer (IPL), ganglion cell layer (GCL), nerve fibre layer (NFL) and inner limiting membrane (ILM). Scale bar is 20μm.

collectively termed a *dyad* (Fig. 4A). However, according to the plane of section, the ribbon may appear remote from a synapse, in which case it is termed a *floating* ribbon (Fig. 4B) and sometimes only one postsynaptic process is present, in which case it is termed a *monad*.

Amacrine cells are most readily distinguished by the formation of a conventional synapse (Fig. 4A & B). Otherwise there may be some ambiguity between bipolar cell terminals and large amacrine cell dendrites.

Ganglion cell dendrites could often easily be distinguished by the presence of numerous ribosomes, rough endoplasmic reticulum and clusters of microtubules. They do not contain synaptic vesicles; however, ganglion cells often contain multivesicular bodies and small lysosomes (Fig. 5).

In neonatal retinae (Fig. 5), the large bipolar cell terminals and large amacrine cell processes, so characteristic of mature retinae (Fig. 6), were observed much less frequently. In general, while presynaptic processes may still be readily identifiable by the presence of ribbon or conventional synapses, the identification of postsynaptic processes was much more uncertain. For that reason a systematic classification of these processes was not attempted. This also ruled out subdividing bipolar cell terminals into rod or cone bipolar cell terminals, since such classification must be based on whether the dyad consisted of two amacrine cells or one amacrine and one ganglion cell, respectively (Kolb, 1979).

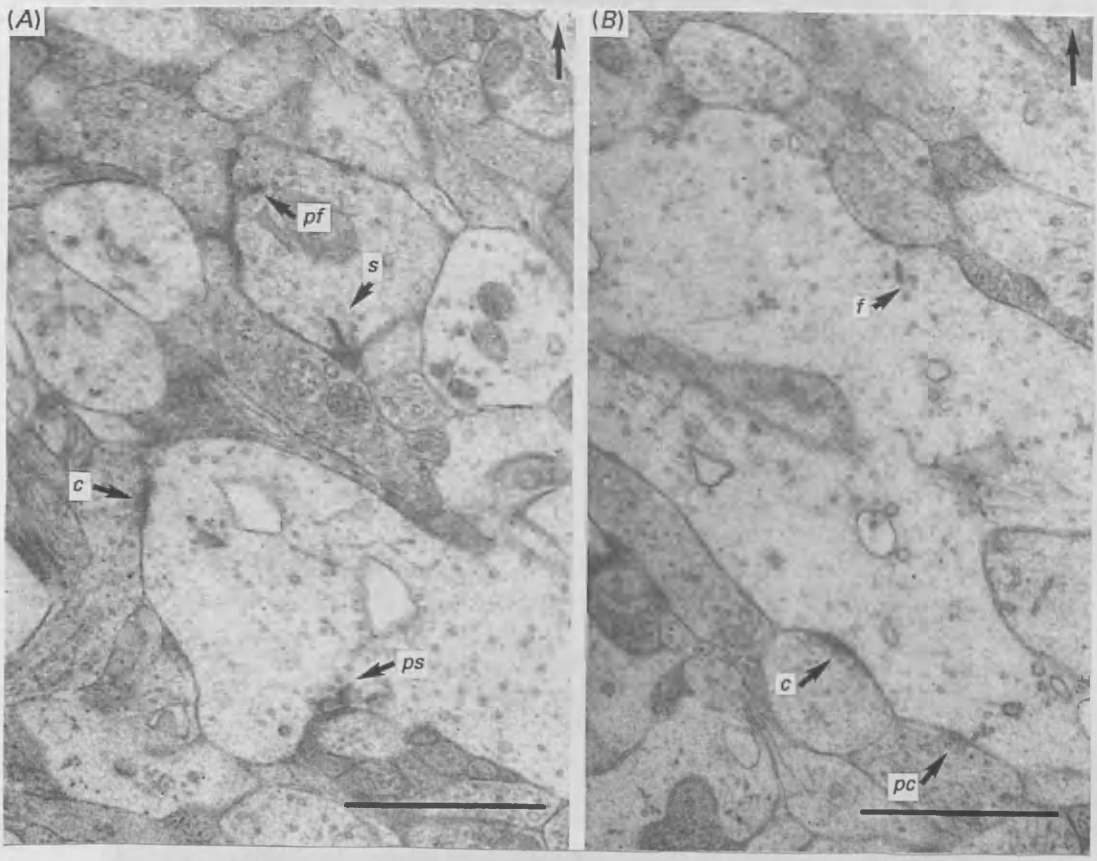

Figure 4

Electron micrograph of IPL of area centralis of 6 day kitten (A & B) showing bipolar cell terminals containing a definite synaptic ribbon (s), a probable synaptic ribbon (ps), a definite floating ribbon (f), a probable floating ribbon (pf) and examples of 2 definite conventional synapse (c) and a probable conventional synapse (pc). Orientation is indicated by arrow (top right) pointing to INL. Scale bar is 1μm.

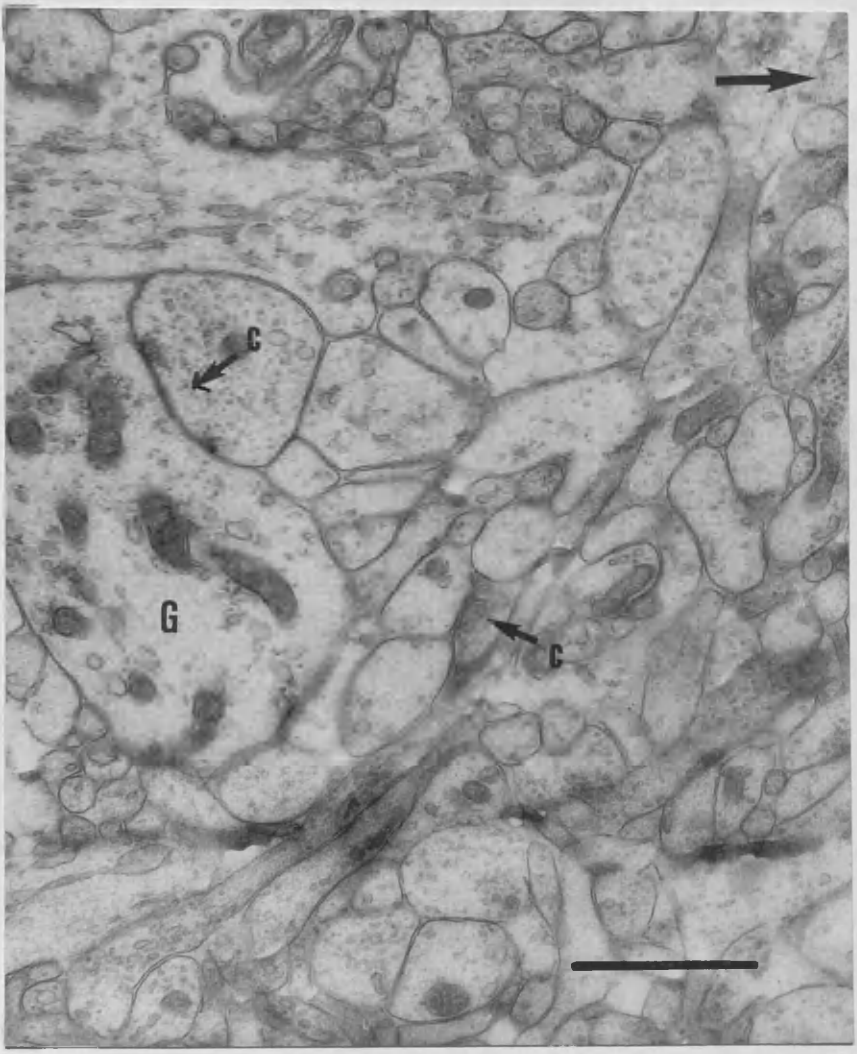

Figure 5

Electron micrograph of IPL of area centralis of newborn kitten, showing examples of 2 definite conventional synapses (c), one of which is located at a ganglion cell dendrite (G). Orientation is indicated by arrow (top right) pointing to INL. Scale bar is 1μm.

3.1.3 Criteria for synapse classification

The profiles of conventional synapses consisted of an accumulation of spherical vesicles located opposite presynaptic and postsynaptic membranes which showed a membrane density (Figs. 4A, 4B, 5 & 6) and may thus be regarded as the counterpart of the Type 1 or E-type synapse of the mammalian brain (Gray, 1959; Uchizono, 1965, respectively). Unequivocal identification of Type 2 synapses or the presence of ellipsoidal vesicles (see Introduction), both of which are indicative of inhibitory transmission, was not made.

Conventional synapses were counted as *definite* when there was no doubt about their classification (Figs. 4A, 4B, 5 & 6). For those where there was an element of doubt, for instance in an oblique section when the pre- and postsynaptic membranes were not clearly revealed, these were classified as *probable* synapses (Fig. 4B). Hence *definite-plus-probable* represents an upper limit to the confidence of the data.

A similar division was used for bipolar cell ribbons, *viz. definite* (Fig. 4A 's') and *probable* (Fig. 4A 'ps'). In addition, the ribbons were also counted as *synaptic* (Figs. 4A and 6) or *floating* (Fig. 4B) and the synapses were counted as *monads* (Fig. 4A lower 'ps') or *dyads* (Fig. 4A upper 's'; Fig 6 's').

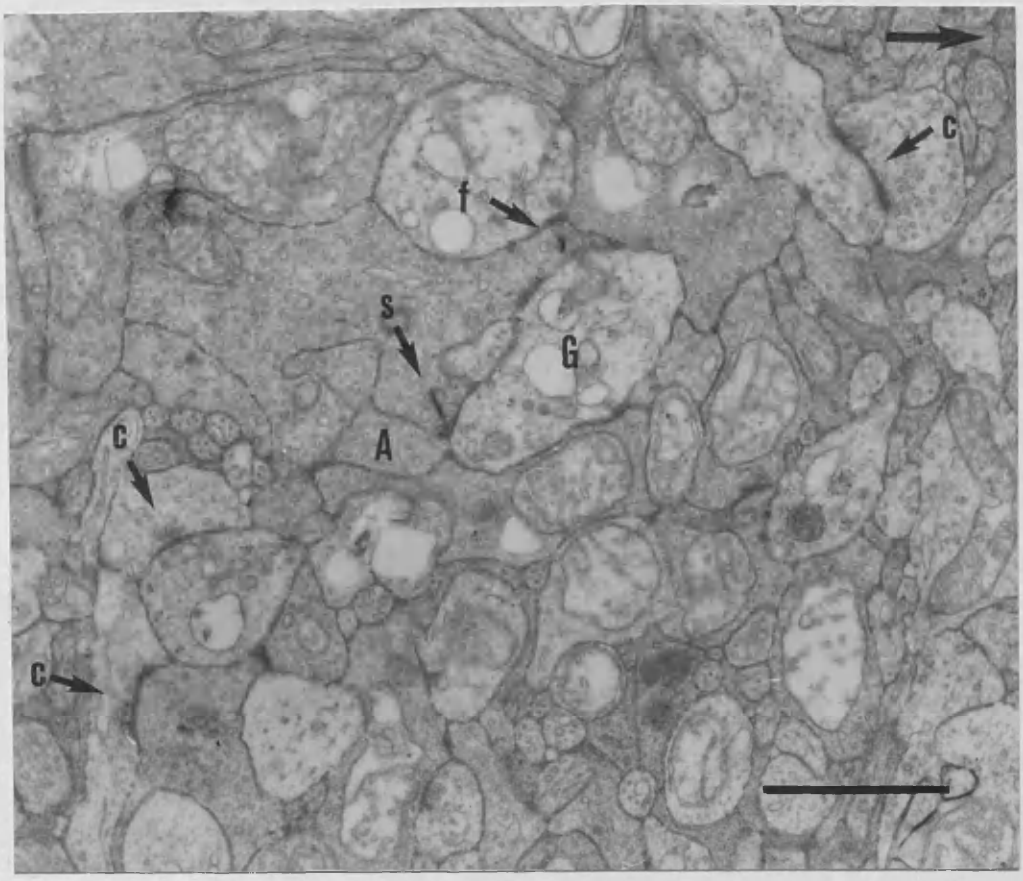

Figure 6

Electron micrograph of IPL of area centralis of adult cat retina, showing a cone bipolar cell terminal containing a definite synaptic ribbon (s), forming a dyad with an amacrine cell neurite (A) and ganglion cell dendrite (G). The bipolar cell terminal also contains a definite floating ribbon (f). Examples of definite conventional synapses (c) are shown. Orientation is indicated by arrow (top right) pointing to INL. Scale bar is 1µm.

3.2 Inner plexiform layer depth

The IPL depth was measured by taking a series of measurements from the montages at intervals equivalent to 10μm with at least 5 depth measurements taken per retina.

The IPL depth had a mean value of 21.7μm in the newborn and 22.7μm in the adult cat. There was no overall change in the IPL depth with linear, logarithmic or square root functions of postnatal age ($-0.16 > r < +0.21$; $P > 0.3$) (Fig. 7; Table 1). However there was an increase in the depth until 18 days, which was significant when plotted with a linear or square root function of age ($r > +0.60$; $P < 0.05$), and of marginal significance with $\log_{10}$age ($r = +0.54$; $0.1 > P > 0.05$). There was a subsequent decrease after 18 days which was significant with linear, logarithmic and square root functions of age ($r > -0.63$; $p < 0.02$).

Since there was a time dependent change in IPL, it was therefore necessary to additionally express the synaptic frequency per μm^2 X depth of the IPL at that age, in order to assess the frequency of synapses in a column across the depth of the IPL.

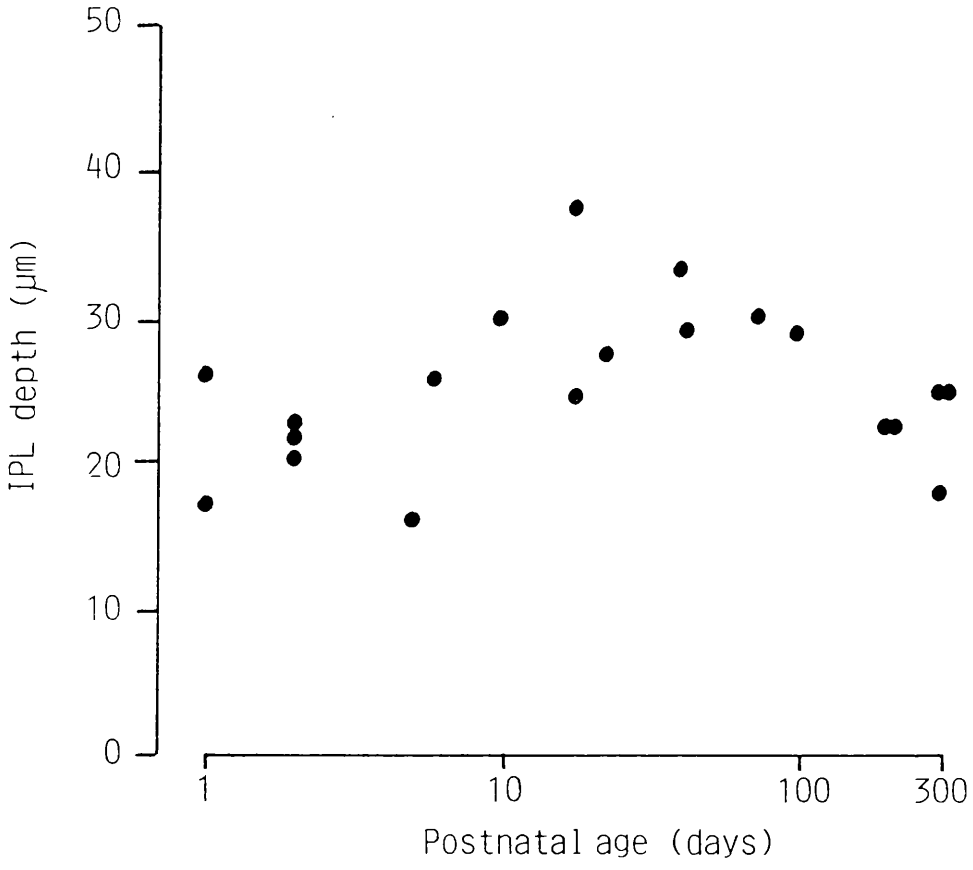

Figure 7
Depth of IPL against increasing age (logarithmic scale).

Table 1. IPL depth with increasing postnatal age.

	Regression equation	S.D. of y	r	P
IPL depth(0-300 days)				
Age(days)	y=26.0 -0.008x	5.6	-0.16	>0.4
Log_{10}Age	y=23.6 +1.34x	5.5	+0.21	>0.3
Sqrt Age	y=25.5 -0.021x	5.6	-0.02	>0.9
IPL depth (0-18 days)				
Age(days)	y=20.1 +0.64x	5.0	+0.62	<0.05
Log_{10}Age	y=19.5 +8.09x	5.3	+0.54	>0.05
Sqrt Age	y=16.8 +3.35x	5.1	+0.60	<0.05
IPL depth (18-300 days)				
Age(days)	y=31.5 -0.032x	3.9	-0.67	<0.02
Log_{10}Age	y=41.3 -7.35x	4.1	-0.63	<0.02
Sqrt Age	y=34.5 -0.70x	4.0	-0.66	<0.02

3.3 Frequency of occurrence of synaptic ribbons

3.3.1 Synaptic ribbon frequency per unit area

Definite synaptic ribbons showed a highly significant increase in frequency with linear, logarithmic and square root functions of age ($r \geq +0.59$; $P<0.01$) Definite-plus-probable synaptic ribbon frequency, which indicates the upper limit to the estimate of synaptic ribbons present, similarly increased significantly with the same functions of age ($r \geq +0.56$; $P<0.01$) (Fig. 8A; Table 2)

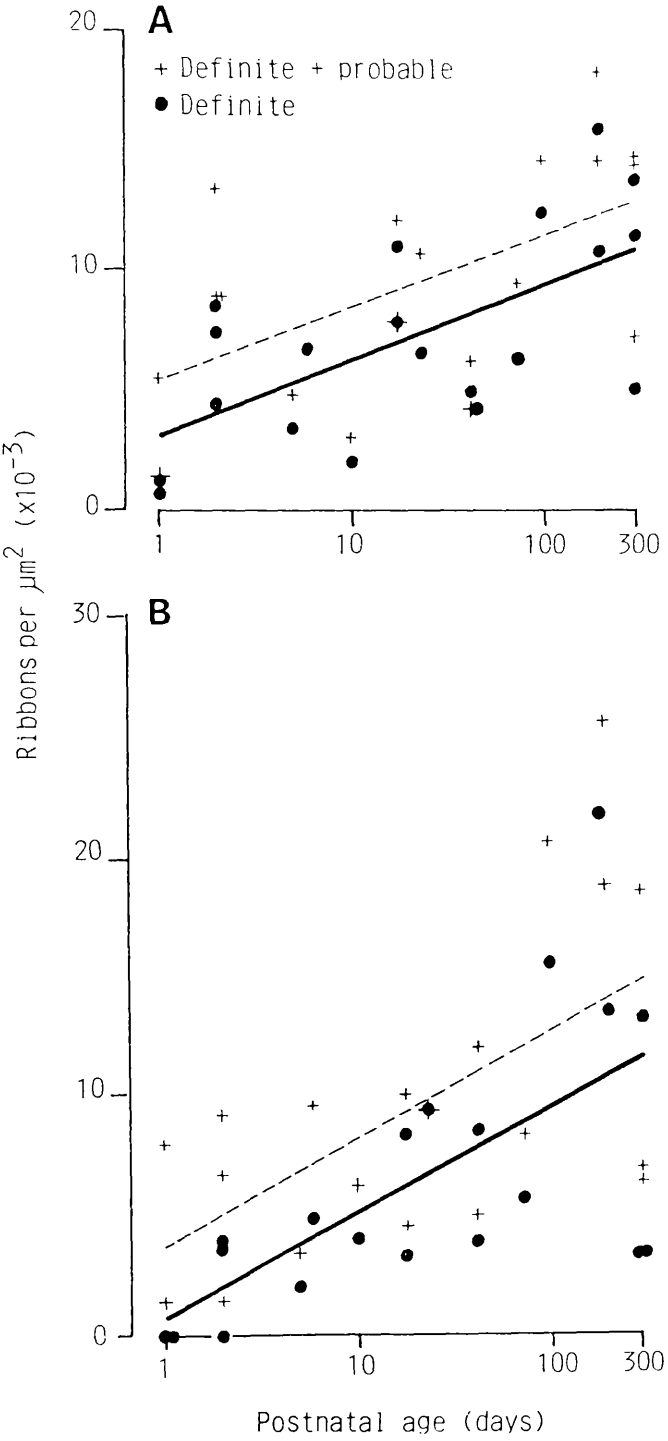

Figure 8

Frequency of synaptic ribbons (A) and floating ribbons (B) with increasing age (logarithmic scale) per μm^2, showing definite ribbons (filled symbols) and definite-plus-probable (crosses).

Table 2 Synaptic ribbon frequency with increasing postnatal age.

A/Definite

	Regression equation	S.D. of y	r	P
Age(days)	y=5.54 +0.023x	3.55	+0.59	<0.01
Log_{10}Age	y=3.13 +3.24x	3.32	+0.66	<0.01
Sqrt Age	y=4.20 +0.46x	3.37	+0.64	<0.01

B/Definite-plus-probable

	Regression equation	S.D. of y	r	P
Age(days)	y=7.64 +0.024x	3.94	+0.56	<0.01
Log_{10}Age	y=5.53 +3.07x	3.91	+0.57	<0.01
Sqrt Age	y=6.34 +0.47x	3.82	+0.60	<0.01

The correlation of synaptic ribbon frequency with log_{10}age and square root of age is higher than with a linear function of age and is, therefore, more appropriate. This indicates an exponential growth of ribbon frequency with levelling out at 100 days, as judged by eye.

3.3.2 Synaptic ribbon frequency per unit area, normalised for IPL depth

Both definite and definite-plus-probable synaptic ribbon frequency per IPL depth showed a significant increase with increasing postnatal age ($r \geq +0.46$; $P<0.05$). In both cases the correlation was again highest with log_{10}age (Fig. 9A; Table 3).

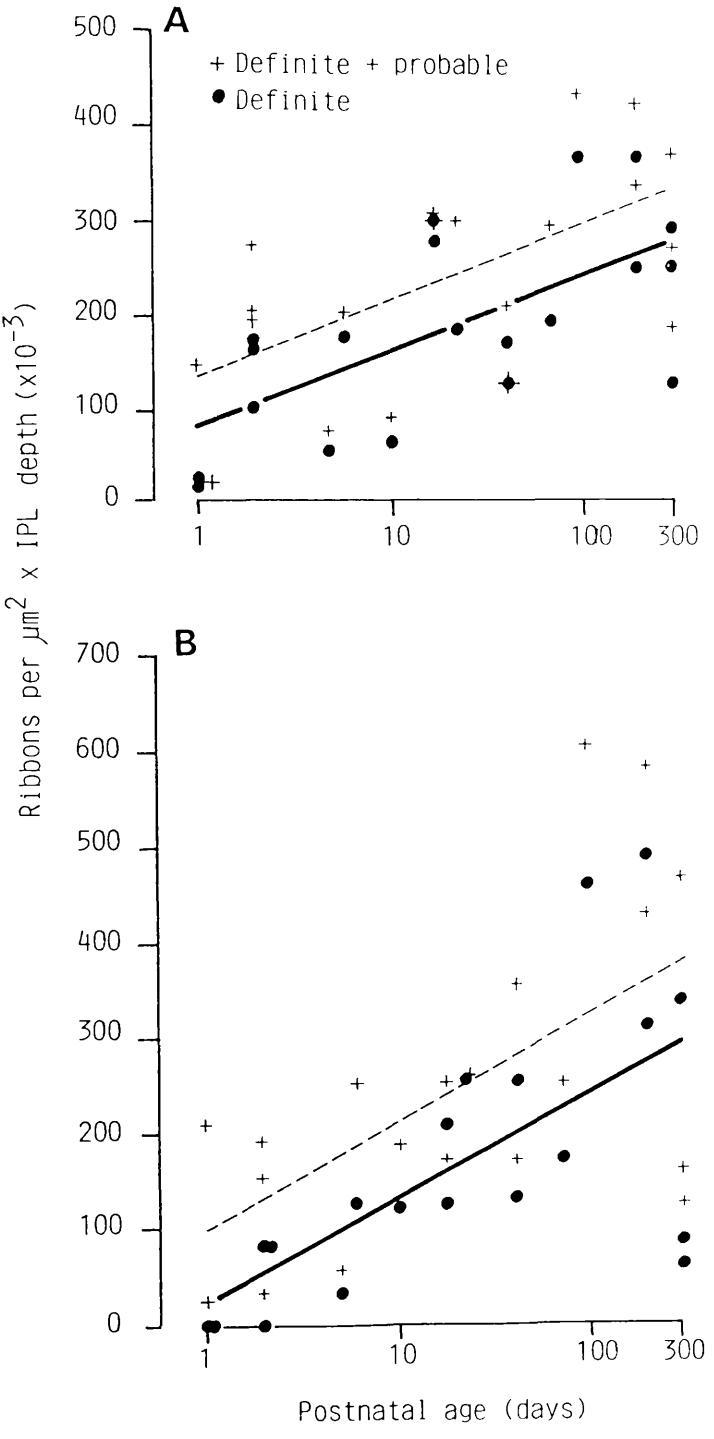

Figure 9

Frequency of synaptic ribbons (A) and floating ribbons (B) with increasing age (logarithmic scale) per μm^2 X depth of IPL, showing definite ribbons (filled symbols) and definite-plus-probable (crosses).

Table 3 Synaptic ribbon frequency per unit area X depth of IPL, with increasing postnatal age.

A/Definite

	Regression equation	S.D. of y	r	P
Age(days)	y=149 +0.44x	95	+0.47	<0.05
Log_{10}Age	y=79.2 +80.8x	79.8	+0.67	<0.01
Sqrt Age	y=116 +10.0x	88	+0.57	<0.01

B/Definite-plus-probable

	Regression equation	S.D. of y	r	P
Age(days)	y=202 +0.46x	101	+0.46	<0.05
Log_{10}Age	y=135 +79.0x	90	+0.62	<0.01
Sqrt Age	y=168 +10.2x	95	+0.55	<0.02

Therefore, there is considerable postnatal synaptogenesis of bipolar cell synaptic ribbons. The more appropriate fit of a logarithmic relationship indicates that synaptogenesis occured at a higher rate in younger retinae than in older retinae.

3.4 Frequency of occurrence of floating ribbons

3.4.1 Floating ribbon frequency per unit area

Definite floating ribbons and definite-plus-probable floating ribbons both showed a significant increase in frequency with linear, logarithmic and square root functions of age ($r \geq +0.46$; $P < 0.05$) (Fig. 8B; Table 4). The correlations with $\log_{10}$age and with square root of age are again the most significant relationships.

Table 4 Floating ribbon frequency with increasing postnatal age.

A/Definite

	Regression equation	S.D. of y	r	P
Age(days)	y=4.61 +0.024x	5.34	+0.46	<0.05
$\log_{10}$Age	y=0.74 +4.42x	4.52	+0.66	<0.01
Sqrt Age	y=2.70 +0.56x	4.92	+0.57	<0.01

B/Definite-plus-probable

	Regression equation	S.D. of y	r	P
Age(days)	y=7.37 +0.029x	5.92	+0.49	<0.05
$\log_{10}$Age	y=3.73 +4.55x	5.42	+0.60	<0.01
Sqrt Age	y=5.35 +0.63x	5.55	+0.57	<0.01

3.4.2 Floating ribbon frequency per unit area, normalised for IPL depth

There was a significant increase in frequency of definite and definite-plus-probable floating ribbons when normalised for IPL depth with logarithmic and square root functions of age ($r \geq +0.53$; $P<0.02$), although there was no significant change in frequency of either definite or definite-plus-probable floating ribbons with age ($r=+0.39$; $r=+0.41$ respectively; $P>0.1$) (Fig. 9B; Table 5). No floating ribbons were observed at 0 days.

Table 5 Floating ribbon frequency per unit area X depth of IPL, with increasing postnatal age.

A/Definite

	Regression equation	S.D. of y	r	P
Age(days)	y=128 +0.52x	138	+0.39	>0.1
Log_{10}Age	y=23.6 +111x	113	+0.66	<0.01
Sqrt Age	y=79.6 +13.0x	127	+0.53	<0.02

B/Definite-plus-probable

	Regression equation	S.D. of y	r	P
Age(days)	y=199 +0.61x	156	+0.41	>0.1
Log_{10}Age	y=95.8 +116x	136	+0.60	<0.01
Sqrt Age	y=147 +14.6x	145	+0.53	<0.02

3.5 Frequency of occurrence of total ribbons

3.5.1 Total ribbon frequency per unit area

When taken together, the total synaptic-plus-floating definite ribbons showed a highly significant increase with all functions of age ($r \geq +0.57$; $P < 0.01$). The total definite-plus-probable ribbons also increased significantly ($r \geq +0.58$; $P < 0.01$) (Fig 10; Table 6). Total definite ribbons were particularly significant when plotted against $\log_{10}$age ($r = +0.73$; $P < 0.001$).

Table 6 Total ribbon frequency with increasing postnatal age.

A/Definite

	Regression equation	S.D. of y	r	P
Age(days)	y=10.2 +0.047x	7.7	+0.57	<0.01
$\log_{10}$Age	y=3.89 +7.65x	6.35	+0.73	<0.001
Sqrt Age	y=6.92 +1.02x	6.92	+0.67	<0.01

B/Definite-plus-probable

	Regression equation	S.D. of y	r	P
Age(days)	y=15.0 +0.052x	8.4	+0.58	<0.01
$\log_{10}$Age	y=9.26 +7.62x	7.79	+0.66	<0.01
Sqrt Age	y=11.7 +1.10x	7.8	+0.65	<0.01

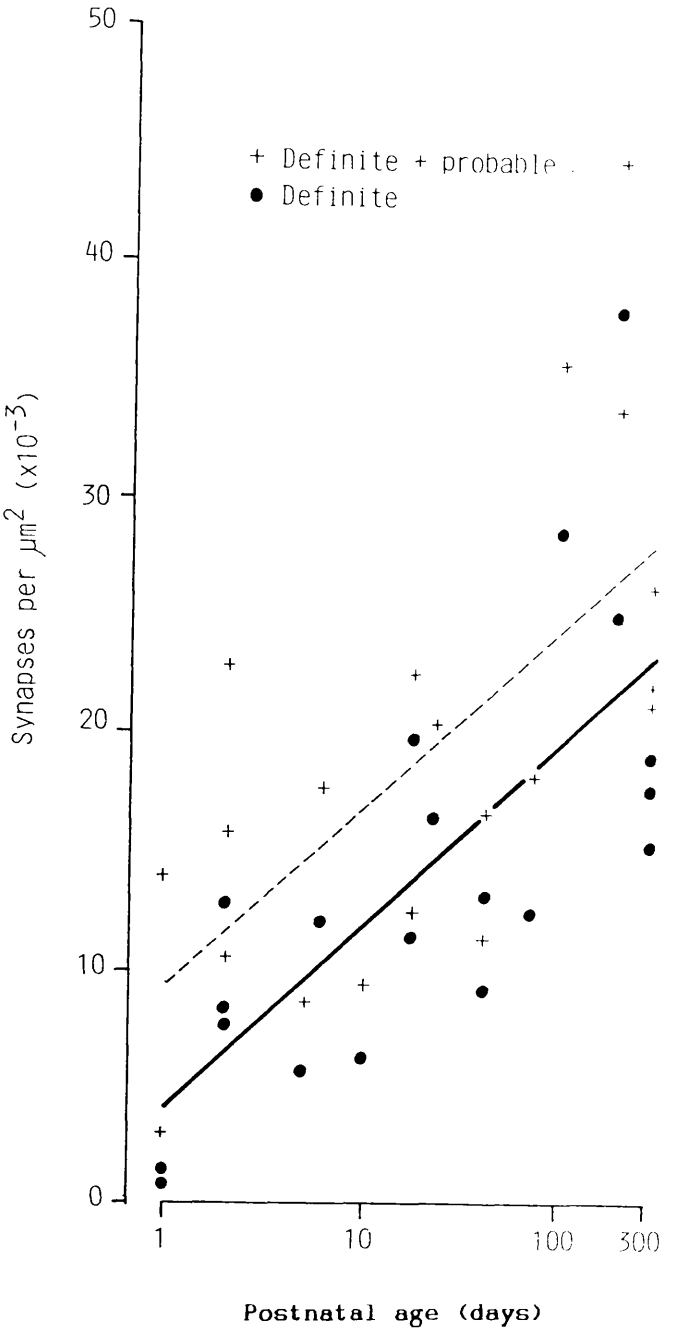

Figure 10

Frequency of total (synaptic-plus-floating) ribbons against increasing age (logarithmic scale) per μm^2, showing definite ribbons (filled symbols) and definite-plus-probable (crosses).

3.5.2 Total ribbon frequency per unit area normalised for IPL depth

After normalising for IPL width, there was again a significant increase in definite and definite-plus-probable total ribbon frequency with increasing postnatal age ($r \geq +0.47$; $P<0.05$). This relationship was most significant with $\log_{10}$age ($r=+0.73$; $P<0.001$). This indicates that the rate of synaptogenesis was high in younger retinae and levelled off in older retinae, particularly at 100 days as judged by eye (Fig. 11; Table 7).

Table 7 Total ribbon frequency per unit area X depth of IPL, with increasing postnatal age.

A/Definite

	Regression equation	S.D. of y	r	P
Age(days)	y=278 +0.96x	206	+0.47	<0.05
$\log_{10}$Age	y=103 +192x	159	+0.73	<0.001
Sqrt Age	y=196 +23.0x	186	+0.61	<0.01

B/Definite-plus-probable

	Regression equation	S.D. of y	r	P
Age(days)	y=400 +1.07x	226	+0.48	<0.05
$\log_{10}$Age	y=231 +195x	189	+0.68	<0.01
Sqrt Age	y=315 +24.9x	206	+0.60	<0.01

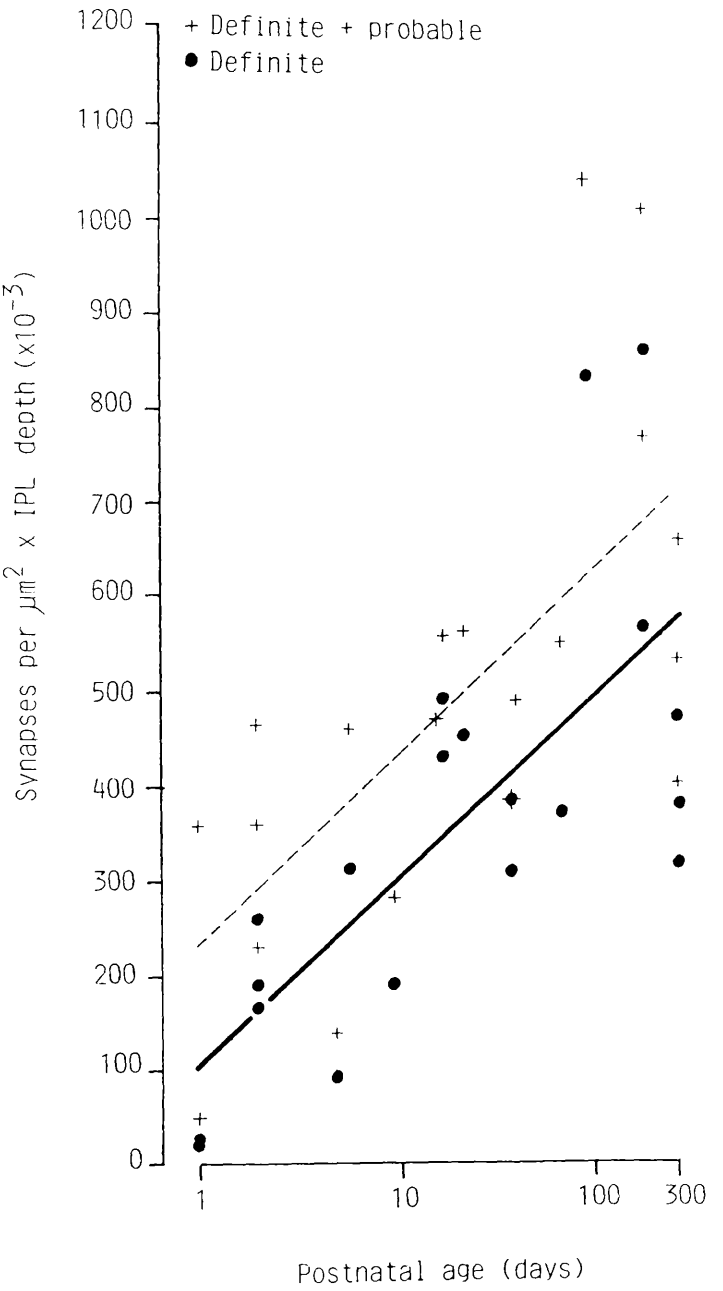

Figure 11

Frequency of total (synaptic-plus-floating) ribbons against increasing age (logarithmic scale) per μm^2 X depth of IPL, showing definite ribbons (filled symbols) and definite-plus-probable (crosses).

3.6 Monads and dyads

3.6.1 Monad and dyad frequency per unit area

In the cat retina, ribbon synapses first pass through a monad stage involving a single post-synaptic process before the mature dyad is formed (Morrison, 1982). Therefore, the profiles of definite ribbon synapses were subdivided into monads and dyads.

There was no increase in monad frequency postnatally (range of $r=-0.032$ to $+0.063$; $P>0.25$) (Fig 12A; Table 8). However, the increase in dyad frequency with increasing postnatal age was highly significant with linear, logarithmic and square root functions of age ($r\geq+0.68$; $P<0.002$) (Fig. 12C; Table 9).

Table 8 Monad frequency with increasing postnatal age.

	Regression equation	S.D. of y	r	P
Age(days)	y=1.69 -0.0005x	1.63	-0.032	>0.25
Log_{10}Age	y=1.50 +0.115x	1.63	+0.063	>0.25
Sqrt Age	y=1.62 +0.0052x	1.63	+0.020	>0.25

Table 9 Dyad frequency with increasing postnatal age.

	Regression equation	S.D. of y	r	P
Age(days)	y=3.57 +0.025x	3.14	+0.68	<0.002
Log_{10}Age	y=0.65 +3.79x	2.63	+0.79	<0.001
Sqrt Age	y=2.07 +0.52x	2.76	+0.76	<0.001

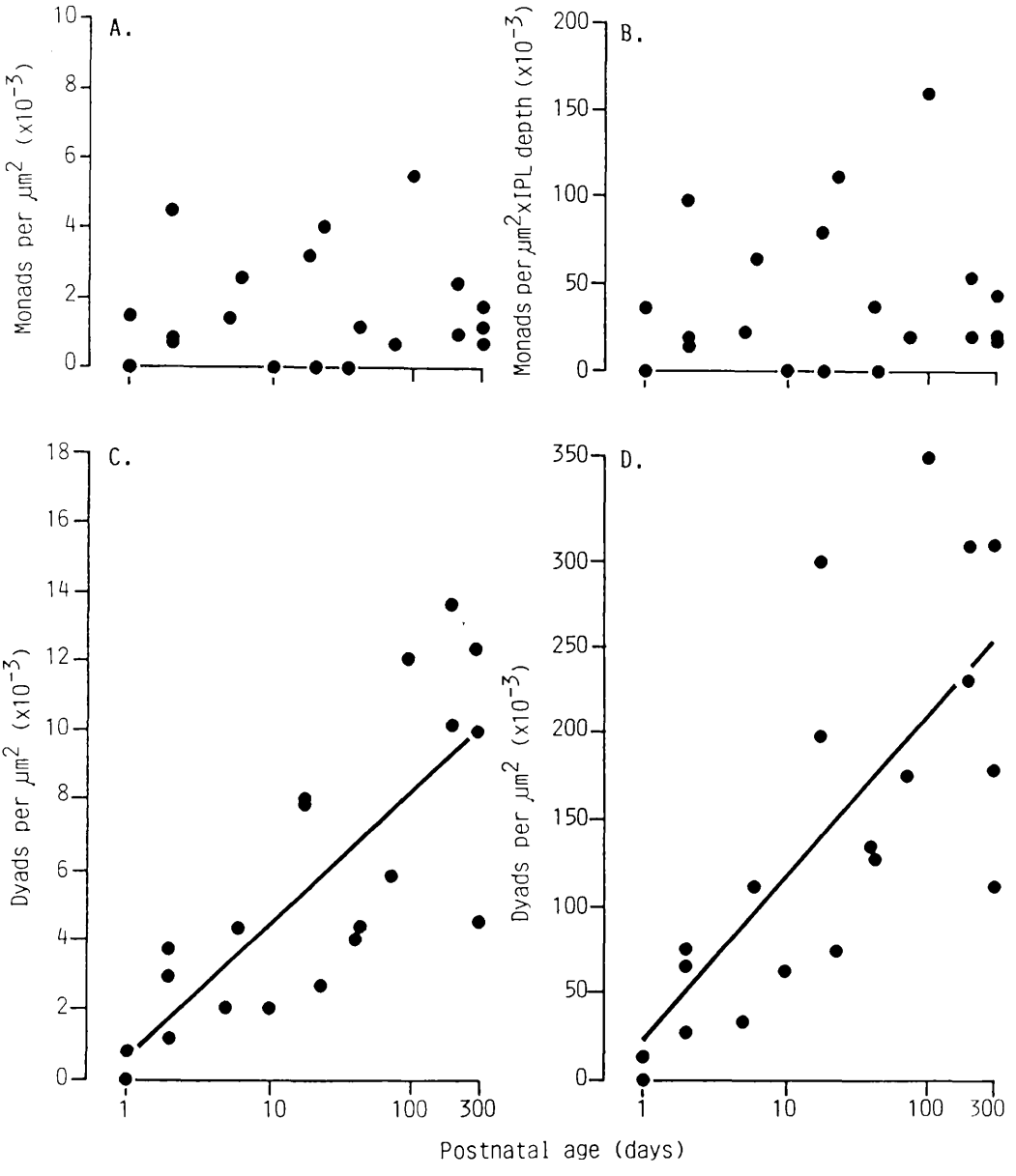

Figure 12

Frequency of monads (A and B) and dyads (C and D) against increasing age (logarithmic scale) per µm² and per µm² X depth of IPL, respectively.

3.6.2 Monad and dyad frequency per unit area normalised for IPL width

When normalised for IPL depth, there was again no change in monad frequency with age (range of r=-0.041 to +0.098; P>0.6) (Fig. 12B; Table 10). Dyad frequency normalised for IPL depth showed a significant increase with linear, logarithmic and square root functions of age (r≥+0.53; P<0.02) (Fig. 12D; Table 11).

Table 10 Monad frequency per unit area, X depth of IPL, with increasing postnatal age.

	Regression equation	S.D. of y	r	P
Age(days)	y=42.8 -0.016x	44.0	-0.041	>0.8
Log_{10}Age	y=35.0 +4.9x	43.9	+0.098	>0.6
Sqrt Age	y=40.0 +0.21x	44.1	+0.030	>0.8

Table 11 Dyad frequency per unit area, X depth of IPL, with increasing postnatal age.

	Regression equation	S.D. of y	r	P
Age(days)	y=103 +0.52x	95	+0.53	<0.02
Log_{10}Age	y=22.8 +92.9x	75.2	+0.74	<0.001
Sqrt Age	y=65.2 +11.7x	84.6	+0.65	<0.01

3.7 Frequency of occurrence of conventional synapses

3.7.1 Conventional synapse frequency per unit area

There was no significant change in the frequency of definite conventional synapses with linear, logarithmic or square root functions of age (range of r=-0.091 to +0.056; P>0.7) (Fig. 13A; Table 12). There was also no change in frequency of definite-plus-probable conventional synapses with age (range of r=-0.040 to +0.11; P>0.6). The high variance values reflect the large scatter of frequency values.

Table 12 Conventional synapse frequency with increasing postnatal age.

A/Definite

	Regression equation	S.D. of y	r	P
Age(days)	y=74.3 +0.014x	28.4	+0.056	>0.8
Log_{10}Age	y=79.3 -2.92x	28.3	-0.091	>0.7
Sqrt Age	y=75.9 -0.061x	28.4	-0.013	>0.9

B/Definite-plus-probable

	Regression equation	S.D. of y	r	P
Age(days)	y=98.2 +0.027x	28.6	+0.11	>0.6
Log_{10}Age	y=102 -1.3x	28.7	-0.040	>0.8
Sqrt Age	y=98.8 +0.23x	28.7	+0.050	>0.8

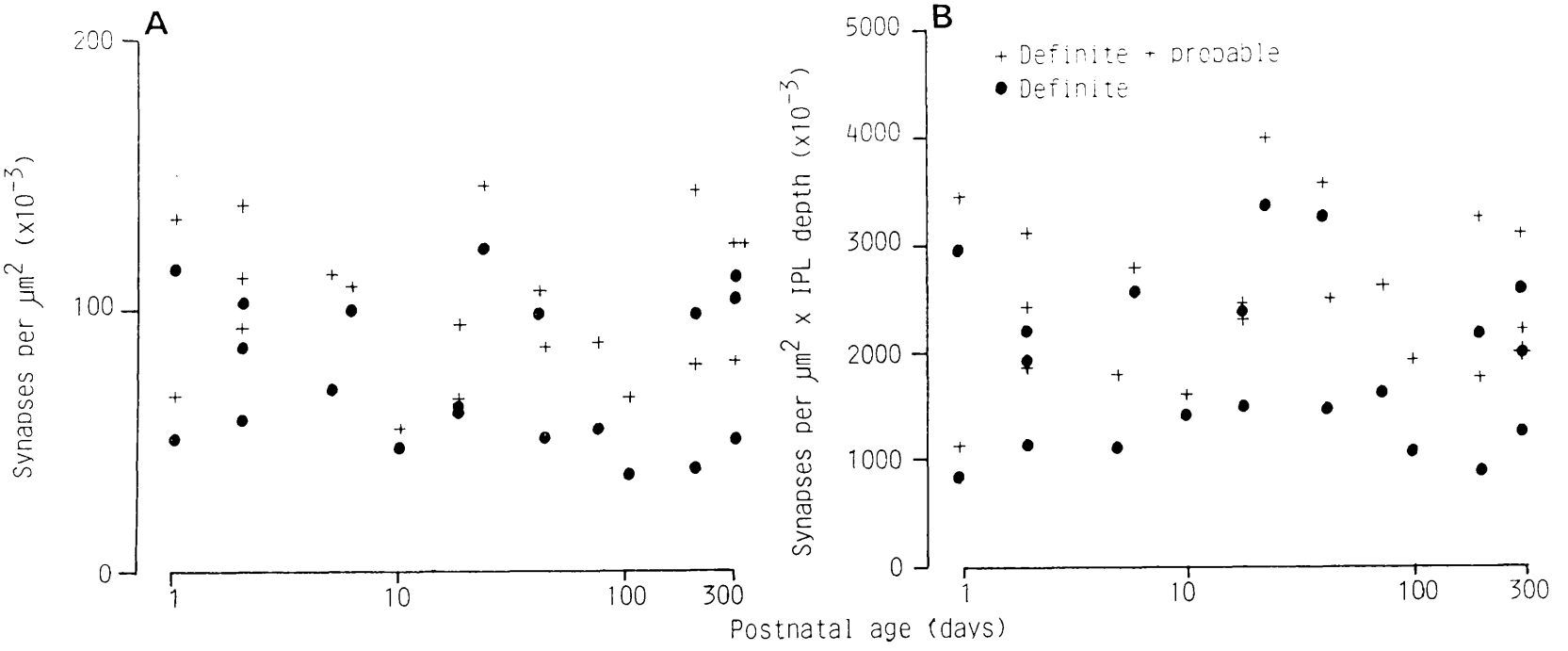

Figure 13

Frequency of conventional synapses with increasing age (logarithmic scale) showing definite synapses (filled symbols) and definite-plus-probable synapses (crosses) per μm^2 (A) and μm^2 X depth of IPL (B).

3.7.2 Conventional synapse frequency per unit area normalised for IPL depth

Similarly, when normalised for IPL depth, there was no significant change in definite conventional synapse frequency with linear, logarithmic and square root functions of age ($r < -0.077$; $P > 0.7$). There was also no significant change in definite-plus-probable conventional synapse frequency with increasing postnatal age (range of $r = -0.028$ to $+0.077$; $P > 0.7$) (Fig. 13B; Table 13).

Table 13 Conventional synapse frequency per unit area, X depth of IPL, with increasing postnatal age.

A/Definite

	Regression equation	S.D. of y	r	P
Age(days)	y=1942 -0.5x	794	-0.077	>0.7
Log_{10}Age	y=1925 -20.6x	797	-0.023	>0.9
Sqrt Age	y=1962 -9.1x	795	-0.070	>0.7

B/Definite-plus-probable

	Regression equation	S.D. of y	r	P
Age(days)	y=2514 -0.2x	761	-0.028	>0.9
Log_{10}Age	y=2412 +65.7x	759	+0.077	>0.7
Sqrt Age	y=2489 +1.5x	761	+0.012	>0.9

3.7.3 Serial conventional synapse frequency

When an amacrine synapse was observed to form a conventional synapse onto another amacrine cell which in turn formed a conventional synapse onto a third process, this was taken to constitute a serial conventional synapse. Such an array was counted as one serial synapse.

Serial synapses were first observed, in low numbers, in the newborn kitten retina. There was no subsequent change in frequency of serial synapses with linear, logarithmic and square root functions of age ($r < -0.10$; $P > 0.25$) (Fig. 14A; Table 14). Similarly, when normalised for IPL depth, there was again no change in serial synapse frequency with age ($r < -0.15$; $P > 0.5$) (Fig. 14B; Table 15).

Table 14 Serial conventional synapse frequency with increasing postnatal age.

	Regression equation	S.D. of y	r	P
Age(days)	y=2.14 -0.0015x	1.90	-0.090	>0.25
Log_{10}Age	y=2.21 -0.145x	1.90	-0.090	>0.25
Sqrt Age	y=2.23 -0.031x	1.90	-0.10	>0.25

Table 15 Serial conventional synapse frequency per unit area, X depth of IPL, with increasing postnatal age.

	Regression equation	S.D. of y	r	P
Age(days)	y=56.1 -0.064x	49.6	-0.15	>0.5
Log_{10}Age	y=51.1 -0.2x	50.2	-0.004	>0.9
Sqrt Age	y=56.7 -0.86x	49.9	-0.11	>0.6

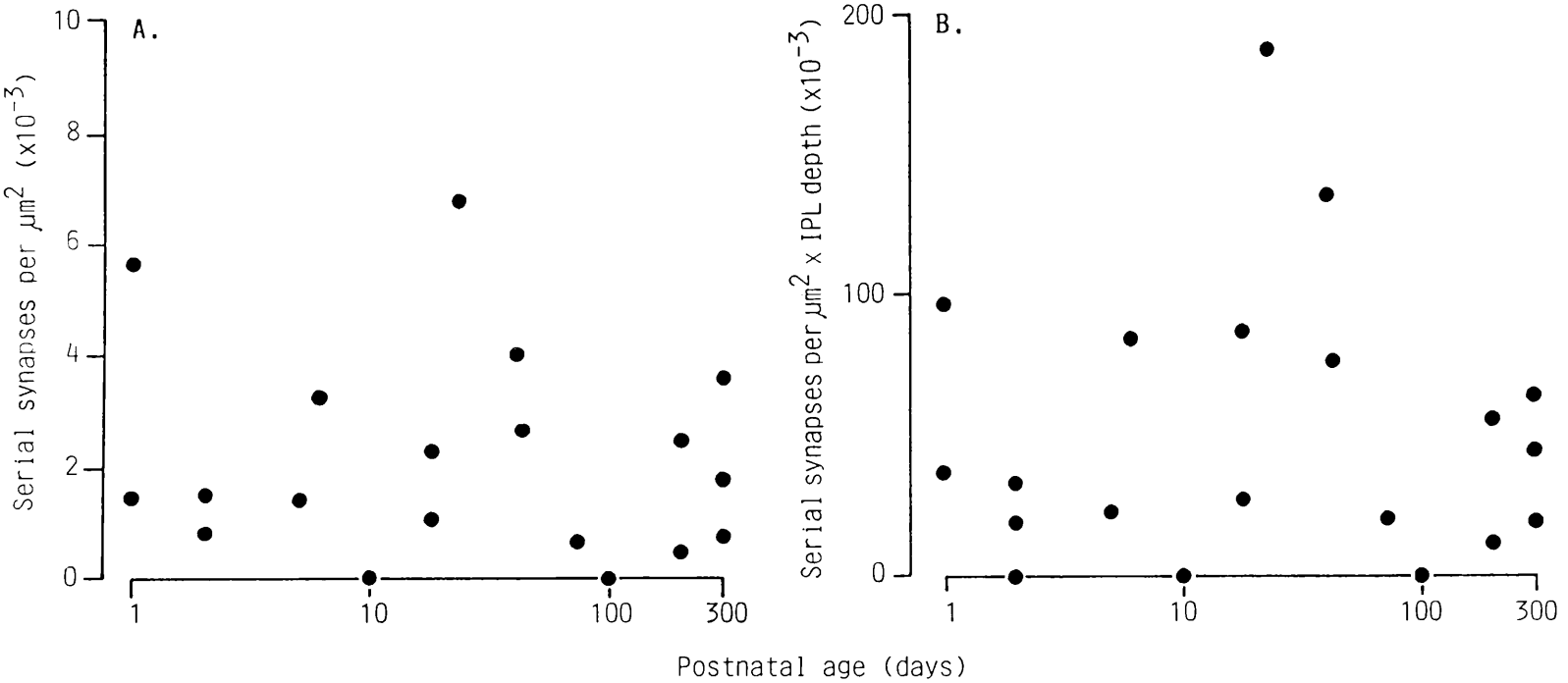

Figure 14

Frequency of definite serial synapses with increasing age (logarithmic scale) per µm² (A) and per µm² X depth of IPL (B).

The lack of significant change with age persisted even when the two outermost points in the newborn and 23 day old kitten were excluded ($r<+0.17$; $P>0.6$) (Tables 16 and 17).

Table 16 Serial conventional synapse frequency (two outlying points removed) with increasing postnatal age.

	Regression equation	S.D. of y	r	P
Age(days)	y=1.44 +0.0013x	1.26	+0.12	>0.6
Log_{10}Age	y=1.21 +0.25x	1.25	+0.17	>0.4
Sqrt Age	y=1.36 +0.026x	1.26	+0.13	>0.6

Table 17 Serial conventional synapse frequency (two outlying points removed) X depth of IPL, with increasing postnatal age.

	Regression equation	S.D. of y	r	P
Age(days)	y=41.4 -0.008x	37.7	-0.025	>0.9
Log_{10}Age	y=33.5 +5.2x	37.4	+0.12	>0.6
Sqrt Age	y=39.7 +0.13x	37.7	+0.022	>0.9

While most serial synapses consisted of two conventional synapses in series, in four cases, a series of three conventional synapses was observed at 0 days, 23 days, 41 days and in the adult cat, thus failing to show any relationship to age.

3.7.4 Reciprocal synapses

The first reciprocal synapse was observed at 5 days postnatal. Therefore, potentially there is feedback from amacrine cells to bipolar cells at least as early as this. Only 4 other reciprocal synapses were observed: in 200 day and adult retinae. The very low numbers of reciprocal synapses, thus, make it impossible to draw any firm conclusion.

3.8 Ribbon/conventional synapses ratio

Since bipolar ribbon synapses appear to be mainly excitatory and conventional synapses appear to be mainly inhibitory (see Introduction), the ratio of definite bipolar ribbons/definite conventional synapses gives an indication of the ratio of excitatory/inhibitory synapses in the IPL. It is also a useful way of standardising the data as the ratio takes into account the scatter of data points present for conventional synapses and eliminates the need for standardising for IPL depth.

The ratios of synaptic ribbons/conventional synapses, floating ribbons/conventional synapses and total ribbons/conventional synapses showed a significant increase with logarithmic and square root functions of age ($r \geq +0.48$; $P<0.05$) although the increase with age was only of marginal significance ($r=+0.38$; $0.1>P>0.05$) (Figs 15 and 16; Table 18). Therefore, this indicates an increase in the amount of excitatory inputs compared to inhibitory inputs in the IPL during postnatal development.

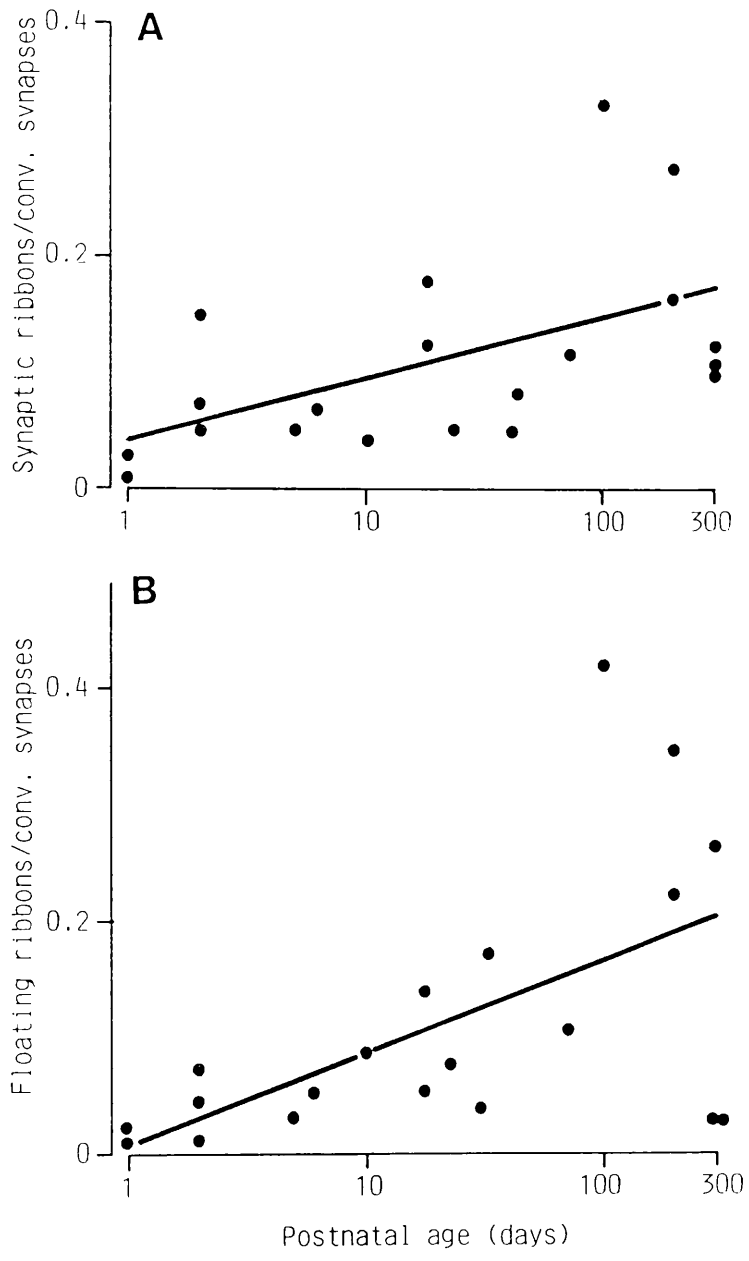

Figure 15

Ratio of definite synaptic ribbons (A) and definite floating ribbons (B) to definite conventional synapses against increasing age (logarithmic scale).

Table 18 Ratio of definite bipolar cell ribbons/ definite conventional synapses with increasing postnatal age.

A/ Synaptic ribbons/conventional synapses

	Regression equation	S.D. of y	r	P
Age(days)	y=0.088 +0.0003x	0.078	+0.38	>0.05
Log_{10}Age	y=0.043 +0.052x	0.071	+0.55	<0.02
Sqrt Age	y=0.065 +0.0067x	0.074	+0.48	<0.05

B/ Floating ribbons/conventional synapses

	Regression equation	S.D. of y	r	P
Age(days)	y=0.079 +0.0004x	0.11	+0.39	>0.05
Log_{10}Age	y=0.0092 +0.079x	0.10	+0.57	<0.01
Sqrt Age	y=0.044 +0.010x	0.11	+0.50	<0.05

C/ Total ribbons/conventional synapses

	Regression equation	S.D. of y	r	P
Age(days)	y=0.164 +0.0007x	0.18	+0.41	>0.05
Log10Age	y=0.046 +0.13x	0.16	+0.60	<0.01
Sqrt Age	y=0.105 +0.017x	0.17	+0.52	<0.02

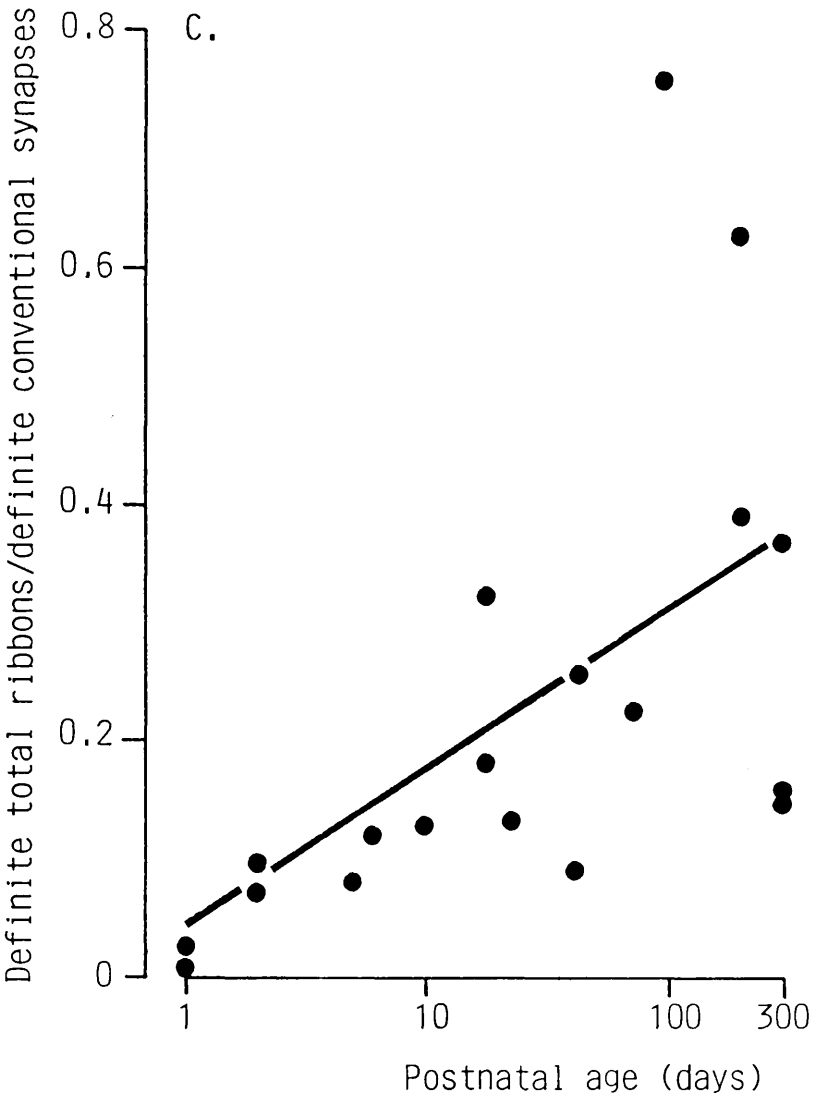

Figure 16

Ratio of definite total ribbons to definite conventional synapses against increasing age (logarithmic scale).

3.9 Bipolar ribbon profile size

3.9.1 Comparison of neonatal and adult bipolar cell ribbon length

Bipolar cell ribbon length was measured to determine whether there was a change in ribbon size with postnatal development. If so, this would have implications for the frequency of synaptic profiles which would then require correction to take account of the fact that larger ribbons would have a greater probability of occurrence in profile.

Synaptic ribbon length ranged from 0.06-0.55μm, with an approximately Gaussian distribution of profile sizes in the newborn and adult retinae (Fig. 17A & B). There was no significant change in synaptic ribbon length between seven retinae aged 0-6 days and three adult retinae, which had been combined to give an adequate sample size ($P>0.45$, t-test) (Table 19).

Table 19 Comparison of mean synaptic ribbon length between seven neonatal and three adult retinae

	Mean length	SD	N
0-6 days	0.143μm	0.050	58
Adult	0.151μm	0.054	44

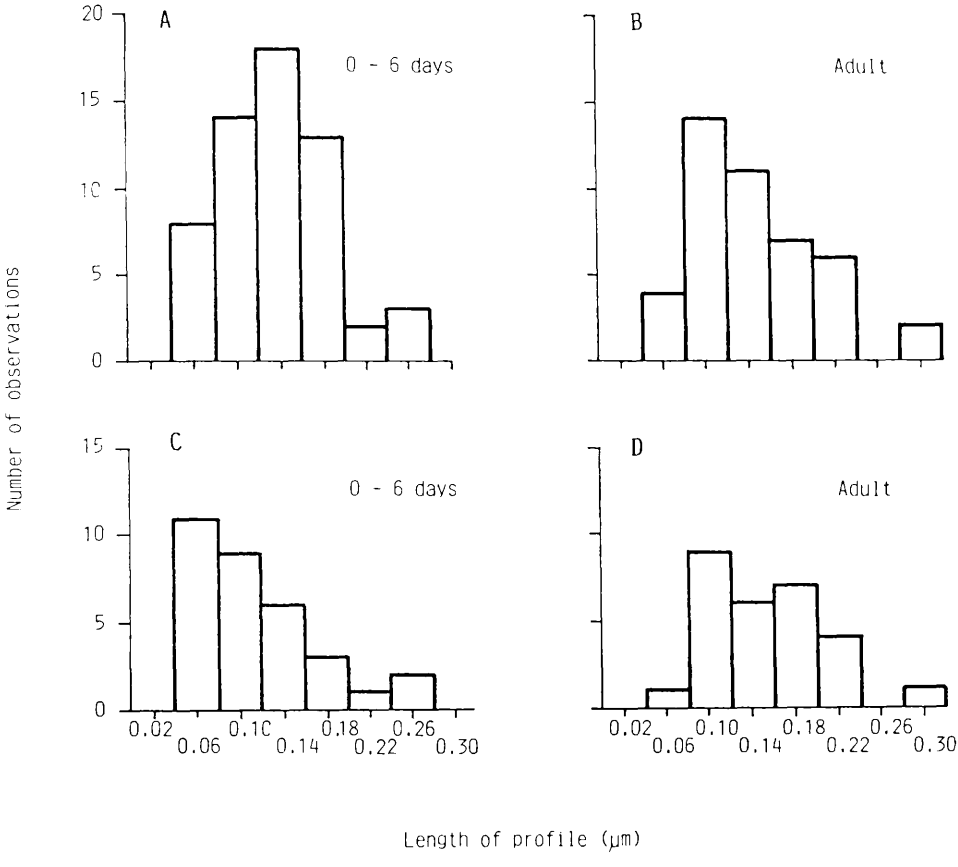

Figure 17

Distributions of lengths of profiles. A. definite synaptic ribbons for 7 retinae ages 0-6 days (n=58); B. definite synaptic ribbons for 3 adult retinae (n=44); C. definite floating ribbons for 7 retinae ages 0-6 days (n=34); D. definite floating ribbons for 3 adult retinae (n=28).

The profile length of floating ribbons ranged from 0.06-0.48μm. Since the distribution of profile lengths appeared by eye and by normality plots to be non-Gaussian (Fig. 17C & D), the Mann-Whitney test was applied. In a comparison of seven retinae aged 0-6 days and three adult retinae, floating ribbons increased significantly in length by 17% (P=0.022, Mann-Whitney test) (Table 20).

Table 20 Comparison of mean floating ribbon length between seven neonatal and three adult retinae

	Mean length	SD	N
0-6 days	0.134μm	0.0834	7
Adult	0.157μm	0.0528	3

This analysis was then extended to analyse the length of ribbons during postnatal development.

3.9.2 Bipolar cell ribbon length with increasing postnatal age

There was no significant change in the mean length of synaptic ribbons when regressed against linear, logarithmic or square root functions of age ($r<-0.17$; $P>0.5$) (Fig. 18A; Table 21).

Table 21 Synaptic ribbon length with increasing postnatal age

	Regression equation	S.D. of y	r	P
Age (days)	y=0.177-0.00008x	0.042	-0.17	>0.5
Log_{10}Age	y=0.176 -0.0027x	0.043	-0.05	>0.8
Sqrt Age	y=0.179 -0.0011x	0.042	-0.14	>0.6

There was found to be no significant change in the length of the floating ribbons when regressed against linear, logarithmic or square root functions of age ($r<+0.47$; $p>0.1$) (Fig. 18B; Table 22).

Table 22 Floating ribbon length with increasing postnatal age

	Regression equation	S.D. of y	r	P
Age (days)	y=0.143 +0.00008x	0.029	+0.27	>0.3
Log_{10}Age	y=0.122 +0.0194x	0.032	+0.47	>0.1
Sqrt Age	y=0.136 +0.002x	0.028	+0.35	>0.2

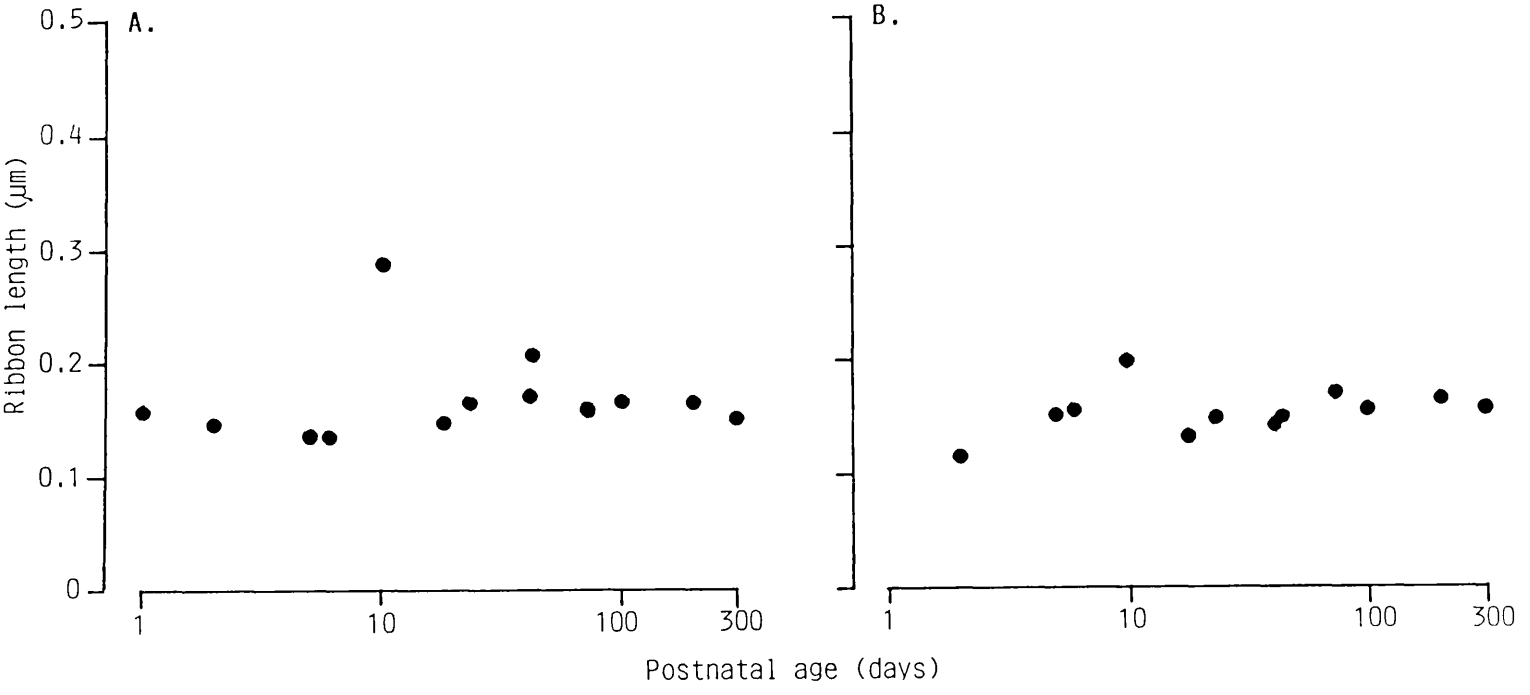

Figure 18

Mean bipolar cell ribbon length with increasing postnatal age. A. definite synaptic ribbons; B. definite floating ribbons.

The apparent increase in floating ribbon length from neonatal to adult retina was not supported by linear regression of the data from all retinae studied. Therefore, it was considered unnecessary to apply a correction factor for ribbon length to the ribbon frequency results.

3.10 Conventional synapse morphology

Conventional synapse profile length was measured as the extent of the synaptic density or, in the absence of a synaptic density, as the extent of the cluster of synaptic vesicles. The frequency distribution of conventional synapse profile size was compared between 2 newborn and 3 adult retinae with the Mann-Whitney test since they were non-Gaussian. The mean conventional synapse frequency was equal in newborn and adult retinae (Fig. 19; Table 24) as indicated by equal mean values.

Table 23 Comparison of mean conventional synapse profile length between two newborn and three adult retinae.

	Mean length	SD	N
Newborn	0.254µm	0.124	211
Adult	0.254µm	0.114	392

There was no significant difference between neonatal (newborn and 2 day old) and adult retinae in the number of synaptic vesicles at definite conventional synapses ($P>0.55$, Mann-Whitney test) (Fig. 20). The majority of both neonatal and mature synapses had 5 or more synaptic vesicles.

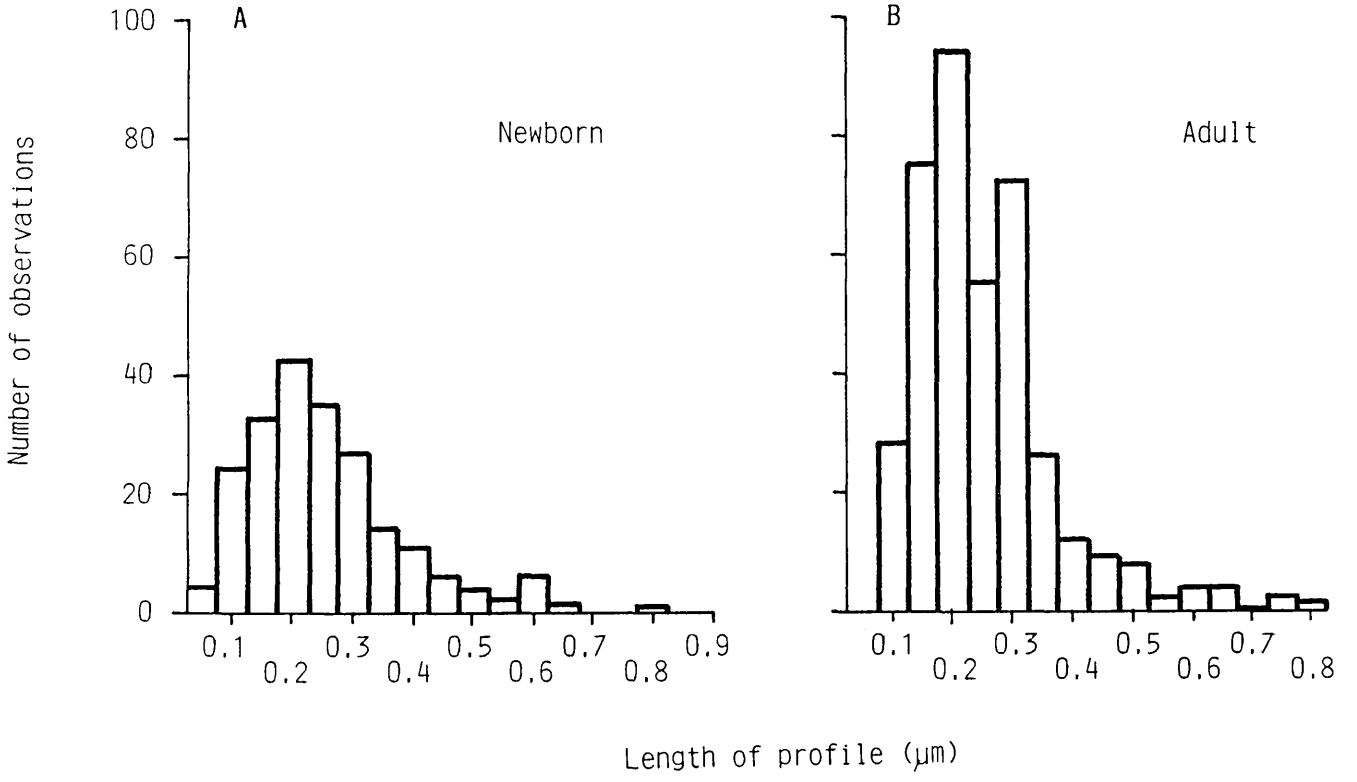

Figure 19

Distributions of lengths of profiles. A. definite conventional synapses for 2 newborn retinae (n=211); B. definite conventional synapses for 3 adult retinae (n=392).

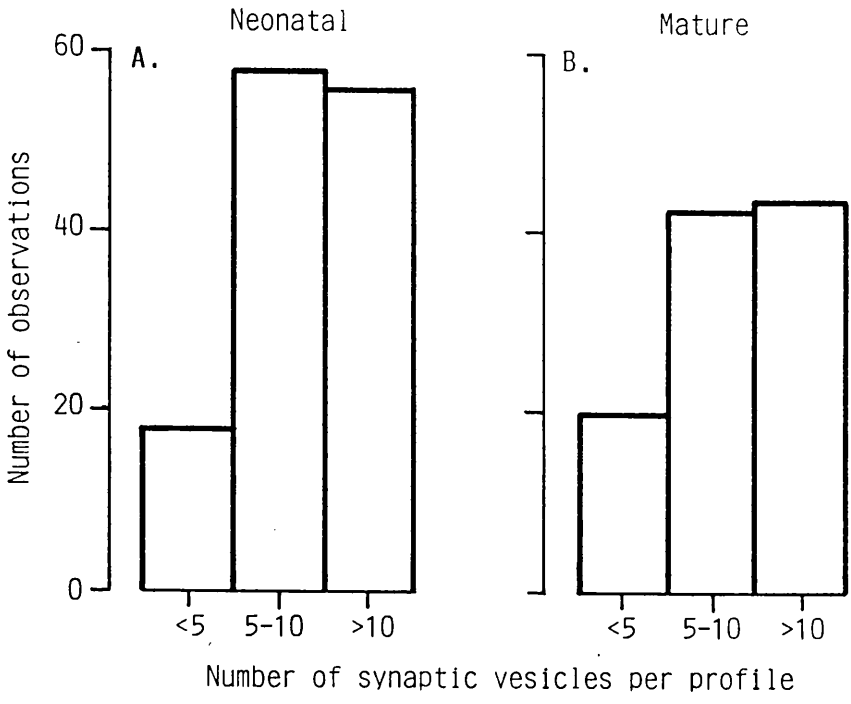

Figure 20

Distributions of the number of synaptic vesicle per conventional synapse. A. for 2 neonatal retinae ages 0-2 days (n=132); B. for 2 adult retinae (n=97).

Thus, conventional synapses had a mature morphology even in the newborn retina.

3.11 Orientation of synaptic profiles

The orientation of conventional synapses and bipolar ribbons was measured, with 0 degree taken parallel to the GCL/IPL border. The distributions of the orientation of neonatal (newborn and 2 day old) and mature (200 day and adult) conventional synapses were both random ($P>0.99$; $P>0.1$ respectively, χ^2-test). There was no significant difference between two neonatal and two mature retinae by the Mann-Whitney test ($P=0.81$) (Fig. 21A and B).

Similarly the distribution of orientations of bipolar cell ribbons for both neonatal (0-6 days) and mature retinae (200 day and adult) was also not different from random distribution ($P>0.99$), χ^2 test) (Fig. 21C and D). There was also no significant difference between the distributions of bipolar cell ribbons between seven neonatal and two mature retinae ($P=0.51$, Mann-Whitney test).

Therefore, no systematic change in orientation of the bipolar cell ribbons or conventional synapses had occurred with age.

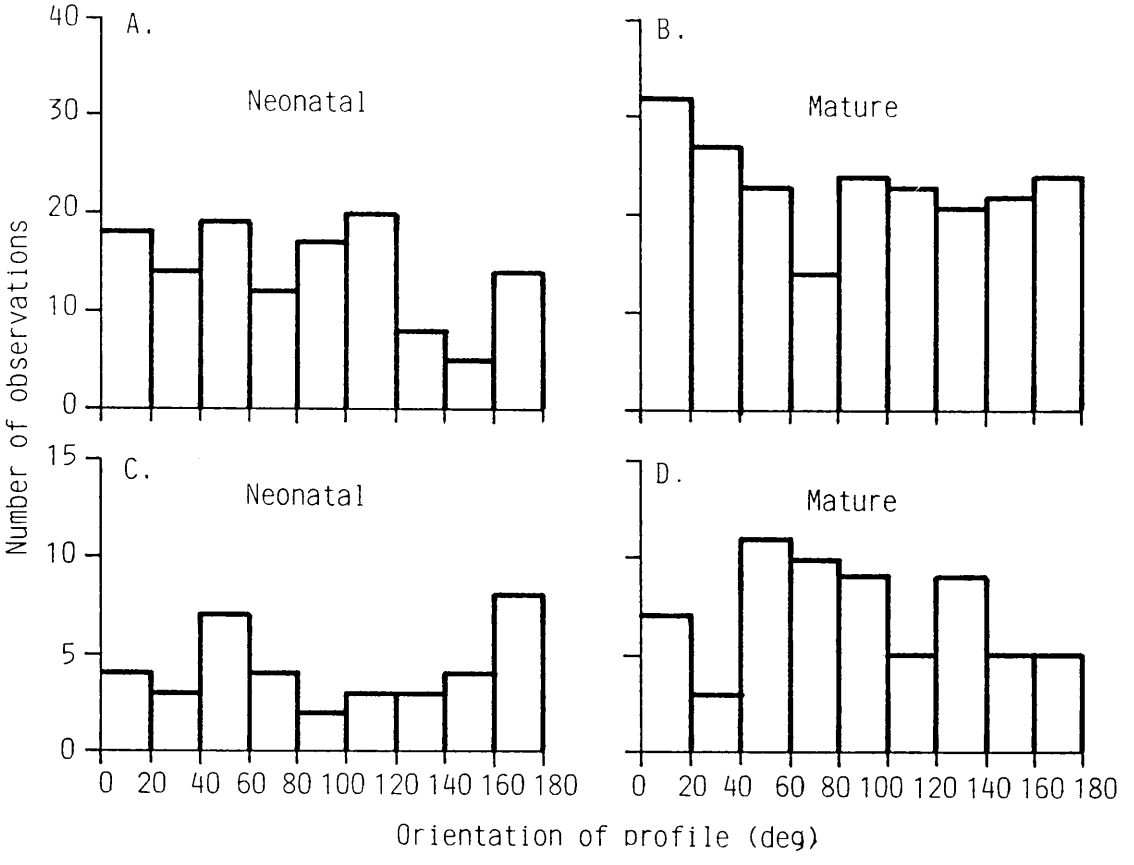

Figure 21

Distributions of orientations of profiles with respect to INL/IPL boundary taken as 0 deg. A. definite conventional synapses for 2 retinae ages 0-2 days (n=127); B. definite conventional synapses for 2 retinae ages 200 days and adult (n=185); C. definite synaptic-plus-floating ribbons for 7 retinae ages 0-6 days (n=38); D. definite synaptic-plus-floating ribbons for 2 retinae ages 200 days and adult (n=64).

3.12 Position of synaptic profiles

3.12.1 Conventional synapses

The position of the profiles of conventional synapses in neonatal retinae (newborn and 2 day) showed a non-random distribution within the five strata measured, with more synapses in stratum 3 than in the other strata ($P<0.005$, χ^2 test) (Fig. 21A). Mature retinae (200 day and adult) showed a similar distribution with more conventional synapses in stratum 3 than the other strata but, in this case, this was of marginal significance ($0.1>P>0.05$, χ^2-test) (Fig. 21B). There was no difference between the distribution of conventional synapses in neonatal and mature retinae ($P>0.99$, Mann-Whitney test). Therefore, conventional synapses are distributed mainly in the middle stratum of the IPL in both neonatal and adult retinae.

3.12.2 Bipolar cell ribbons

The distribution of bipolar ribbons in neonatal (0-6 days) retinae was not significantly different from a random distribution ($P>0.1$, χ^2 test) (Fig. 21C). However, the distribution was not random in mature retinae (200 day and adult), with more ribbons in strata 3 and 4 ($P<0.01$, χ^2 test) (Fig 21D). The change of distribution with age was of borderline significance ($P=0.079$, Mann-Whitney test).

Since the measured frequencies of bipolar cells were in any case obtained from the entire depth of the IPL, no adjustment to take account of the change in distribution is required.

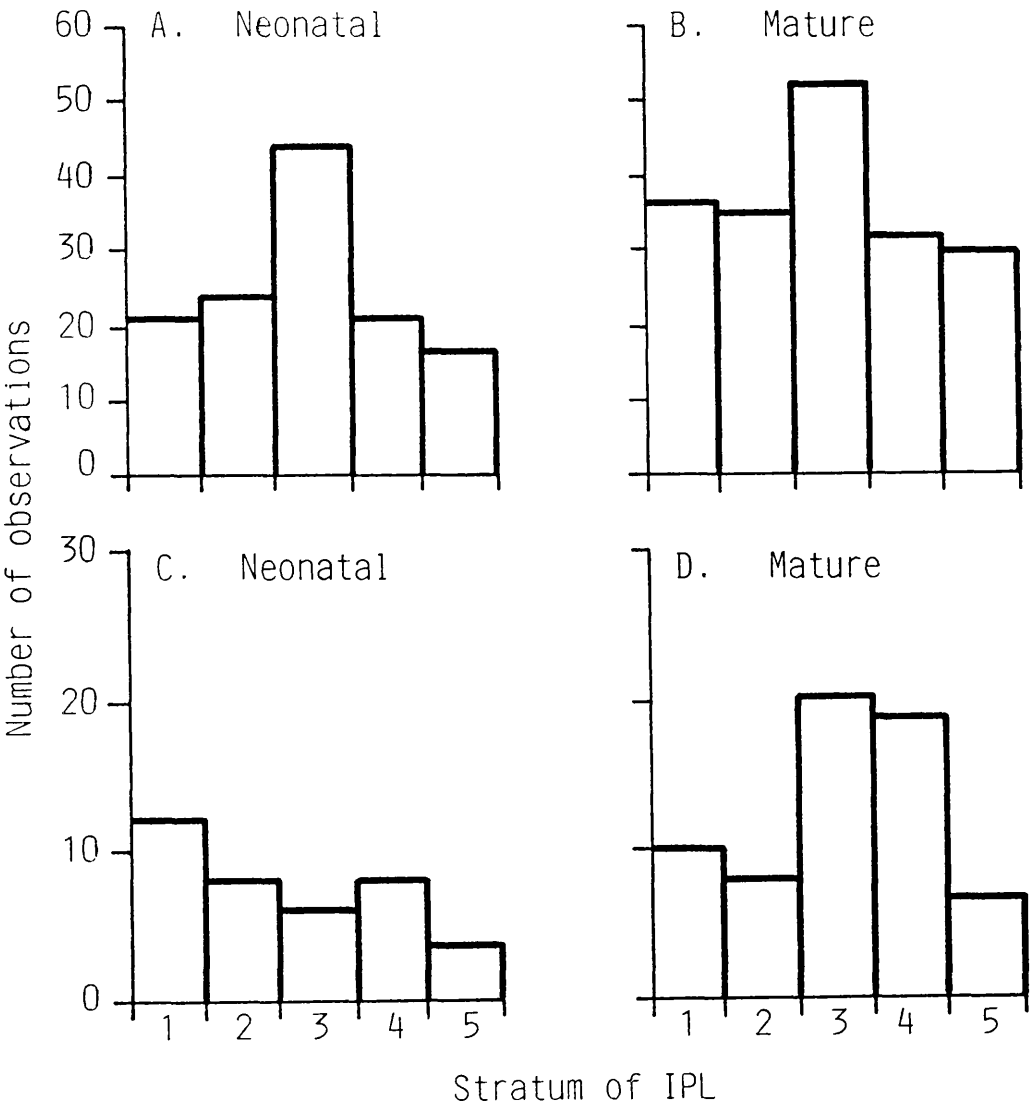

Figure 22

Distributions of profiles into 5 strata of equal depth across the IPL (with stratum 1 adjacent to the INL and stratum 5 adjacent to the GCL). A. definite conventional synapses for 2 retinae ages 0-2 days (n=127); B. definite conventional synapses for 2 retinae ages 200 days and adult (n=185); C. definite synaptic-plus-floating ribbons for 7 retinae ages 0-6 days (n=38); D. definite synaptic-plus-floating ribbons for 2 retinae ages 200 days and adult (n=64).

DISCUSSION

4.1 Main conclusions

The development of the synapses of the IPL was studied in a reproducible area of cat retina which was chosen to be the area centralis. In addition to its distinctive histology, the area centralis is the region of highest spatial resolution and is positioned on the visual axis. The main excitatory synapses seem to arise from the bipolar cells, the terminals of which are characterised by the presence of a synaptic ribbon, while the main inhibitory synapses seem to be mediated through conventional synapses formed by amacrine cells. However, there is evidence for bipolar cells which release the inhibitory transmitter glycine and amacrine cells which release the excitatory transmitter acetylcholine. Neither the excitatory nor inhibitory synapse types, however, are distinguishable by conventional transmission microscopy, thus precluding an allowance for their possible presence in cat retina: the relative proportions of these synapses in cat retina remains to be evaluated.

Synaptogenesis in the IPL has, therefore, been expressed as the number of bipolar cell ribbons and conventional synapses present at different stages of development. The number of synaptic ribbons and floating ribbons was counted, irrespective of the postsynaptic configuration. The reason for this was that these data constitute a more realistic assessment of the synaptic output of these neurones rather than by solely counting

synapses which, due to their three dimensional structure, may appear as a spectrum of different profiles in ultrathin sections. In addition, the profiles of the actual bipolar cell ribbon synapses were then also subdivided into monads and dyads. In scoring the presence of ribbons, there is always an element of ambiguity which may arise, for example, as a result of a plane of section nearly parallel to the synaptic membranes, thus presenting a profile lacking in the sharp, contrasted features of an orthogonal section. Strangely, this problem which was counted to be of considerable importance does not previously appear to have been given the consideration which it deserves. Hence, throughout the study, two main estimates - of definite and definite-plus-probable profiles - has been adopted. It was also noted that to express the number of synaptic profiles per unit area of IPL had its shortcomings, due to the differences in the depth of the IPL at different ages. The relevance here is that the measure of synaptic input to the ganglion cell dendritic tree should be thought of in terms of a column of IPL. In particular, these columns should ideally be based upon the extent of the dendritic tree of the different types of ganglion cells in sublaminae *a* and *b*, at the different stages of development. At the time of this study, this task had yet to be undertaken and, therefore, a less refined indicator has been adopted, using a a column extending through the entire depth of the IPL. More recently, Dann, Buhl & Peichl (1988) found that there was, in fact, no change in dendritic field area in the

tangential plane of either alpha- or beta-ganglion cells at the area centralis during development, thus vindicating this initial assumption.

By whatever method of measurement used - whether synaptic ribbons, floating ribbons or total ribbons, definite or definite-plus-probable ribbons, or per unit area or per column of the IPL - a very considerable degree of bipolar cell synaptogenesis was shown to occur in the postnatal period (Figs. 8-10). This synaptogenesis followed an exponential growth pattern, levelling off at about 100 days of age. This change, which was in the order of five-fold, was not dependent upon any age related shift in ribbon size (Figs 17 & 18) or orientation (Fig. 21), although a relative concentration of ribbons within the inner strata of the IPL was noted with increasing age (Fig. 22). This would not affect the measurements which extended the entire depth of the IPL. Thus, it may be inferred that the retinal ganglion cells must receive a considerable increase in their excitatory input during the postnatal period. The degree to which this may be balanced by a growth in the inhibitory inputs is unknown and would require immunocytochemical studies at the electron microscopic level. It must also be pointed out that considerable refinement of the data is possible in future work. Bipolar cell terminals may be classified into their three main types: invaginating cone, flat cone and rod bipolar cells on the basis of the identity of the postsynaptic processes and the level of the terminal arborisations in the IPL. Such work

would require three dimensional reconstruction of the synaptic complexes on a scale much greater than has been previously reported.

In marked contrast to the ribbon synapses of bipolar cells, conventional synapses remained invariant in number during postnatal development (Fig. 13). This was valid for the frequency per unit area and frequency per depth of IPL of definite and definite-plus-probable synapses. In addition, the length of the profile of the synapse (Fig. 19) and the number of vesicles per synapse (Fig. 20) remained constant. Furthermore, the range of orientations (Fig. 21) and distribution (Fig. 22) through the depth of the IPL was mature at birth and the number of serial synapses was mature (Fig. 14). As such, this is not surprising since genesis of conventional synapses commences at E45 in the cat retina, whereas that of bipolar cells only commences at birth (Maslim & Stone, 1986). Of particular importance would be the frequency of the different types of postsynaptic process i.e. whether amacrine, bipolar, ganglion or interplexiform cell processes, which would require further investigations involving the tracing of the origin of these processes. Since conventional electron microscopy of IPL is unable to distinguish between excitatory and inhibitory synapses, immunocytochemical studies at the electron microscopic level would be necessary to reveal whether the proportion of neurones with different neurotransmitters showed a consistent change with development.

4.2 Validation of results

4.2.1 Comparison with other quantitative studies

To be confident of the synaptic frequency results, the mean results for definite synaptic profiles of 200 day and adult retinae of the present study were compared to those of previous studies (Table 24).

Table 24 Comparison of the frequency of the conventional synapse, serial synapse and bipolar cell ribbon synapse in different species, at maturity.

		Number per μm^2		
		Conventional	Serial	Ribbon
Present study (definite synapses)		0.11	0.0018	0.017
Dubin (1970)	(cat)	0.07	0.0057	0.025
Sosula & Glow (1970)	(rat)	0.06	0.006	0.008
Fifkova (1972)	(rat)	0.12	0.005	0.011
McArdle et al (1977)	(rabbit)	0.13	0.006	0.025
Fisher (1979)	(mouse)	0.07	-	0.017
Nishimura & Rakic (1985)	(monkey)	0.16	-	0.037

The conventional synapse frequency and total bipolar cell ribbon frequency results obtained for mature cats in the present study show reasonably close agreement to previously reported quantitative studies. In quantifying serial synapses, Dubin (1970), Sosula & Glow (1970), Fifkova (1972) and McArdle et al

(1977) counted the individual conventional synapses rather than the serial synapse arrays which was done in the present study. Since these each consisted of 2, or occasionally 3 conventional synapses, the present results are thus reasonably comparable with the data of other investigators shown in Table 24.

Comparisons have also been made of the lengths of conventional synapses and of total bipolar cell ribbons with those previously reported. As shown in Table 25, there is very close agreement with previous data from a range of species.

Table 25 Comparison of the profile length of conventional synapses and bipolar cell ribbons in different species at maturity.

	Length of profile (μm)	
	Conventional	Ribbon
Present study (definite)	0.24	0.16
Dubin (1970) (cat)	0.25	0.18
McArdle et al (1977) (rabbit)	0.25	0.15
Fisher (1979) (mouse)	0.28	0.13
Nishimura & Rakic (1985) (monkey)	0.31	-

Therefore, given the close correspondence to published data for a variety of species including cat, the validity of the present methods of measurement may be accepted with confidence.

4.2.2 Control measurements

Measurements of synaptic profile size and their orientation and distribution within the IPL were taken. These were important in case there was a systematic change with age which would affect the measured frequency of occurrence of the profiles.

Conventional synapse size (Fig. 19) and orientation (Fig. 21) were the same in both newborn and adult retinae; therefore, no correction was required. The length of synaptic ribbons also did not change postnatally (Figs. 17 & 18). There was found to be a 17% increase in floating ribbon length from 0-6 days old to adult (Fig. 17). However, when floating ribbon length in all retinae was regressed with age, no significant change was found (Fig. 18). This, therefore, casts doubt upon the validity of the apparent difference between neonatal and adult retinae. In any case, if, for simplicity, bipolar ribbons are assumed to be circular, this would have caused a 17% increase in the frequency of floating ribbons observed (Weibel, 1980). Since floating ribbons were observed to increase fivefold in frequency, it was considered unnecessary to apply a correction factor to ribbon frequency. The orientation of bipolar ribbons was similar in both neonatal and adult retinae, thus having no effect on the measurement of synaptic frequency.

Conventional synapses were distributed similarly in both neonatal and mature retinae (Fig. 22), with most synapses in stratum 3. Bipolar cell ribbons were uniformly distributed throughout the 5 strata of the IPL in the neonatal retina whilst

a peak was present in strata 3 and 4 in the mature retina (Fig. 2-). The measured frequencies of bipolar ribbons were, in any case, obtained from the entire depth of the IPL; therefore, no adjustment to take account of the change in distribution is required.

4.2.3 Scatter of results

It was notable that, in the present study, there was considerable range of scatter of the data for both conventional synapses and bipolar cell ribbons. This may be accounted for by the fact that, in the cat, age is not necessarily a good indicator of developmental status even though a reproducible area of retina was studied, as noted earlier (Morrison, 1982). This was again highlighted more recently in a comparison between two litters of kittens which had an almost twofold difference in body weight at a given age and in which the effect of unilateral tenotomy of the lateral rectus muscle on interocular alignment was different between litters (though it was consistent within a litter) (Devlin, Jay & Morrison, 1990). A closer correspondence between developmental status and age may reasonably be expected in a reproducible strain of mice or rabbits, though an absence of scatter also occurred in rhesus monkey even though a reproducibly identifiable area of retina was not taken (Nishimura & Rakic, 1985). This may have been influenced by the fact that, in the present study, a smaller number of large montages from each retina was studied, while Nishimura & Rakic counted from five strips of IPL of 10μm wide in each retina.

4.3 Discussion of results

4.3.1 IPL depth

It was shown that the IPL increases in depth until about 18 days and then subsequently decreases (Fig. 7). Although there have been several histological studies on the developing cat retina (e.g. Donovan, 1966; Vogel, 1978; Morrison, 1982; Maslim & Stone, 1986) no investigators have previously reported IPL depth with age. In quantitative studies in the mouse (Fisher, 1979) and hamster (Greiner & Weidman, 1980), it was found that the depth of the IPL increased with age until an adult value was attained. However, in an earlier study in the rat, Braekevelt & Hollenberg (1970) found that the IPL depth in the posterior retina increased until 20 days and, after 40 days postnatal, it subsequently decreased, although in peripheral retina there was no subsequent decrease. The present finding is, thus, new information, indicating a similar pattern of growth to the rat.

To determine whether the decreasing depth of IPL after 18 days was due to 'stretching' of the neuropil as the eye increased in size, the volume of IPL at 18 days and in the adult was calculated from IPL depth X area of retina. Mastronarde, Thibeault & Dubin (1984) measured the area of retina containing 100 alpha-ganglion cells to determine the growth or stretching of the area centralis with development. From 2-6 weeks there was negligible growth (0.03% per week); therefore, a reduction in IPL depth as reported in the present study must correspond to a decrease in IPL volume subtended by 100 alpha-ganglion cells. From 6 weeks to adult there was a 2.7% increase in the area of

retina containing 100 alpha cells (*ibid*). Thus, from 2 weeks to adult, it can be calculated from the present results and those of Mastronarde et al (1984) that the volume of IPL at the area centralis in the adult cat is 74% of that in the area centralis in the 2 week old kitten. Unfortunately, figures are not available to calculate the changes in area centralis volume prior to 2 weeks postnatal. Since the area centralis thus increases in area by just 2.8% from 18 days to adult (Mastronarde et al, 1984), which is insufficient to account for the decrease in IPL depth, there must be an additional decrease in IPL depth after 18 days not due to stretching of the retina. The mechanism by which this thinning of the IPL occurs is at present unclear, since by about 18 days the processes of the IPL already appear to have become mature in size and appear to be 'compacted' within the IPL without the large extracellular spaces that are seen in neonatal retinae (personal observations). A quantitative study by Maslim & Stone (1989) showed that there is only a slight decrease in the amount of extracellular space after P14. Other factors which may affect the volume of the IPL are the number of ganglion cells and the morphology of their dendrites. The number of ganglion cells was reported to have decreased to an adult value by P15 (Ng & Stone, 1982); so after that time, the number cannot affect IPL volume. The number of branches of a ganglion cell dendritic tree and the number of dendritic spines decreases postnatally until the end of the first postnatal month (Ramoa, Campbell & Shatz, 1988). This might cause a decrease in IPL volume but this is presumably

offset, at least to some extent, by the increase in calibre of the remaining ganglion cell dendrites (*ibid*).

The change in size of the IPL depth has implications for the method of expressing the frequency of synaptic profiles which will affect the apparent frequency per unit area. For example, conventional synapse frequency per unit area did not change with increasing age. However, because of the decrease in IPL volume after 18 days, this result implies that the actual number of conventional synapses present in the area centralis (rather than the synaptic frequency) subsequently decreases. Therefore, it was considered desirable also to express the results in terms of a column of IPL.

4.3.2 Bipolar cell ribbons

In the IPL of cat retina, previous studies of synaptogenesis have been qualitative (Cragg, 1975; Vogel, 1978; Greiner & Weidman, 1980; Morrison, 1982; Maslim & Stone, 1986). The present quantititative findings are consistent with the commencement of ribbon formation in central retina at birth (Maslim & Stone, 1986), although the present study, along with Morrison (1982), who also observed ribbons at the area centralis at birth did not examine prenatal retinae. It is now possible to extend these data by adding that the rate of growth is exponential with levelling off at about 100 days. This compares with the more rapid synaptogenesis seen in the rabbit retina (from P9 to P20 days) (McArdle et al, 1977) and mouse retina (P11 to P16) (Fisher, 1979). Even in rhesus monkey IPL, the

time course of synaptogenesis, which occurs mainly prenatally, is somewhat shorter (E99-E149) (Nishimura & Rakic, 1985).

Bipolar cell ribbons first appear floating in the cytoplasm, as shown by the serial reconstructions by Morrison (1982) and Nishimura & Rakic (1987). These floating ribbons then become apposed to a synaptic site to form first a monad with one postsynaptic process before another postsynaptic process becomes aligned to form a dyad (McArdle et al, 1977, Morrison, 1982). In a single ultrathin section of the IPL, the profile of a floating ribbon may, thus, be either a truly floating ribbon or a synaptic ribbon in which the section has omitted the postsynaptic processes. Thus, if the real number of synaptic ribbons were to increase, it is likely that the number of profiles of floating ribbons would also increase. This expectation has been confirmed by the present results.

By the same reasoning, if monads may also be considered to consist of true monads and dyads which have been sectioned through one postsynaptic process, the expectation might therefore be that as the number of dyads increased, that of the monads would also increase. This expectation was not fulfilled: in fact the number of monads remained constant. The circumstances in which this might occur would be if true monads which are an intermediate stage in dyad formation were eliminated during development (though some true monads do exist in adult retina (Kolb, 1979)). Hence the present finding of constancy in the number of monads with development, despite increasing dyad frequency, is consistent with the sequence of

dyad formation which involves the intermediate formation of a monad.

While the length of synaptic ribbon profiles did not change postnatally, that of floating ribbons may be slightly smaller in neonatal than adult retinae (Fig. 17) although the regression of floating ribbon length in all retinae does not support this finding (Fig. 18) (see 4.2.2). The inconsistency in the analysis of the present results reinforces the desirability to study as large a sample of ribbons as possible. However, the difference in growth pattern between floating and synaptic ribbons, ***if real***, would indicate that the floating ribbon profiles in neonatal kittens probably arose from genuine floating ribbons rather than from sections of synaptic ribbons, which is quite likely since at this stage the number of synaptic ribbons was relatively low. The alternative explanation is a change in ribbon shape during early development. For example, the ribbon may have been elliptical in neonatal retinae with the short axis orthogonal to the postsynaptic processes. If the short axis increased in length during development, this would explain the higher number of short floating ribbon profiles observed in neonatal retinae compared with mature retinae, as well as the increase in mean floating ribbon size with maturity in the absence of an increase in synaptic ribbon size. However, serial sections would be required to properly elucidate this. Fisher (1979) has also found that the length of bipolar cell ribbons in the developing mouse IPL increased by 30% over the first 4 days of synaptogenesis although he did not distinguish between

synaptic and floating ribbons. The present result showing a constancy of synaptic ribbon profile length is also at variance with Morrison's (1982) observation in the cat, that at birth the synaptic ribbon usually occupied the thickness of only one ultrathin section compared with 4 or more sections in older retinae. This is probably due to the limited number of ribbons which were serial sectioned in his study and reinforces the desirability to study as large a sample of ribbons as possible.

4.3.3 Conventional synapses

The frequency and morphology of conventional synapses has been shown to be mature at birth: their size did not change postnatally and the number of synaptic vesicles in neonatal retinae was mature. Also serial conventional synapses were present in adult numbers at birth. In cat retina, Maslim & Stone (1986) reported the first conventional synapses at E45, with a subsequent increase in frequency until at least E62 in central and peripheral retina, though this was not quantified. Postnatally, Morrison (1982) reported the impression of an increase in the number of conventional synapses at the area centralis in older retinae. Hence, the present data have established on a quantitative basis that this was not the case and that the frequency remained constant postnatally, though this by no means excludes a change in the proportion of conventional synapses sub-types or indeed a change in their relative efficacy.

In rabbit and mouse, the presence of conventional synapses was observed at birth and P3, respectively, with an increase in both species until P20 (McArdle et al, 1977; Fisher, 1979, respectively). Nishimura & Rakic (1985) showed that conventional synapses in the rhesus monkey were first observed at E78 and reached adult frequency at E99-114. Conventional synapses were observed to be mature in size before they reached adult frequency levels in rabbit and mouse (McArdle et al, 1977; Fisher, 1979, respectively). In addition, McArdle et al (1977) and Nishimura & Rakic (1985) found fewer synaptic vesicles at conventional synapses in the immature retina than in the mature retina.

By the time conventional synapses have reached adult numbers in the rabbit, serial synapses are also already found in adult numbers (McArdle et al, 1977). The present results are consistent with this. The maturity of serial synapse frequency in neonatal retinae implies amacrine-amacrine synapses are present in adult numbers in the neonatal kitten, since at least one amacrine-amacrine conventional synapse must be contained in each serial synapse. It is not possible to determine whether amacrine-bipolar and amacrine-ganglion synapses are also present in adult numbers at this stage. Certainly, amacrine-bipolar synapses are definitely present at 5 days, when a reciprocal synapse was first observed, if not before; but it is not easy to positively identify ganglion cell dendrites in the immature IPL. The study of reciprocal synapses from amacrine cells to bipolar cells, which were also presynaptic to those amacrine cells was

difficult, since only a total of 5 such synapses were unequivocally observed. Since the earliest was present at P5, this indicates that reciprocal synapses were present early. Maslim & Stone (1986), studying prenatal development, observed that amacrine-amacrine conventional synapses were first formed at E45 which was prior to amacrine-ganglion synapses at E56. In the rhesus monkey, Nishimura & Rakic (1987) found the reverse; that amacrine-amacrine conventional synapses were initially observed more frequently than amacrine-ganglion synapses. However, the identification of ganglion cell dendrites and amacrine cell neurites at such an early age, in the absence of tracing back to the parent cell body, must be regarded, at best, as hopeful. Both studies agree that conventional synapses to bipolar synapses form later. Morrison (1982) reported that bipolar, amacrine and ganglion cells were all postsynaptic at conventional synapses at birth.

4.3.4 Comparison of bipolar cell ribbon and conventional synapse development

It is clear from the present study that bipolar cell synaptogenesis only commences once conventional synapses have attained maturity, at least in terms of numbers and morphology. Similarly Nishimura & Rakic (1985) showed that, in the rhesus monkey, conventional synapses had virtually reached their adult complement at E99-114 when bipolar cell ribbons were first observed. In the mouse, bipolar cell synaptogenesis occurred within the period of conventional synapse formation, with

conventional synapses formed from P2-P20 and bipolar cell ribbons from P10-16 (Fisher, 1979). While the first conventional synapses in the rabbit predated ribbon synapses which were first observed at P9, the main increase in conventional synapse and synaptic ribbon frequency occurred simultaneously, reaching adult levels by about P20 (McArdle et al, 1977). In addition, previous qualitative studies also show that conventional synapses predate ribbon synapses in the cat (Greiner & Weidman, 1980; Maslim & Stone, 1986) and mouse (Olney, 1968), although Smelser, Ozanics, Rayburn & Sagun (1974) found that conventional synapses and ribbon synapses appeared virtually simultaneously in the IPL of rhesus monkey.

Therefore, the present result is in agreement with previous studies that conventional synapses start to appear before bipolar cell ribbons and further adds that, in the cat, conventional synapses are present at adult levels when bipolar cell ribbons start forming, as also reported for rhesus monkey IPL (Nishimura & Rakic, 1985).

The significance of the prior formation of conventional synapses compared with ribbon synapses is not certain. There may be an actual requirement for the conventional synapses to be in place before bipolar cell ribbon synaptogenesis commences or it may merely reflect the earlier differentiation of amacrine cells compared with bipolar cells (Sidman, 1961).

4.3.5 Distribution of synapses within the IPL

The highest number of conventional synapses were found to lie in the middle stratum of the IPL in both neonatal and adult retinae between which there was no significant difference (Fig. 22). While Dubin (1970) found a uniform distribution of conventional synapses across the IPL in the adult cat, Nishimura & Rakic (1987) described the initial formation of these synapses to occur mainly in the middle stratum of the IPL of the rhesus monkey, lending support that this region is indeed important with respect to conventional synapses. Furthermore, it may be said from the present results that conventional synapses have reached maturity in distribution, as well as in terms of numbers and morphology.

Bipolar cell ribbons were distributed uniformly across the neonatal IPL whereas, in the adult IPL, a definite accumulation of ribbons was present in strata 3 and 4 (Fig. 22). This is again contrary to the report of Dubin (1970), who found constancy in ribbon frequency across the depth of the IPL in adult cat. Possible reasons for this discrepancy between Dubin's results and the present study may be the larger areas of montages used in the present study or variation between animals. Previous qualitative developmental studies first reported bipolar ribbons to occur more frequently in the outer aspect of the IPL (Olney, 1968; Smelser et al, 1974; McArdle et al, 1977). This may simply be due to differences in sample size, species variation or to a subjective impression not supported by quantitative data. There are several possible explanations for

the present findings that the distribution of ribbons within the IPL changes with development. First, it may simply reflect the migration of newly-formed ribbons from the outer towards the inner strata of the IPL. Second, ganglion cells at the area centralis do not become unistratified until P3 (Maslim & Stone, 1988), so there may also be a change in the level of stratification of bipolar cells and the position of their synapses. Third, the present finding may imply that an increased number of ribbons are forming in invaginating cone bipolar cell axon terminals which lie in sublamina *b*. Invaginating cone bipolar cells mainly depolarise when the retina is exposed to light (Nelson, Kolb, Robinson & Mariani, 1981) and, by inference, provide the inputs to ON-centre ganglion cells (Nelson et al, 1978). The two main studies on development of retinal ganglion cell responses (Rusoff & Dubin, 1977; Hamasaki & Sutija, 1979), however, did not differentiate between ON- and OFF-centre ganglion cells. Mastronarde (1984) noted that X-ON axons were located further from the pial surface of the optic tract than X-OFF fibres, indicating that the ON fibres were generated earlier. However, the time of generation in the optic tract may not necessarily reflect the time-course of synaptogenesis in the IPL. Fourth, although Kolb (1979) found that the ribbon synapses of rod bipolar cells were only present in the axon terminals, deeper in the IPL adjacent to the GCL (Kolb & Famiglietti, 1974; Kolb, 1979), McGuire, Stevens & Sterling (1984) found that rod bipolar cells also formed ribbon synapses, at a lower frequency, in strata 3 and 4. Thus,

particularly considering the previous observation by Morrison (1982) of the later development of rod bipolar cell ribbon synapses, the increase in frequency of ribbons in strata 3 and 4 could be due to synaptogenesis in rod bipolar cells.

It remains to be determined whether the new ribbons were added to newly developed or to existing bipolar cell terminals. However, at birth the full complement of bipolar cells is already present in central retina (Johns et al, 1977) and the impression gained was that they arose in existing terminals, which is consistent with the considerable enlargement of terminals which occurs postnatally (Morrison, 1978).

4.4 Comparison with ganglion cell development

4.4.1 Ganglion cell excitability

The response amplitude and response sensitivity of ganglion cells was found to be smaller in 3 week old than in mature retinae (Hamasaki & Flynn, 1977). However the converse was reported by Rusoff & Dubin (1977) who found a greater response in the three-week-old kitten. Both groups of investigators found that there was a lower rate of spontaneous activity in the kitten than in the adult. If it were the case that the increased bipolar cell synaptogenesis indicated an increased excitatory drive to the ganglion cells, the present findings would thus be consistent with the increased rate of spontaneous activity in older retinae, and would be consistent with an increased response amplitude and sensitivity during development.

4.4.2 Ganglion cell receptive field development

Retinal ganglion cell receptive fields are immature at 3 weeks of age (earliest studied) (Rusoff & Dubin, 1977; Hamasaki & Flynn, 1977). At this time, the receptive fields, measured in degrees of visual angle, are large and the cells cannot be classified into adult categories (Rusoff & Dubin, 1977), although this was not at the area centralis and, therefore, would represent a slightly earlier developmental stage.

The diameter of the receptive field centre of identifiable X-ganglion cells, measured in degrees of visual angle, may be translated into linear dimensions using the unpublished data of Thorn & Gollender quoted by Rusoff (1979) and that of Hamasaki & Flynn (1977) and Vakkur, Bishop & Kozak (1963). Intuitively, this shows a reduction in receptive field centre size with age in the data of Hamasaki & Flynn (1977) and Hamasaki & Sutija (1979) while the data of Rusoff & Dubin (1977) indicate an increase in the linear size of the receptive field centre size in the adult (Table 26). The data of Rusoff & Dubin (1977) can also be seen to be considerably lower than the data of Hamasaki & Flynn (1977) and Hamasaki & Sutija (1979), which is presumably due to different methods of measurement. The apparent decrease in the data of Hamasaki & Flynn (1977) and Hamasaki & Sutija (1979) was not significant ($P>0.1$), though the analysis is compromised by the large variance.

Table 26 Dimensions of receptive field centres of X-ganglion cells

		Hamasaki & Flynn, 1977		Hamasaki & Sutija, 1979		Rusoff & Dubin, 1977	
Age	PND	Deg	μm	Deg	μm	Deg	μm
wks	mm						
3	7.9	2.2	303	2.4	331		
4	7.8			2.6	354	1.3	177
5-6	8.3			2.0	290	1.1	160
7-8	9.5			1.9	342	1.0	166
10-12	10.3			1.4	252		
Adult	12.5	1.2	262	1.3	283	0.9	196

Also, consistent with this are the results for cats with a surgically-induced squint in which the ganglion cells had a receptive field centre and surround twice as large in the squinting eye compared to the normal eye (Ikeda & Tremain, 1979). If it were the case that an arrest of development had occurred, as seems to be the case in the lateral geniculate nucleus (Ikeda, Tremain & Einon, 1978), then the results of Ikeda & Tremain (1979) would be a reflection of the immature stage of ganglion cell development.

Thus, all groups of investigators have described a decrease in the angular size of the receptive field centre with age. It is not clear whether there is a change in linear dimensions but there may be some evidence of a decrease in linear size with

development (Hamasaki & Flynn, 1977; Hamasaki & Sutija, 1979; Ikeda & Tremain, 1979).

The antagonistic receptive field surround of identifiable X-cells was first observed at 4 weeks. The outside diameter of the receptive field surround decreases in both degrees of visual angle ($P<0.02$) and in linear dimensions ($P<0.001$) with increasing postnatal age (Rusoff & Dubin, 1977) (Table 27).

Table 27 Dimensions of receptive field surrounds of X-ganglion cells

		Rusoff & Dubin, 1977	
Age	PND	Deg	μm
wks	mm		
4	7.8	6.8	925
5-6	8.3	6.2	899
7-8	9.5	5.3	880
Adult	12.5	3.2	714

4.4.3 Comparison of the development of ganglion cell receptive field dimensions with IPL synapse development

If the linear size of the receptive field centre does indeed decrease with postnatal development, as found by Hamasaki & Flynn (1977) and Hamasaki & Sutija (1979) and as implied by the work of Ikeda & Tremain (1979), this might be explained by an increased inhibition by the antagonistic surround, causing it to

encroach upon the receptive field centre. However, if the receptive field surround is surmised to be mediated by conventional synapses, then this has to be reconciled with the constancy of conventional synapse frequency during postnatal development and their apparent morphological maturity at birth. This might be explained by a possible increase in efficacy or a redistribution of sub-types of conventional synapses with development which are further discussed in sections 4.4.4 and 4.5.

The data of Rusoff & Dubin (1977), that the receptive field centre is greater in the adult cat than in the kitten, might be explained by an increased excitatory input to ganglion cells. This is consistent with the findings of the present study that there is considerable bipolar cell synaptogenesis postnatally. The size of the inhibitory surround decreases with development (Rusoff & Dubin, 1977) but the strength of the inhibitory surround is apparently stronger in the mature compared to the immature retina (Ikeda & Tremain, 1979). Therefore, depending upon the balance of the receptive field surround and its strength, there may or may not be a change in the amount of inhibitory input to ganglion cell surround. Certainly, a lack of change would be consistent with the present results that there was no change in conventional synapse frequency or morphology after birth.

Thus, while the physiological evidence of the development of receptive field parameters remains to be clarified, the present findings are most consistent with the data of Rusoff & Dubin (1977).

4.4.4 Reduced selectivity and sensitivity of receptors in the immature retina and possible redistribution of synapses with development

Ikeda & Robbins (1985) found that, in the adult cat, GABA and glycine selectively inhibit the visually induced excitation of ON- and OFF-centre ganglion cells, respectively (although Bolz, Thier, Voigt & Wassle (1985) reported glycine to be inhibitory to all ganglion cells). However, in 7-9 week old kittens, Ikeda & Robbins (1985) found that GABA also inhibited OFF-centre ganglion cells while glycine also inhibited ON-centre ganglion cells to some extent. Thus, there was less selectivity to GABA and glycine in the kitten retina compared to the adult. Ikeda & Robbins also observed a lower sensitivity to GABA and glycine, but a greater sensitivity to their antagonists, in the kitten compared to the adult retina. Thus, both the selectivity and the sensitivity of postsynaptic receptors on the ganglion cells to exogenous inhibitory transmitter increases during development.

The excitatory action of dopamine antagonists on immature but not on adult ganglion cells implied that physiologically active dopaminergic innervation was present on immature ganglion cells but was subsequently eliminated during the course of postnatal development. In addition, the application of exogenous

dopamine, L-sulpiride (a D_2 antagonist) and α-flupenthixol (a D_1 antagonist) indicates that both D_1 and D_2 receptors are present in immature cells but only D_2 receptors remain in the adult (Ikeda, Robbins & Wakakuwa, 1987). Thus, inhibitory dopamine inputs are actually eliminated during development.

In the present study, not only was the frequency of conventional synapses constant during postnatal development, but conventional synapses were also morphologically mature in both size and the number of vesicles per synapse. Thus, if the receptive field surround were surmised to be mediated by conventional synapses which cause a reduction of the receptive field centre during development (see section 4.4.2), this has to be reconciled with the constancy of conventional synapse frequency during postnatal development and their apparent morphological maturity at birth. There may be a redistribution of types of conventional synapse, with those that are initially excitatory becoming inhibitory in function, or even those that are initially inhibitory may subsequently change to a different inhibitory neurotransmitter to give a more potent inhibition on ganglion cells. In this respect, a quantitative study of different putative transmitters at the electron microscope level would be particularly useful. Also, although the synapses appear to be morphologically mature, the structural maturity of the the receptors cannot be determined, although increasing sensitivity to GABA and glycine with development (Ikeda & Robbins, 1985) indicates immaturity of receptors or of receptor populations at this age.

4.5 Possible mechanisms for redistribution of synapses

As described earlier, Ramoa et al (1988) found that the number of branches and dendritic spines reached a peak by the first week of postnatal life and then decreased abruptly to reach near-adult levels by the end of the first postnatal month. Also, immature ganglion cell dendritic trees initially branch diffusely in the IPL and then go through a bistratified stage before becoming unistratified to either sublamina *a* or sublamina *b* (Maslim & Stone, 1988), with the dendritic trees of ganglion cells in the area centralis becoming unistratified at P3 (Maslim & Stone, 1988). The number of retinal ganglion cell axons increases from E30 to E45-E55. The number then falls rapidly, reaching a mature level by P15 (Ng & Stone, 1982). These changes in the structure and size of the ganglion cell dendritic tree and the number of ganglion cells may thus cause elimination of synapses. The depth and volume of the IPL at the area centralis apparently decreases after 18 days (See 4.3.1) although it was not determined what the volume of IPL is prior to this. This has implications for the present results, particularly for conventional synapses which are at an adult frequency at birth. It suggests that some of these synapses may be formed onto ganglion cells that subsequently die or onto spines or branches of ganglion cell dendritic trees that subsequently regress. In order to maintain a constant frequency of conventional synapses throughout postnatal life while the IPL volume is changing, new conventional synapses are likely to be formed onto other ganglion cells. The soma size and dendritic calibre diameter of

ganglion cells increase with development (Ramoa et al, 1988), which would permit formation of new synapses onto the remaining ganglion cells. However, if there is a redistribution of conventional synapses they may also form onto other amacrine cells, bipolar cells and interplexiform cells.

4.6 The 'push-pull' hypothesis - the possible role of putative inhibitory bipolar cell ribbon synapses

Although the majority of bipolar cells was stated by morphological evidence to be excitatory (Raviola & Raviola, 1982), more recently several sub-types of cone bipolar cell that appear to contain glycine have been identified using autoradiographical and immunocytochemical techniques (Cohen & Sterling, 1986; Wässle et al, 1986; Pourcho & Goebel, 1987a; 1987b). However, the actual degree of labelling in the autoradiographic studies is low compared to the amount of [^{3}H] glycine accumulated by amacrine cells, for which there is evidence of inhibitory transmission (Wässle et al, 1986). In fact, the two most highly labelled cone bipolar cell types demonstrated glycine accumulation which was only about 40% that of the most heavily labelled amacrine cell. In addition, some cone bipolar cells did not label much more strongly for glycine than did GABAergic amacrine cells which also showed a slight reaction to glycine, indicating the possibility of a background stain (Pourcho & Goebel, 1987a). Cohen & Sterling (1986) have suggested that the reason so many cone bipolar cells label for glycine is because of leakage through gap junctions which they

form with glycinergic amacrine cells. Pourcho & Goebel (1987b), however, believe that since the distribution of endogenous glycine as visualised by immunoreactivity confirms the results shown by autoradiography, this supports the identification of glycinergic cone bipolar cells.

The putative glycinergic bipolar cells could be involved in the centre response of the ganglion cell. McGuire et al (1984) observed that 4 types of cone bipolar cell terminated in sublamina *a*, all making synapses onto OFF-beta ganglion cells, while 3 types of cone bipolar cell terminated in sublamina *b* and made synapses with ON-beta ganglion cells. In a further study (McGuire et al, 1986), they found, from reconstruction of serial sections of two ganglion cells, that 3 types of cone bipolar cell made synapses onto one ON-beta ganglion cell and that 2 types of cone bipolar cell made synapses onto one OFF-beta ganglion cell. From those studies and from other work on the properties of the cone bipolar cells involved (Nelson & Kolb, 1983), McGuire et al (1984; 1986) have postulated a mechanism - the 'push-pull' hypothesis - to explain the centre response of beta-ganglion cells by simultaneous excitation from one bipolar cell and disinhibition from another bipolar cell.

If an inhibitory input to ganglion cells came via bipolar cells, the findings of Rusoff & Dubin (1977) that ganglion cells were more excitable at 3 weeks than in adult retinae could be reconciled with the findings of the present study if some of the increase of ribbon synapse frequency observed after 3 weeks was due to an increase in the number of inhibitory ribbon synapses.

However, as was previously mentioned, Hamasaki & Flynn (1977) found immature ganglion cells to give a smaller response than mature ganglion cells (section 4.5.1).

McGuire et al (1986) also suggested that the surround inhibition could be generated, at least in part, by bipolar cell surrounds, since illumination of the cone bipolar surround would lead to withdrawal of its excitation upon the ganglion cell. However, as yet, only one sub-type of cone bipolar cell has been observed to have a surround (Nelson & Kolb, 1983); so if there are no other bipolar cells with a surround, the surround of ganglion cells must presumably be mediated by amacrine cells.

Only 10-15% of bipolar cells in the cat retina appear to contain or accumulate glycine, all of which are cone bipolar cells (Wässle et al, 1986; Pourcho & Goebel, 1987b) while 45-50% of amacrine cells do so (Wässle et al, 1986; Pourcho & Goebel, 1987b). In addition, there is no evidence to suggest that bipolar cells may contain any other inhibitory transmitter, while the inhibitory neurotransmitter GABA has been shown to be accumulated (Freed et al, 1983; Bolz, Frumkes, Voigt & Wässle, 1985) and synthesized (Bolz, Frumkes, Voigt & Wässle, 1985) in several subtypes of amacrine cell.

Thus, while there is evidence that some cone bipolar cells have an inhibitory function, with glycinergic transmission, their role is not yet clear and no other inhibitory transmitters appear to be involved in bipolar cell transmission. On the other

hand, there is substantial evidence that the majority, if not all, bipolar cells are excitatory (see Introduction) and that many amacrine cells synthesize and accumulate inhibitory transmitter substances.

4.7 Excitatory amacrine cell conventional synapses and interplexiform cell conventional synapses

Not all conventional synapses in the IPL are inhibitory amacrine cell synapses. There also appear to be excitatory amacrine cell conventional synapses, since two sub-types of amacrine cells appear to accumulate and synthesize acetylcholine (Pourcho & Osman, 1986; Schmidt et al, 1987). In the rabbit, it has been found that some amacrine cells accumulate both acetylcholine and GABA (Vaney & Young, 1988).

Other conventional synapses are formed by interplexiform cells. The role of interplexiform cell conventional synapses in the IPL is unclear at present but they are probably presynaptic to both bipolar cells and amacrine cells as well as being postsynaptic to amacrine cells (Kolb & West, 1977; Nakamura et al, 1980). In the OPL, interplexiform cells are presynaptic to rod and cone bipolar cells and also pre- and postsynaptic to other interplexiform cells (Kolb & West, 1977). Although Boycott et al (1975) found interplexiform cells to be fairly rare, they concluded, because they did not stain readily with the Golgi technique, that these cells did, in fact, occur fairly frequently. Nishimura & Rakic (1987) made the assumption that, in the developing rhesus monkey retina, interplexiform cell

synapses must form either at the same time as amacrine-bipolar cell synapses or later. This assumption was made on the basis of interplexiform cells being only presynaptic to bipolar cells, since amacrine-bipolar were positively identified from serial sections at E105 (the earliest age that bipolar cells were found to be postsynaptic at conventional synapses). However, in the cat, interplexiform cells are probably also presynaptic to amacrine cells as well as to bipolar cells (Kolb & West, 1977; Nakamura et al, 1980). Thus, the significance of the interplexiform cell conventional synapses, their number in the adult cat and the timing of their development is an unknown factor in the present study.

4.8 Comparison of IPL synaptogenesis to other developmental events in the cat's visual system

To gain a proper perspective of the timing of synaptogenesis in the IPL, the present results were compared with other physiological and anatomical developmental events in the visual system (Fig. 23). This was to explore which events might influence IPL synaptogenesis and whether IPL synaptogenesis might in turn influence the other developmental events.

4.8.1 Development of the ocular media

The kitten's eyes are closed at birth and do not open until P7-10 (personal observations; Windle, 1930). The eyes undergo extensive growth between birth and adulthood, with the axial dimensions more than doubling (Thorn, Gollender & Erickson,

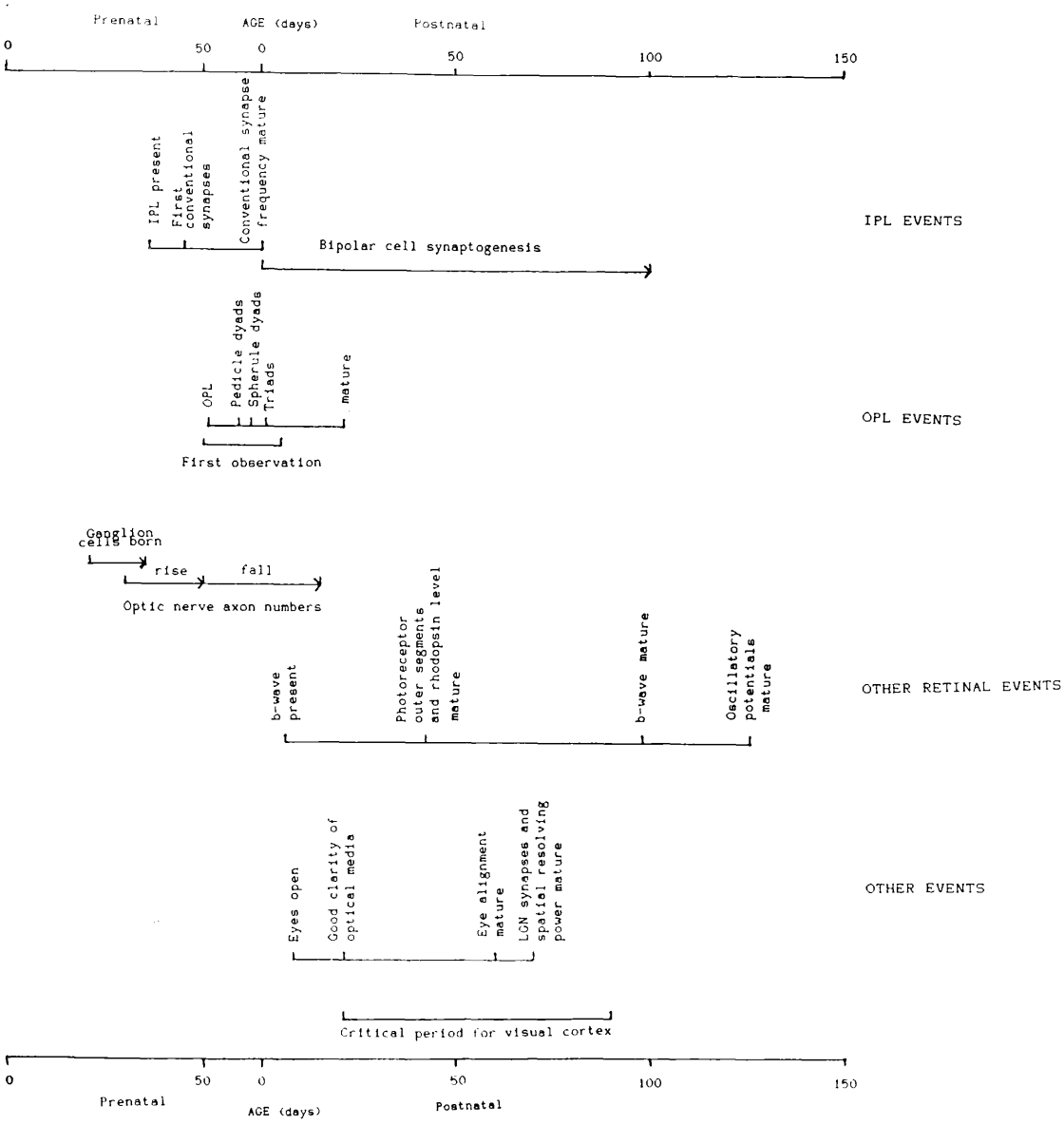

Figure 23

Summary diagram of developmental events in the cat's visual system. See text for details.

1976). Eye alignment changes with development from being strongly divergent at the time of eye opening to being almost parallel. A mature alignment is reached at about P60-P70 (von Grunau, 1978; Olson & Freeman, 1978).

The ocular media appear opaque in the kitten, thus limiting the amount of light reaching the retina and causing light scattering. This is due to a dense vascular network, the tunica vasculosa lentis, attached to the posterior surface of the lens and the dense pupillary membrane to which it is joined on the anterior surface of the lens. The pupillary membrane and the tunica vasculosa lentis begin to disappear during the third postnatal week (Thorn et al, 1976). Bonds & Freeman (1978) calculated values for the modulation transfer function at different ages in the kitten and concluded that clarity of the ocular apparatus is not likely to be a factor limiting visual acuity by 3 weeks of age. The cornea is already morphologically mature by 11 days postnatal (Freeman & Lai, 1978). However, corneal curvature at 20 days (earliest studied) is sometimes irregular and is greater in the kitten, even at 100 days postnatal, than in the adult (Freeman, Wong & Zezula, 1978).

The formation of conventional synapses does not appear to require visual experience since they are present in adult numbers at birth. However, any redistribution of conventional synapses postnatally might depend on the clarity of the ocular media in transmitting a sharp retinal image. Ocular clarity may also be necessary for normal bipolar cell synaptogenesis after 3

weeks of age. This is supported by the effect of light deprivation on IPL synaptogenesis in the rat (Fifkova, 1972; see section 4.8.6).

4.8.2 Photoreceptor development

Photoreceptor outer segments have reached an adult length by about 5-6 weeks postnatal (Donovan, 1966; Tucker, Hamasaki, Labbie & Muroff, 1979; Morrison, 1982). At the same time, rhodopsin becomes present in an adult level although rhodopsin levels were found to be higher at 7-11 weeks than in the adult cat (Faulkner, Jacobson, Ikeda & Kemp, 1982). Photoreceptor activity, as measured by the late receptor potential, is present at P9-10 (the earliest age studied) and is already mature in terms of both threshold value and amplitude at 3-4 weeks which is earlier than when the outer segments reach their adult length (Tucker et al, 1979).

In the OPL, at the area centralis, cone pedicles and rod spherules form a dyad before entering into a triad synaptic arrangement (Morrison, 1982). Morrison observed that cone pedicles formed synapses with a bipolar dendrite at birth. Rod spherules developed over a slower time course and were first observed to form synapses with rod bipolar cell dendrites at the start of the second postnatal week, reaching maturity in the fifth week postnatal. Maslim & Stone (1986) observed that a few ribbon synapses of a dyad configuration were present at E59 and observed cone pedicles and, less frequently rod spherules, forming triads at birth. A quantitative study by Rapaport (1989)

indicated that the *total* number of ribbons in the OPL increased in frequency until P3 and then decreased after P11 to reach an adult frequency at P60. This study did not differentiate between rod spherules and cone pedicles and the presence of multiple ribbons in immature rod spherules make it difficult to determine the true time course of the development of ribbon synapses.

Photoreceptors have, therefore, reached a high degree of maturity by 5 weeks. Since their synapses in the OPL only start forming at E59, it is unlikely that their development influences conventional synapse formation in the IPL though they may well influence bipolar cell synaptogenesis, which, as shown in the present study, commences at about this age and indicates a coincidence between photoreceptor synapses and bipolar cell synaptogenesis.

4.8.3 Development of the electroretinogram

The b-wave of the electroretinogram (ERG) arises as the result of radial K^+ current flow into the Müller glial cells. Two main current sinks are located at the outer and inner margins of the INL. Since the K^+ ions arise initially from depolarising neurons in the INL, the b-wave is, thus, a reflection of INL function (Kline, Ripps & Dowling, 1978; Newman, 1980). The b-wave was recorded in the developing retina by Zetterstrom (1955), who reported its presence by P6-10. Hamasaki & McGuire (1985) found that the b-wave amplitude elicited by high stimulus intensities attain adult size at 5-7 weeks, while it was not until 10 weeks that the b-wave elicited

by lower stimulus intensities reached adult size, by which time the implicit time of the b-wave had also reached an adult value. Jacobson et al (1987) found that cone-mediated ERGs appeared to take a longer time to develop, as the b-wave was not adult-like until after 14 weeks, although the implicit time was mature at 12 weeks postnatal. Oscillatory potentials, which have been suggested to indicate IPL activity, were found to be mature at 18 weeks postnatal (Hamasaki & McGuire, 1985).

The maturity of the b-wave thus follows a similar time course to bipolar cell synaptogenesis. This would be consistent with a relationship between bipolar cell synaptogenesis and the functional status of these cells if, indeed, the b-wave is a reflection of their activity. Oscillatory potentials follow a similar or slightly more extended time course to bipolar cell synaptogenesis. This is what might be expected if they do indeed reflect IPL activity. The slightly longer time course of oscillatory potential development than bipolar cell synaptogenesis may not be significant but if so, it may indicate that morphological maturity of bipolar cell ribbon synapses may not be associated with functional maturity in terms of oscillatory potentials.

4.8.4 Ganglion cell morphological development

The full complement of medium and large ganglion cells have been generated by E35 (Walsh et al, 1983). Ganglion cell death is largely complete by birth but continues until P15 (Ng & Stone, 1982). The structure of the ganglion cell dendritic tree

also changes with development. The segregation of ganglion cell dendrites into sublaminae in the IPL begins around birth and is complete at the area centralis by P3 (Maslim & Stone, 1988).

If the viability of a ganglion cell is dependent upon synaptic inputs, then, since most ganglion cell death occurs prenatally, conventional synapses rather than bipolar ribbon synapses would be responsible. It is interesting that most bipolar cell synaptogenesis occurs after the segregation of ganglion cell dendrites into sublaminae. It may be necessary for ganglion cell dendrites to have segregated into sublaminae before ribbon synapses from the appropriate bipolar cell (i.e. flat or invaginating cone bipolar cells) can form onto ganglion cells. Alternatively, the stimulus to segregation may be the initial formation of bipolar cell synapses. The delayed segregation of ganglion cell dendrites in peripheral retina which occurs at the same time as the first ribbon synapses are formed in peripheral retina, at P5 (Maslim & Stone, 1986), further supports the association between dendritic segregation and bipolar cell synaptogenesis.

The decrease in the number of branches of the ganglion cell dendritic tree and the number of spines on the dendrites with development (see section 4.6) occur both in the prenatal period and continue until the end of the first postnatal month (Ramoa et al, 1988). The decrease in the number of branches and spines on the ganglion cell dendritic tree may also involve elimination of both conventional and ribbon synapses in the IPL.

4.8.5 Development of the lateral geniculate nucleus

The synapses from retinal ganglion cell axons onto LGN relay cells are already present at P1 (Winfield & Powell, 1980) and subsequently decrease in frequency until about P60-70 (Winfield, Hiorns & Powell, 1980). Terminals of retinal origin were identifiable because they were the largest with asymmetric synapses and made numerous synaptic contacts with other profiles in a single section. Over the same period, corticogeniculate synapses (identified as the symmetrical synapses in the glomeruli), increase in frequency. Daniels, Pettigrew & Norman (1978) found that before 3 weeks postnatal, LGN cells were immature, most having large receptive fields without surround inhibition. In the 4th week, many cells could be identified physiologically as X- or Y-cells. Many X-cells had attained maturity by this time, while Y-cells developed mature receptive fields later than 5 weeks (Daniels et al, 1978). The spatial resolving power of LGN X-cells receiving their input from the area centralis reaches a near adult level by 10 weeks postnatal (Ikeda & Tremain, 1978).

The LGN thus reaches maturity at approximately the same time as bipolar ribbon frequency, suggesting there may be an association between the development of the LGN and the retina.

4.8.6 Development of the visual cortex

There has been debate as to whether the response characteristics of cortical neurones are determined innately or by visual experience. It appears that the basic properties of

orientation selectivity, organisation into orientation columns, directionality and binocularity are all present very early in development (Hubel & Wiesel, 1963, Albus & Wolf, 1982). However, although the basic adult characteristics are reached by the fourth postnatal week (Albus & Wolf, 1982), it seems that the 'tuning' of these neurones becomes more specific to a particular stimulus (such as a particular orientation) with postnatal development (see Pettigrew, 1978). Disparity detection appears to be the property most dependent on visual experience (Pettigrew, 1974). It has been suggested by Pettigrew (1978) that the innate characteristics of orientation selectivity may be determined by the W-cell pathway and that the X- and Y-cell pathways are more susceptible to environmental influence.

The work of Hubel & Wiesel (reviewed by Wiesel, 1982) demonstrated a critical period, during which visual deprivation caused diminished efficacy of inputs from the deprived eye onto binocularly driven neurones. This was reversible within the critical period but was irreversible once the critical period was over. The extent of this critical period in cat was from about 3 weeks to 3 months postnatal, which is approximately simultaneous with bipolar cell synaptogenesis. So it is possible that synaptogenesis in the IPL may be related to the sensitive period in the visual cortex. However, the normality of the LGN neuronal responses after monocular deprivation in cat and primate suggested that the impairment of vision was cortical in origin rather than retinal (Wiesel & Hubel, 1963; Blakemore & Vital-Durand, 1986, respectively). In cat, monocular occlusion

appears to be without effect on the responsiveness of both LGN X-cells (Sherman, Hoffman & Stone, 1972; Shapley & So, 1980; Derrington & Hawken, 1981), (although Maffei & Fiorentini (1976) did report reduced acuity) and retinal X-ganglion cells in the cat (Kratz, Mangel, Lehmkuhle & Sherman, 1979; Cleland, Mitchell, Gillard-Crewther & Crewther, 1980). In addition, unilateral and bilateral occlusion in the cat have virtually no effect on the normal morphological development of LGN cells (Winfield & Powell, 1980) or LGN synapse frequency (Winfield et al, 1980). In monocularly deprived rats, Fifkova (1972) found that the frequency of bipolar ribbon synapses of both closed and open eye was lower than in the control animals. Conventional synapses in the closed eye occurred more frequently than in the control, while those in the open eye were less frequent than in the controls. Other studies in the rat (Sosula & Glow, 1971) and primate (von Noorden, 1973) also indicated that occlusion had an effect on IPL synapse frequency. However, the two latter studies compared only two retinae and thus must be regarded as preliminary.

On the other hand, esotropia, experimentally induced at 3 weeks, resulted in LGN X-cells that had diminished spatial resolution in the central representation (Ikeda & Wright, 1976). Ikeda & Tremain (1979) found that the resolution of retinal X-ganglion cells was also appreciably reduced following esotropia, while Y-cells were only minimally affected. The retinal X-ganglion cells had an enlarged receptive field and diminished inhibitory surround. The loss of X-cell resolution has

subsequently been confirmed for LGN (Jones, Kalil & Spear, 1984) and retina (Chino, Shansky & Hamasaki, 1980). Although Cleland, Crewther, Crewther & Mitchell (1982), who induced esotropia at the time of eye opening by section of the lateral rectus muscle, reported unchanged retinal X-ganglion cell resolution, a subsequent study following Ikeda's surgical procedure did show a 20% reduction in resolution of retinal X-ganglion cells (Crewther, Crewther & Cleland, 1985). In addition, Devlin, Jay & Morrison (1990) found that esotropia resulted in a delayed time-to-peak of the pattern electroretinogram, which may reflect the summed activity of the retinal ganglion cells (Maffei & Fiorentini, 1981). Similarly the binocularity of visual cortical neurones is reduced by experimentally induced strabismus in cats (Kalil, Spear & Langsetmo, 1984) and primates (Crawford & von Noorden, 1979).

In general, it appears that the effects of experimentally-induced monocular deprivation and esotropia produce different effects on the visual system. While esotropia appears to affect the normal development of LGN and retinal neurones, monocular deprivation appears to cause little, if any, change.

4.8.7 Conclusions

This study of cat has shown that there is substantial bipolar cell synaptogenesis postnatally while conventional synapses are at a mature frequency at the time of birth. Bipolar cell synaptogenesis occurs simultaneously with growth of the eye and the clarity of the ocular media, photoreceptor development, the development of the ERG, the maturation of the ganglion cell dendritic tree and LGN development. It is completed at the same time as the end of the critical period for the visual cortex.

The increase in bipolar cell synaptogenesis indicated by the increased numbers of ribbons in postnatal development indicates an increased excitatory input to the retinal ganglion cells. This is consistent with the electrophysiological data (Hamasaki & Flynn, 1977) showing that the response amplitude of ganglion cells was smaller in 3 weeks old than in mature retinae, though not with the data of Rusoff & Dubin (1977) who reported greater excitability. An increased excitatory input to ganglion cells with development is also consistent with the results of Rusoff & Dubin (1977) that the ganglion cell receptive field centre ***increases*** in linear size with development. However, the data of Hamasaki & Flynn (1977) and Hamasaki & Sutija indicate a ***decrease*** in centre size which may be caused by an encroachment of the inhibitory surround upon the centre. If this is the case, the constancy of conventional synapse frequency with development may indicate an increased efficacy of inhibitory transmission or a redistribution of sub-types of conventional synapses. In this

respect, a quantitative study of different putative transmitter substances at the electron microscope level would be particularly valuable.

Bipolar cell synaptogenesis in the cat occurs simultaneously to developmental events in the LGN and cortex. Therefore, it would be interesting to see whether abnormal visual experience affecting the development of the LGN and cortex also affects bipolar cell synaptogenesis. Although there is evidence in the rat and monkey that monocular occlusion affects bipolar cell and amacrine cell synaptogenesis, there have been no previous studies on the effects of monocular deprivation or esotropia on synaptogenesis in the IPL of cat retina. Electrophysiological evidence from monocular occlusion in the cat indicates that there is little change in the retina or LGN and that there is no morphological change in the LGN neurones. Present electrophysiological evidence indicates that strabismus has an effect on normal retinal and LGN development which would seem to justify the examination of the effect of strabismus on IPL synaptogenesis.

REFERENCES

Albus, K. & Wolf, W. (1984). Early post-natal development of neuronal function in the kitten's visual cortex: a laminar analysis. Journal of Physiology 348, 153-185.

Barlow, H.B., Fitzhugh, R. & Kuffler, S.W. (1957). Change of organization of the receptive field of the cat's retina during dark adaptation. Journal of Physiology 137, 338-354.

Bishop, P.O., Kozak, W. & Vakkur, G.J. (1962). Some quantitative aspects of the cat's eye: axis and plane of reference, visual field co-ordinates and optics. Journal of Physiology 163, 466-502.

Blakemore, C. & Vital-Durand, F. (1986). Effects of visual deprivation on the development of the monkey's lateral geniculate nucleus. Journal of Physiology 380, 493-511.

Bloomfield, S.A. & Dowling, J.E. (1985). Roles of aspartate and glutamate in synaptic transmission in rabbit retina. II. Inner plexiform layer. Journal of Neurophysiology 53, 714-725.

Bolz, J., Frumkes, T., Voigt, T. & Wässle, H. (1985). Action and localization of γ-aminobutyric acid in the cat retina. Journal of Physiology 362, 369-393.

Bolz, J., Thier, P., Voigt, T. & Wässle, H. (1985). Action and localization of glycine and taurine in the cat retina. Journal of Physiology 362, 395-413.

Bonds, A.B. & Freeman R.D. (1978). Development of optical quality in the kitten eye. Vision Research 18, 391-398.

Boycott, B.B., Dowling, J.E., Fisher, S.K., Kolb, H. & Laties, A.M. (1975). Interplexiform cells of the mammalian retina and their comparison with catecholamine containing retinal cells. Proceedings of the Royal Society of London B 191, 353-368.

Boycott, B.B. & Wässle, H. (1974). The morphological types of ganglion cells of the domestic cat's retina. Journal of Physiology 240, 397-419.

Braekevelt, C.R. & Hollenberg, M.J. (1970). The development of the retina of the albino rat. American Journal of Anatomy 127, 281-302.

Cajal, R.S. (1892). The structure of the retina. Compiled and translated by Thorpe, S.A. & Glickstein, M., Illinois. Thomas, C.C..

Chino, Y.M., Shansky, M.S. & Hamasaki, D.I. (1980). Development of receptive field properties of retinal ganglion cells in kittens raised with a convergent squint. Experimental Brain Research 39, 313-320.

Cleland, B.G., Crewther, D.P., Crewther, S.G. & Mitchell, D.E. (1982). Normality of spatial resolution of retinal ganglion cells in cats with strabismic amblyopia. Journal of Physiology 326, 235-249.

Cleland, B.G., Mitchell, D.E., Gillard-Crewther, S. & Crewther, D.P. (1980). Visual resolution of retinal ganglion cells in monocularly-deprived cats. Brain Research 192, 261-266.

Cohen, E. & Sterling, P. (1986). Accumulation of (^{3}H)glycine by cone bipolar neurons in the cat retina. Journal of Comparative Neurology 250, 1-7.

Cragg, B.G. (1975). The development of synapses in the visual system of the cat. Journal of Comparative Neurology 160, 147-166.

Crawford, M.L.J. & von Noorden, G.K. (1979). The effects of short term experimental strabismus on the visual system of Macaca mulatta. Investigative Ophthalmology and Visual Science 18, 496-505.

Crewther, S.G., Crewther, D.P. & Cleland, B.G. (1985). Convergent strabismic amblyopia in cats. Experimental Brain Research 60, 1-9.

Crooks, J. & Morrison, J.D. (1986). Synaptogenesis in the inner plexiform layer of area centralis of kitten retina. Journal of Physiology 380, 74P.

Crooks, J. & Morrison, J.D. (1989). Synapses of the inner plexiform layer of the area centralis of kitten retina during postnatal development: a quantitative study. Journal of Anatomy 163, 33-47.

Daniels, J.D., Pettigrew, J.D. & Norman, J.L. (1978). Development of single-neuron responses in kitten's lateral geniculate nucleus. Journal of Neurophysiology 41, 1373-1393.

Dann, J.F., Buhl, E.H., & Peichl, L. (1988). Postnatal dendritic maturation of alpha and beta ganglion cells in the cat retina. Journal of Neuroscience 8, 1485-1499.

Derrington, A.M. & Hawken, M.J. (1981). Spatial and temporal properties of cat geniculate neurones after prolonged deprivation. Journal of Physiology 314, 107-120.

Devlin, M.L., Jay, J.L. & Morrison, J.D. (1990). Abnormality of the pattern electroretinogram and pattern visual evoked cortical response in esotropic cats. Documenta Ophthalmologica. In press.

Donovan, A. (1966). The postnatal development of the cat retina. Experimental Eye Research 5, 249-254.

Dowling, J.E. (1968). Synaptic organization of the frog retina: an electron microscopic analysis comparing the retinas of frogs and primates. Proceedings of the Royal Society of London B 170, 205-228.

Dowling, J.E. (1987). The retina. An approachable part of the brain. Cambridge, Massachusetts. Harvard University Press.

Dowling, J.E. & Boycott, B.B. (1966). Organization of the primate retina: electron microscopy. Proceedings of the Royal Society of London B 166, 80-111.

Dubin, M.W. (1970). The inner plexiform layer of vertebrate retina: a quantitative and comparative electron microscopic analysis. Journal of Comparative Neurology 140, 479-506.

Estable-Puig, J.F., Bauer, W.C. & Blumberg, J.M. (1965). Technical note; paraphenylenediamine staining of osmium-fixed plastic-embedded tissue for light and phase microscopy. Journal of Neuropathology and Experimental Neurology 24, 531-535.

Famiglietti, E.V. & Kolb, H. (1976). Structural basis for ON- and OFF-center responses in retinal ganglion cells. Science 194, 193-195.

Faulkner, D.J., Ikeda, H., Jacobson, S.G. & Kemp, C.M. (1982). Rhodopsin levels and rod electroretinogram thresholds during development in the cat. Journal of Physiology 330, 58-59P.

Fifkova, E. (1972). Effect of visual deprivation and light on synapses of the inner plexiform layer. Experimental Neurology 35, 458-469.

Fisher, L.J. (1979). Development of synaptic arrays in the inner plexiform layer of neonatal mouse retina. Journal of Comparative Neurology 187, 359-372.

Freed, M.A., Nakamura, Y. & Sterling, P. (1983). Four types of amacrine in the cat retina that accumulate GABA. Journal of Comparative Neurology 219, 295-304.

Freeman, R.D. & Lai, C.E. (1978). Development of the optical surfaces of the kitten eye. Vision Research 18, 399-407.

Freeman, R.D., Wong, S. & Zezula, S. (1978). Optical development of the kitten cornea. Vision Research 18, 409-414.

Gray, E.G. (1959). Axo-somatic and axo-dendritic synapses of the cerebral cortex: an electron microscope study. Journal of Anatomy 93, 420-433.

Gray, E.G. & Pease, H.L. (1971). On understanding the organisation of the retinal receptor synapses. Brain Research 35, 1-15.

Greiner, J.V. & Weidman, T.A. (1980). Histogenesis of the cat retina. Experimental Eye Research 30, 439-453.

Hamasaki, D.I. & Flynn, J.T. (1977). Physiological properties of retinal ganglion cells of 3-week-old kittens. Vision Research 17, 275-284.

Hamasaki, D.I. & McGuire, G.W. (1985). Physiological development of the kitten's retina: an ERG study. Vision Research 25, 1537-1543.

Hamasaki, D.I. & Sutija, V.G. (1979). Development of X- and Y-cells in kittens. Experimental Brain Research 35, 9-23.

Hinds, J.W. & Hinds, P.L. (1979). Differentiation of photoreceptors and horizontal cells in the embryonic mouse retina: an electron microscopic, serial section analysis. Journal of Comparative Neurology 187, 495-512.

Hinds, J.W. & Hinds, P.L. (1983). Development of retinal amacrine cells in the mouse embryo: evidence for two modes of formation. Journal of Comparative Neurology 213, 1-23.

Hochstein, S. & Shapley, R.M. (1976). Linear and non-linear spatial subunits in Y cat retinal ganglion cells. Journal of Physiology 262, 265-284.

Hubel D.H. & Wiesel T.N. (1963). Receptive fields of cells in striate cortex of very young, visually inexperienced kittens. Journal of Neurophysiology 26, 994-1002.

Ikeda, H. & Robbins, J. (1985). Postnatal development of GABA- and glycine-mediated inhibition of feline retinal ganglion cells in the area centralis. Developmental Brain Research 23, 1-17.

Ikeda, H., Robbins, J. & Wakakuwa, K. (1987). Evidence for dopaminergic innervation on kitten retinal ganglion cells. Developmental Brain Research 35, 83-89.

Ikeda, H. & Sheardown, M.J. (1982a). Acetylcholine may be an excitatory transmitter mediating visual excitation of 'transient' cells with the periphery effect in the cat retina: iontophoretic studies in vivo. Neuroscience 7, 1299-1308.

Ikeda, H. & Sheardown, M.J. (1982b). Aspartate may be an excitatory transmitter mediating visual excitation of "sustained" but not "transient" cells in the cat retina: iontophoretic studies in vivo. Neuroscience 7, 25-36.

Ikeda, H. & Sheardown, M.J. (1983). Functional transmitters at retinal ganglion cells in the cat. Vision Research 23, 1161-1174.

Ikeda, H. & Tremain, K.E. (1978). The development of spatial resolving power of lateral geniculate neurones in kittens. Experimental Brain Research 31, 193-206.

Ikeda, H. & Tremain, K.E. (1979). Amblyopia occurs in retinal ganglion cells in cats reared with convergent squint without alternating fixation. Experimental Brain Research 35, 559-582.

Ikeda, H., Tremain, K.E. & Einon, G. (1978). Loss of spatial resolution of lateral geniculate nucleus neurones in kittens raised with convergent squint produced at different stages in development. Experimental Brain Research 31, 207-220.

Ikeda, H. & Wright, M.J. (1976). Properties of LGN cells in kittens reared with convergent squint: a neurophysiological demonstration of amblyopia. Experimental Brain Research 25, 63-77.

Ito, S. & Winchester, R.J. (1963). The fine structure of the gastric mucosa in the bat. Journal of Cell Biology 16, 541-577.

Jacobson, S.G., Ikeda, H. & Ruddock, K. (1987). Cone-mediated retinal function in cats during development. Documenta Ophthalmologica 65, 7-14.

Johns, P.R., Rusoff, A.C. & Dubin, M.W. (1979). Postnatal neurogenesis in the kitten retina. Journal of Comparative Neurology 187, 545-556.

Jones, K.R., Kalil, R.E. & Spear, P.D. (1984). Effects of strabismus on responsivity, spatial resolution, and contrast sensitivity of cat lateral geniculate neurons. Journal of Neurophysiology 52, 538-552.

Kalil, R.E., Spear, P.D. & Langsetmo, A. (1984). Response properties of striate cortex neurons in cats raised with divergent and convergent strabismus. Journal of Neurophysiology 52, 514-537.

Kidd, M. (1962). Electron microscopy of the inner plexiform layer of the retina in the cat and the pigeon. Journal of Anatomy 96, 179-188.

Kline, R.P., Ripps, H. & Dowling, J.E. (1978). Generation of b-wave currents in the skate retina. Proceedings of the National Academy of Sciences of the U.S.A. 75, 5727-5731.

Kolb, H. (1979). The inner plexiform layer in the retina of the cat: electron microscopic observations. Journal of Neurocytology 8, 295-329.

Kolb, H. & Famiglietti, E.V. (1974). Rod and cone pathways in the inner plexiform layer of cat retina. Science 186, 47-49.

Kolb, H., Nelson, R. & Mariani, A. (1981). Amacrine cells, bipolar cells and ganglion cells of the cat retina: a Golgi study. Vision Research 21, 1081-1114.

Kolb, H. & West, R. (1977). Synaptic connections of the interplexiform cell in the retina of the cat. Journal of Neurocytology 6, 155-170.

Kratz, K.E., Mangel, S.C., Lehmkuhle, S. & Sherman, S.M. (1979). Retinal X- and Y-cells in monocularly lid-sutured cats: normality of spatial and temporal properties. Brain Research 172, 545-551.

Lia, B., Williams, R.W. & Chalupa, L.M. (1987). Formation of retinal ganglion cell topography during prenatal development. Science 236, 848-851.

Maffei, L. & Fiorentini, A. (1976). Monocular deprivation in kittens impairs the spatial resolution of geniculate neurones. Nature 264, 754-755.

Maffei, L. & Fiorentini, A. (1981). Electroretinographic responses to alternating gratings before and after section of the optic nerve. Science 211, 953-955.

Mann, I.C. (1928). The process of differentiation of the retinal layers in vertebrates. British Journal of Ophthalmology 12, 449-478.

Masland, R.H., Mills, J.W. & Cassidy, C. (1984). The functions of acetylcholine in the rabbit retina. Proceedings of the Royal Society of London B 223, 121-139.

Masland, R.H., Mills, J.W. & Hayden, S.A. (1984). Acetylcholine-synthesizing amacrine cells: identification and selective staining by using radioautography and fluorescent markers. Proceedings of the Royal Society of London B 223, 79-100.

Maslim, J. & Stone, J. (1986). Synaptogenesis in the retina of the cat. Brain Research 373, 35-48.

Maslim, J. & Stone, J. (1988). Time course of stratification of the dendritic fields of ganglion cells in the retina of the cat. Developmental Brain Research 44, 87-93.

Maslim, J. & Stone, J. (1989). Extracellular space in the developing retina assessed by electron microscopy: laminar and topographic distribution. Neuroscience Letters 100, 40-46.

Massey, S.C. & Miller, R.F. (1988). Glutamate receptors of ganglion cells in the rabbit retina: evidence for glutamate as a bipolar cell transmitter. Journal of Physiology 405, 635-655.

Mastronarde, D.N. (1984). Organization of the cat's optic tract as assessed by single-axon recordings. Journal of Comparative Neurology 227, 14-22.

Mastronarde, D.N., Thibeault, M.A. & Dubin, M.W. (1984). Non-uniform postnatal growth of the cat retina. Journal of Comparative Neurology 228, 598-608.

McArdle, C.B., Dowling, J.E. & Masland, R.H. (1977). Development of outer segments and synapses in the rabbit retina. Journal of Comparative Neurology 175, 253-274.

McGuire, B.A., Stevens, J.K. & Sterling, P. (1984). Microcircuitry of bipolar cells in cat retina. Journal of Neuroscience 4, 2920-2938.

McGuire, B.A., Stevens, J.K. & Sterling, P. (1986). Microcircuitry of beta ganglion cells in cat retina. Journal of Neuroscience 6, 907-918.

Morrison, J.D. (1978). Development of photoreceptor and bipolar cell terminals in kitten retina. Journal of Physiology 284, 118-119P.

Morrison, J.D. (1982). Postnatal development of the area centralis of the kitten retina: an electron microscopic study. Journal of Anatomy 135, 255-271.

Morrison, J.D. (1983). Morphogenesis of photoreceptor outer segments in the developing kitten retina. Journal of Anatomy 136, 521-533.

Nakamura, Y., McGuire, B.A. & Sterling, P. (1980). Interplexiform cells in cat retina: identification by uptake of γ-[^{3}H]amino-butyric acid and serial reconstruction. Proceedings of the National Academy of Sciences of the U.S.A. 77, 658-661.

Nelson, R., Famiglietti, E.V. & Kolb, H. (1978). Intracellular staining reveals different levels of stratification for on- and off-center ganglion cells in cat retina. Journal of Neurophysiology 41, 472-483.

Nelson, R. & Kolb, H. (1983). Synaptic patterns and response properties of bipolar and ganglion cells in the cat retina. Vision Research 23, 1183-1195.

Nelson, R., Kolb, H., Robinson, M.M. & Mariani, A.P. (1981). Neural circuitry of the cat retina: cone pathways to ganglion cells. Vision Research 21, 1527-1536.

Newman, E.A. (1980). Current source - density analysis of the b-wave of frog retina. Journal of Neurophysiology 43, 1355-1366.

Newman, E.A. (1984). Regional specialization of retinal glial cell membrane. Nature 309, 155-157.

Ng, A.Y.K. & Stone, J. (1982). The optic nerve of the cat: appearance and loss of axons during normal development. Developmental Brain Research 5, 263-271.

Nishimura, Y. & Rakic. P. (1985). Development of the rhesus monkey retina. I. Emergence of the inner plexiform layer and its synapses. Journal of Comparative Neurology 241, 420-434.

Nishimura, Y. & Rakic. P. (1987). Development of the rhesus monkey retina. II. A three-dimensional analysis of the sequences of synaptic combinations in the inner plexiform layer. Journal of Comparative Neurology 262, 290-313.

Olney, J.W. (1968). An electron microscopic study of synapse formation, receptor outer segment development, and other aspects of developing mouse retina. Investigative Ophthalmology 7, 250-268.

Olson, C.R. & Freeman, R.D. (1978). Eye alignment in kittens. Journal of Neurophysiology 41, 848-859.

Pettigrew (1974). The effect of visual experience on the development of stimulus specificity by kitten cortical neurones. Journal of Physiology 237, 49-74.

Pettigrew, J.D. (1978). The paradox of the critical period for striate cortex. In 'Neuronal Plasticity', pp 311-330. Ed. Cotman, C.W. New York. Raven Press.

Pourcho, R.G. & Goebel, D.J. (1987a). A combined Golgi and autoradiographic study of ^{3}H-glycine-accumulating cone bipolar cells in the cat retina. Journal of Neuroscience 7, 1178-1188.

Pourcho, R.G. & Goebel, D.J. (1987b). Visualization of endogenous glycine in cat retina: an immunocytochemical study with Fab fragments. Journal of Neuroscience 7, 1189-1197.

Pourcho, R.G. & Osman, K. (1986). Cytochemical identification of cholinergic amacrine cells in cat retina. Journal of Comparative Neurology 247, 497-504.

Ramoa, A.S., Campbell, G. & Schatz, C.J. (1988). Dendritic growth and remodeling of cat retinal ganglion cells during fetal and postnatal development. Journal of Neuroscience 8, 4239-4261.

Rapaport D.H. (1989). Quantitative aspects of synaptic ribbon formation in the outer plexiform layer of the developing cat retina. Visual Neuroscience 3, 21-32.

Rapaport, D.H. & Stone, J. (1983). Time course of morphological differentiation of cat retinal ganglion cells: influences on soma size. Journal of Comparative Neurology 221, 45-52.

Raviola, E. & Dacheux, R.F. (1987). Excitatory dyad synapse in rabbit retina. Proceedings of the National Academy of Science of the USA 84, 7324-7328.

Raviola, G. & Raviola, E. (1967). Light and electron microscopic observations on the inner plexiform layer of the rabbit retina. American Journal of Anatomy 120, 403-426.

Raviola, E. & Raviola, G. (1982). Structure of the synaptic membranes in the inner plexiform layer of the retina: a freeze-fracture study in monkeys and rabbits. Journal of Comparative Neurology 209, 233-248.

Reynolds, E.S. (1963). The use of lead citrate at high pH as an electron-opaque stain in electron microscopy. Journal of Cell Biology 17, 208-212.

Rusoff, A.C. (1979). Development of ganglion cells in the retina of the cat. In "Developmental Neurobiology of Vision" Ed. Freeman, R.D. pp 19-29. New York: Plenum Press.

Rusoff, A.C. & Dubin, M.W. (1977). Development of receptive-field properties of retinal ganglion cells in kittens. Journal of Neurophysiology 40, 1188-1198.

Ryan, B.F., Joiner, B.L. & Ryan, T.A. (1985). Minitab Handbook, 2nd Edition. Boston: Duxbury Press.

Schmidt, M., Humphrey, M.F. & Wässle, H. (1987). Action and localization of acetylcholine in the cat retina. Journal of Neurophysiology 58, 997-1015.

Shapley, R. & So, Y.T. (1980). Is there an effect of monocular deprivation on the proportions of X and Y cells in the cat lateral geniculate nucleus? Experimental Brain Research 39, 41-48.

Shatz, C.J. The prenatal development of the cat's retinogeniculate pathway. Journal of Neuroscience 3, 482-499.

Sherman, S.M., Hoffman, K-P. & Stone, J. (1972). Loss of a specific cell type from dorsal lateral geniculate nucleus in visually deprived cats. Journal of Neurophysiology 35, 532-541.

Sidman, R.L. (1961). Histogenesis of mouse retina studied with thymidine-H^3. In 'The Structure of the Eye', pp 487-506. Ed. Smelser G.K. New York & London: Academic Press.

Smelser, G.K., Ozanics, V., Rayborn, M. & Sagun, D. (1974). Retinal synaptogenesis in the primate. Investigative Opthalmology & Visual Science 13, 340-361.

Sosula, L. & Glow, P.H. (1970). A quantitative ultrastructural study of the inner plexiform layer of the rat retina. Journal of Comparative Neurology 140, 439-478.

Sosula, L. & Glow, P.H. (1971). Increase in the number of synapses in the inner plexiform layer of light deprived rat retinae: quantitative electron microscopy. Journal of Comparative Neurology 141, 427-452.

Steinberg, R.H., Reid, M. & Lacey, P.L. (1973). The distribution of rods and cones in the retina of the cat (Felis domesticus). Journal of Comparative Neurology 148, 229-248.

Stempak, J.G. & Ward, R.T. (1964). An improved staining method for electron microscopy. Journal of Cell Biology 22, 697-701.

Stone, J. (1965). A quantitative analysis of the distribution of ganglion cells in the cat's retina. Journal of Comparative Neurology 124, 337-352.

Stone, J. (1978). The number and distribution of ganglion cells in the cat's retina. Journal of Comparative Neurology 180, 753-772.

Thorn, F., Gollender, M. & Erickson, P. (1976). The development of the kitten's visual optics. Vision Research 16, 1145-1149.

Toyoda, J.-I. & Fujimoto, M. (1984). Application of transretinal current stimulation for the study of bipolar-amacrine transmission. Journal of General Physiology 84, 915-925.

Tucker, G.S. (1978). Light microscopic analysis of the kitten retina: postnatal development in the area centralis. Journal of Comparative Neurology 180, 489-500.

Tucker, G.S., Hamasaki, D.I., Labbie, A. & Muroff, J. (1979). Anatomic and physiologic development of the photoreceptor of the kitten. Experimental Brain Research 37, 459-474.

Uchizono, K. (1965). Characteristics of excitatory and inhibitory synapses in the central nervous system of the cat. Nature 207, 642-643.

Vakkur, G.J., Bishop, P.O. & Kozak, W. (1963). Visual optics in the cat, including posterior nodal distance and retinal landmarks. Vision Research 3, 289-314.

Vaney, D.I. & Young H.M. (1988). GABA-like immunoreactivity in cholinergic amacrine cells of the rabbit retina. Brain Research 438, 369-373.

Vogel, M (1978). Postnatal development of the cat's retina. Advances in Anatomy, Embryology and Cell Biology 54, 1-66.

von Grunau, M.W. (1979). The role of maturation and visual experience in the development of eye alignment in cats. Experimental Brain Research 37, 41-47.

von Noorden, G.K. (1973). Histological studies of the visual system in monkeys with experimental amblyopia. Investigative Ophthalmology 12, 727-738.

Walls, G.L. (1942). The vertebrate eye and its adaptive radiation. Michigan. The Cranbrook Press.

Walsh, C. & Polley, E.H. (1985). The topography of ganglion cell production in the cat's retina. Journal of Neuroscience 5, 741-750.

Walsh, C., Polley, E.H., Hickey, T.L. & Guillery, R.W. (1983). Generation of cat retinal ganglion cells in relation to central pathways. Nature 302, 611-614.

Wässle, H., Schäfer-Trenkler, I. & Voigt, T. (1986). Analysis of a glycinergic inhibitory pathway in the cat retina. Journal of Neuroscience 6, 594-604.

Weibel, E.R. (1980). Stereological Methods. Vol. 2 Theoretical Foundations. London: Academic Press.

Wiesel, T.N. (1982). Postnatal development of the visual cortex and the influence of environment. Nature 299, 583-591.

Wiesel, T.N. & Hubel, D.H. (1963). Effects of visual deprivation on morphology and physiology of cells in the cat's lateral geniculate body. Journal of Neurophysiology 26, 978-993.

Windle, W.F. (1930). Normal behavioural reactions of kittens correlated with the postnatal development of nerve-fiber density in the spinal gray matter. Journal of Comparative Neurology 50, 479-503.

Winfield, D.A., Hiorns, R.W. & Powell, T.P.S. (1980). A quantitative electron-microscopical study of the postnatal development of the lateral geniculate nucleus in normal kittens and in kittens with eyelid suture. Proceedings of the Royal Society B 210, 211-234.

Winfield, D.A. & Powell, T.P.S. (1980). An electron-microscopical study of the post-natal development of the lateral geniculate nucleus in the normal kitten and after eyelid suture. Proceedings of the Royal Society of London B 210, 197-210.

Zetterstrom B. (1955). The effect of light on the appearance and development of the electroretinogram in newborn kittens. Acta Physiologica Scandinavica 35, 272-279.

APPENDIX 1

FIXATIVE

Buffer A/ $Na_2HPO_4.2H_2O$ = 8.9g

Make up to 250 ml with distilled water.

Buffer B/ $Na_2HPO_4.H_2O$ = 3.12g

Make up to 100 ml with distilled water.

PRIMARY FIXATIVE (0.05M Phosphate)

25% glutaraldehyde = 4 ml

10% paraformaldehyde = 5 ml

Buffer A = 20.25 ml

Buffer B = 4.75 ml

Distilled water = 60ml

Adjust to pH 7.4 and make up to 100ml with distilled water.

Osmolality ≈ 300 mOsm/kg

BUFFER WASH (0.15M Phosphate)

Buffer A = 60.75 ml

Buffer B = 14.25 ml

Adjust to pH 7.4 and make up to 100 ml with distilled water

Osmolality ≈ 300 mOsm/kg

POST-FIXATIVE (0.15M Phosphate)

Buffer A = 60.75 ml

Buffer B = 14.25 ml

Adjust to pH 7.4.

Buffer = 3 parts

4% OsO_4 = 1 part

STAINING PROCEDURES

1µm Sections

1µm sections were mounted on gelatin/ chrome alum coated slides then stained using one of the following techniques.

A/ TOLUIDINE BLUE/ PYRONIN Y (Ito & Winchester, 1963)

Sodium Tetraborate (Borax) = 0.8g

Distilled water =100 ml

Dissolve, then add in order

Toluidine Blue = 0.8g

Pyronin Y = 0.2g

Filter before use

Stain at room temperature until desired colour is obtained. Wash in running water, air dry and mount in immersion oil or synthetic mounting medium.

B/ PARAPHENYLENEDIAMINE (Estable-Puig, Bauer & Blumberg, 1965)

1% solution of paraphenylenediamine

Filter before use

Stain at room temperature for 30 minutes.

Rinse slides in distilled water for 2 minutes.

Dehydrate in 2 changes in 96% or absolute alcohol.

Air dry and mount in immersion oil or synthetic mounting medium.